Imaging cortical plasticity in the human motor system

I n a u g u r a l – D i s s e r t a t i o n

zur

Erlangung des Doktorgrades

der Mathematisch-Naturwissenschaftlichen Fakultät

der Universität zu Köln

vorgelegt von

Charlotte Maria Nettekoven

aus Siegburg

2015

Berichterstatter: Prof. Dr. Ansgar Büschges

(Gutachter) Prof. Dr. Christian Grefkes

Tag der mündlichen Prüfung: 23.06.2015

Table of Content

Table of Figures

Abbreviations

AP – anterior-posterior

B_0 – static magnetic MRI field

BA – Brodmann area

BOLD – blood oxygenation level dependent

BV – blood volume

CBF – cerebral blood flow

cTBS – continuous theta-burst stimulation

DCM – dynamic causal modeling

dPMC – dorsal premotor cortex

D-wave – direct-wave

EMG – electromyography

fMRI – functional magnetic resonance imaging

GABA – γ-aminobutric acid

GAD – glutamate decarboxylase

HRF – hemodynamic response function

iTBS – intermittent theta-burst stimulation

I-wave – indirect-wave

LM – latero-medial

LTD – long-term depression

LTP – long-term potentiation

M1 – primary motor cortex

MDM – magnetic dipole moment

MEP – motor-evoked potential

MRS – magnetic resonance spectroscopy

M_{xy} – transversal magnetization

M_z – longitudinal magnetization

NMDA – N-Methyl-D-Aspartate

PA – posterior-anterior

PMC – premotor cortex

RF – radiofrequency

ROI – region of interest

rTMS – repetitive transcranial magnetic stimulation

rsFC – resting-state functional connectivity

S1 – primary somatosensory cortex

SMA – supplementary motor area

T1 – longitudinal relaxation

T2 – transversal relaxation

TBS – theta-burst stimulation

TMS – transcranial magnetic stimulation

vPMC – ventral premotor cortex

Abstract

Intermittent theta-burst stimulation (iTBS) is a novel form of repetitive transcranial magnetic stimulation (rTMS) inducing increases in cortical excitability that last beyond stimulation. Compared to conventional rTMS protocols iTBS induces strong and long-lasting aftereffects with shorter stimulation time and less stimulation intensity. However, mechanisms underlying iTBS-induced aftereffects as well as factors contributing to a high inter-individual variability between subjects are still poorly understood. The aim of the present study was to gain some new insights into these mechanisms by combining non-invasive brain stimulation with neuroimaging and connectivity analyses of the human motor system.

Previous studies suggested a link between rTMS aftereffects and activity as well as connectivity of the stimulated region. However, the mechanisms underlying iTBS-induced plasticity on the systems level are still incompletely understood. Hence, the aim of the first study of the present thesis was to investigate how neural activity and connectivity of the motor system are related to aftereffects of iTBS. Therefore, 12 healthy, right-handed volunteers underwent functional magnetic resonance imaging (fMRI) during rest (resting-state fMRI, rs-fMRI) and while performing a simple hand motor task. Based on this data, resting-state functional connectivity (rsFC) and task-induced activation as well as task-related effective connectivity were assessed. In separate sessions, aftereffects of iTBS applied over the left, primary motor cortex (M1) and the parieto-occipital vertex (sham) were tested for up to 25 min by measuring motor-evoked potentials (MEPs). High MEP increases post stimulation correlated with low movement-induced blood oxygenation level dependent (BOLD) activity in the stimulated M1. MEP changes also correlated positively with the effective connectivity between M1 and different premotor regions. However, no correlation could be found for rsFC. Therefore, our data suggest that changes in cortical plasticity induced by iTBS not only depend on local properties of the stimulated region, but also on activity-dependent properties of the cortical motor system.

Furthermore, different studies recently aimed at enhancing iTBS aftereffects by increasing the dose. However, no additive aftereffects could be observed. This may result from the incomplete understanding of the mechanisms underlying the dose-dependent induction of cortical plasticity in humans. The second study, therefore, aimed at investigating the dose-dependency of iTBS aftereffects by applying multiple stimulation blocks within a short time-interval. Possible mechanisms underlying cortical plasticity should be revealed by combining iTBS with connectivity analyses of the motor system. 16 healthy, right-handed subjects received three serially applied blocks of iTBS with an interstimulus-interval of 15 min. Each subject underwent M1- and sham-iTBS in two separate sessions. Aftereffects were tested on both MEP amplitudes as well as rsFC leading to a total of four sessions: M1-iTBS_MEPs, sham-iTBS_MEPs, M1_rs-fMRI, sham_rs-fMRI. For the first time, a dose-dependent buildup of aftereffects after the third block could be found both on the local level (MEPs) as well as on the systems level (rsFC). These increases in MEP amplitudes and rsFC were not linearly correlated, thus, possibly representing two parallel mechanisms underlying iTBS-induced plasticity. Of note, similar dose-dependent alterations of cortical protein expression of distinct subgroups of GABAergic inhibitory interneurons were observed following multiple iTBS blocks in an animal model. Hence, possibly suggesting a similar mechanism to be involved in iTBS aftereffects in humans.

Recently, a considerable number of studies addressing the variability of TBS aftereffects reported strong variations across subjects often resulting in no overall effects on the group level. The reasons for this variability remain poorly understood. Moreover, the question arises whether non-responders to iTBS can be turned into responders by increasing the dose. Therefore, in the third study, the data of the second study were re-analyzed with respect to the individual susceptibility to iTBS. Subjects were grouped into responders (n=7) and non-responders (n=9) according to their increase in MEP amplitudes after one iTBS block. When taking the individual responsiveness to iTBS into account a higher rsFC between M1 and premotor areas before stimulation could be found for non-responders compared to responders. Interestingly, non-responders to iTBS after one block could not be turned into responders by increasing the dose, i.e., applying a second or third block of iTBS. In contrast, responders after one block of iTBS featured a dose-dependent increase in MEP amplitudes as well as rsFC after all three iTBS blocks. Hence, our data suggest that responsiveness to iTBS at the local level (i.e., M1 excitability) is related to the capability of modulating network connectivity of the stimulated region (i.e., motor network). A ceiling effect at the systems level might underlie non-responsiveness to iTBS since higher levels of pre-interventional connectivity precluded a further increase upon iTBS.

Taken together, the findings of the present thesis add to the understanding of the mechanisms underlying iTBS aftereffects as well as the factors contributing to the high inter-individual variability. Furthermore, our data might help to improve the usefulness of iTBS in both basic research and as a therapeutic intervention.

Zusammenfassung

Die intermittierende Theta-Burst Stimulation (iTBS) ist eine neue Form der repetitiven transkraniellen Magnetstimulation (rTMS), mit welcher man die kortikale Erregbarkeit über die Stimulationsdauer hinaus erhöhen kann. Im Vergleich zu konventionellen rTMS-Protokollen induziert iTBS starke und langanhaltende Effekte mit dem Vorteil einer kürzeren Stimulationsdauer und geringerer Stimulationsintensitäten. Die den iTBS-induzierten Effekten zu Grunde liegenden Mechanismen sind jedoch noch nicht vollständig verstanden. Ziel der vorliegenden Arbeit war es daher mit Hilfe von nicht-invasiver Gehirnstimulation (d.h., iTBS) in Kombination mit funktioneller Bildgebung und Konnektivitätsanalysen des humanen Motokortexes neue Einblicke in diese Mechanismen zu gewinnen.

Vorherige Studien fanden bereits Hinweise, dass die Effekte der rTMS von der Aktivität und Konnektivität des stimulierten Areals abhängen. Unklar ist jedoch, welche Mechanismen der iTBS-induzierten Plastizität auf systemischer Ebene unterliegen. Ziel der ersten Studie dieser Arbeit war es daher zu untersuchen, inwiefern die neurale Aktivität und Konnektivität des motorischen Systems mit den iTBS-Effekten auf die kortikale Erregbarkeit zusammenhängen. 12 gesunde, rechtshändige Probanden wurden mittels funktioneller Magnetresonanztomographie (fMRT) in Ruhe (resting-state fMRT, rs-fMRT) und während der Ausübung einer motorischen Aufgabe gemessen. Mit Hilfe dieser Daten wurden die Aufgaben-abhängige Aktivierung, die Aufgaben-abhängige effektive Konnektivität und die funktionelle Ruhekonnektivität (rsFC) untersucht. iTBS wurde in separaten Sitzungen über dem primären motorischen Kortex (M1) und dem parieto-occipitalen Vertex (sham) appliziert und die Effekte für bis zu 25 Minuten nach Stimulation durch Ableitung von motorisch-evozierten Potentialen (MEPs) untersucht. Ein hoher Anstieg der MEPs nach iTBS korrelierte mit einer niedrigen bewegungs-induzierten BOLD- (blood oxygenation level dependent) Aktivität im stimulierten M1. Veränderungen der MEP-Amplituden korrelierten außerdem positiv mit der effektiven Konnektivität zwischen M1 und verschiedenen prämotorischen Regionen. Eine Korrelation mit rsFC konnte nicht gefunden werden. Unsere Daten deuten also darauf hin, dass Änderungen in der iTBS-induzierten kortikalen Plastizität nicht nur auf lokalen Eigenschaften der stimulierten Region (M1-Erregbarkeit), sondern auch auf aktivitäts-abhängigen Eigenschaften des kortikalen motorischen Systems beruhen.

Weiterhin haben verschiedene Studien versucht die Effekte der iTBS durch eine Erhöhung der Dosis zu verstärken. Hierbei konnten jedoch keine additiven Effekte gezeigt werden. Ein Grund dafür könnte das unvollständige Verständnis der Mechanismen sein, die der dosisabhängigen Induktion kortikaler Plastizität beim Menschen unterliegen. Ziel der zweiten Studie war es daher, die Dosisabhängigkeit von iTBS-Effekten durch Applikation mehrerer Stimulationsblöcke innerhalb eines kurzen Zeitintervalls zu erforschen. Mögliche Mechanismen, die der kortikalen Plastizität zu Grunde liegen, sollten hierbei durch die Kombination mit Konnektivitätsanalysen des motorischen Systems untersucht werden. 16 gesunde, rechtshändige Probanden erhielten dafür seriell-applizierte iTBS-Blöcke mit einem Interstimulus-Intervall von jeweils 15 Minuten. Jeder Proband erhielt sowohl M1- als auch sham-iTBS in verschiedenen Sitzungen. Außerdem wurden sowohl iTBS-Effekte auf MEP-Amplituden als auch auf rsFC untersucht, so dass jeder Proband insgesamt an vier Sitzungen teilnahm: M1-iTBS_MEPs, sham-iTBS_MEPs, M1-iTBS_rs-fMRT, sham-iTBS_rs-fMRT. Es konnte zum ersten Mal gezeigt werden, dass die Applikation

von mehreren iTBS-Blöcken zu einem dosis-abhängigen Anstieg sowohl auf dem lokalen Level (MEPs) als auch auf dem systemischen Level (rsFC) nach dem dritten Block führt. Obwohl die Zunahme in den MEPs nicht mit der Zunahme in der rsFC korrelierte, scheinen sie parallele Mechanismen iTBS-induzierter Plastizität darzustellen. Eine Tierstudie konnte ähnliche dosis-abhängige Änderungen nach mehreren iTBS-Blöcken auf die Proteinexpression unterschiedlicher Subgruppen GABAerger inhibitorischer Interneurone zeigen. Diese könnten daher einen möglichen Mechanismus darstellen, der iTBS-induzierten Plastizitätsprozessen auch beim Menschen unterliegt.

Darüber hinaus haben verschiedene Studien berichtet, dass die iTBS-Effekte zwischen den Probanden hoch variabel sind und die Stimulation oft keinen Effekt über die gesamte Gruppe hat. Die Gründe für diese Variabilität sind jedoch noch unklar. Außerdem stellt sich die Frage, ob „Non-Responder“ nach iTBS durch eine Erhöhung der Stimulationsdosis zu „Respondern“ gemacht werden können. In der dritten Studie wurden daher die Daten der zweiten Studie unter Berücksichtigung der individuellen Suszeptibilität für iTBS neu analysiert. Die Probanden wurden anhand ihres Anstiegs in MEP-Amplituden nach dem ersten iTBS-Block in Responder (n=7) und Non – Responder (n=9) unterteilt. Unter Berücksichtigung der individuellen Ansprechempfindlichkeit konnte eine höhere rsFC zwischen M1 und prämotorischen Arealen vor Stimulation bei Non-Respondern im Vergleich zu Respondern gefunden werden. Interessanterweise wurden Non-Responder durch eine Erhöhung der Stimulationsdosis, d.h. Applikation eines zweiten oder dritten Blocks, nicht zu Respondern. Nur Responder nach einem iTBS-Block zeigten einen dosis-abhängigen Anstieg in MEP-Amplituden und der rsFC nach allen drei iTBS-Blöcken. Unsere Daten suggerieren daher, dass die iTBS-Ansprechempfindlichkeit auf dem lokalen Level (M1-Erregbarkeit) mit der Fähigkeit die Konnektivität der stimulierten Region zu modulieren im Zusammenhang steht. Die negative Ansprechempfindlichkeit scheint also einem Deckeneffekt auf systemischer Ebene zu unterliegen, da eine hohe prä-interventionelle Konnektivität einen weiteren Anstieg durch iTBS verhindert hat.

Zusammengefasst haben die Ergebnisse der vorliegenden Arbeit zum Verständnis der Mechanismen, die den iTBS-Effekten unterliegen, sowie den Faktoren, die zu der hohen inter-individuellen Variabilität zwischen den Probanden führen, beigetragen. Weiterhin könnten unsere Daten die Nutzbarkeit von iTBS sowohl in der Grundlagenforschung als auch in der therapeutischen Anwendung verbessern.

1. Introduction and aim of the thesis

1.1 The human motor system

The human motor system is composed of several cortical and subcortical areas, which are distinctly involved in the planning, execution and control of movements. At the cortical level, key regions of the motor system comprise the primary motor cortex (M1), which corresponds to Brodmann Area (BA) 4 (Brodmann, 1909), and the premotor cortex (PMC) or BA 6 (Figure 1). Both areas (BA 4, BA 6) are situated in the frontal lobe of the brain. BA 4 occupies the anterior wall of the central sulcus as well as a limited part of the exposed surface of the precentral gyrus (Geyer et al., 2000; Rademacher et al., 2001). BA 6 is located anterior to M1.

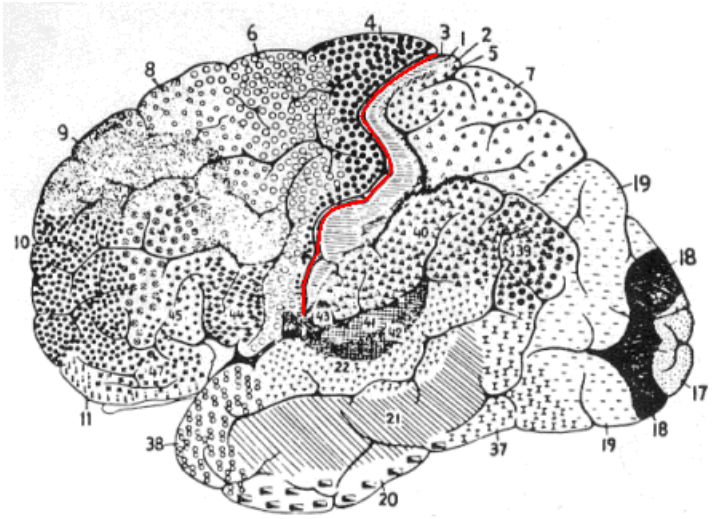

(Brodmann, 1909)

Figure 1: The human motor cortex. In 1909, Korbinian Brodmann divided the human cortex into 47 areas according to differences in cytoarchitecture. BA 4: primary motor cortex, BA 6: premotor cortex, BA 3, 1, 2: primary somatosensory cortex, the central sulcus is colored in red.

Directly adjacent and posterior to BA 4, BA 3 (3a, 3b), 1 and 2 can be found on the postcentral gyrus as typical representatives of the granular, six-layered isocortex (Brodmann, 1909; Geyer et al., 2000; Grefkes et al., 2001). Because of intense axonal connections between the motor cortex (BA 4, 6) and the somatosensory cortex (BA 3, 1, 2), both regions form a functional entity, the sensorimotor cortex.

The cytoarchitectonic hallmark of the cortical motor areas is a missing layer IV ('agranular cortex') and the presence of Betz giant cells in layer V, especially in M1 (BA 4) (Brodmann, 1909; Geyer et al., 2000). The Betz giant cells are the primary origin of efferent motor fibers forming the corticospinal tract. The nerve fibers pass down to the internal capsule and cross below the medulla oblongata on the contralateral site. Most of the axons (about 90%) descend the lateral corticospinal tract and innervate the α-motoneurons in the anterior horn of the spinal cord either directly or indirectly via interneurons (Amunts and Zilles, 2007). Finally, the motoneurons innervate the skeletal muscles contralateral to M1 via peripheral nerves. Thereby, the pyramidal tract controls mainly the voluntary movements of distal muscles. About 10% of the axons do not cross over at the medulla oblongata and form the ventral corticospinal tract. They cross to the contralateral site at the level of the spinal cord, before they innervate the motoneurons. The ventral corticospinal tract mainly controls posture, balance and gross truncal movements (Amunts and Zilles, 2007).

Based on cytoarchitectonical and histochemical studies in macaque monkeys a more complex parcellation of the motor cortex has been suggested than that initially described by Korbinian Brodmann in 1909. It could be shown that the motor cortex is not homogenous, but consists of seven distinct subregions (F1-F7, Figure 2) (Matelli et al., 1985, 1991; Rizzolatti and Fadiga, 1998). A similar parcellation in humans could be inferred from functional imaging studies (Picard and Strick, 1996; Fink et al., 1997). Area F1 corresponds to M1 (BA 4), whereas areas F2 - F7 mainly lie in the PMC (BA 6). Respectively, the PMC can be subdivided into (i) the supplementary motor area (SMA, F3) and the pre-SMA (F6), (ii) the dorsal premotor cortex (dPMC, F2) and the pre-dPMC (F7) as well as (iii) the caudal part of the ventral premotor cortex (vPMC, F4) and the rostral portion of the vPMC (F5). Similar to M1, all premotor areas project to the spinal cord as identified via retrograde tracer studies in macaques (Dum and Strick, 1991; He et al., 1993, 1995). Moreover, all non-primary motor areas (expect of pre-SMA and pre-dPMC) project to M1 (Dum and Strick, 2002, 2005).

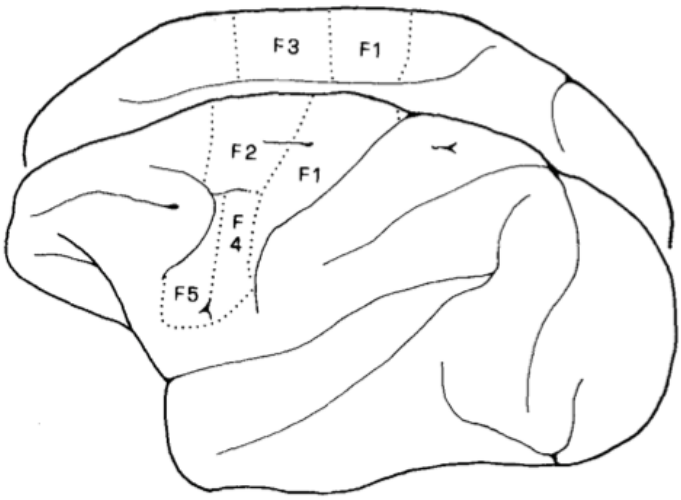

(Matelli et al., 1991)

Figure 2: Parcellation of the agranular frontal cortex in macaque monkeys, according to a histochemical study of Matelli and colleagues in 1985. Area F1 corresponds to BA 4 (M1) in the human motor cortex. Area F2 and F7 (not shown) are located in the superior part of BA 6 (dPMC), whereas area F4 and F5 are located in the superior part of BA 6 (vPMC). Area F3 and F6 (not shown) correspond to the mesial part of BA 6 (SMA and pre-SMA).

Both, invasive studies in macaque monkeys and non-invasive functional neuroimaging studies in humans have investigated the functional properties of these areas. Accordingly, the SMA is important for movement sequencing and bimanual coordination (Roland et al., 1980; Gerloff et al., 1997), the dPMC is involved in response selection based on arbitrary cues and in the control of arm movements (Kurata and Wise, 1988; Picard and Strick, 2001; Chouinard et al., 2005) and the vPMC plays a role in grasping and discrimination of bodily actions (Murata et al., 1997; Rizzolatti and Fadiga, 1998; Grezes et al., 2003). Certain anatomical landmarks such as, e.g., the hand knob on the precentral gyrus marking the motor hand area (Yousry et al., 1997), may help in identifying human motor areas.

1.2 Cortical plasticity

The brain has the ability to adapt to the continuously changing environment by means of structural and functional modifications. As such, cortical plasticity is an intrinsic property of the brain underlying processes like neural repair, learning and memory.

Most importantly, plasticity occurs not only on the local level (e.g., stimulated region), but also at the network level (e.g., functionally distinct, but interconnected areas). Using transcranial magnetic stimulation (TMS) or functional magnetic resonance imaging (fMRI) it is possible to non-invasively study the mechanisms underlying local as well as network plasticity in the human brain (Pascual-Leone et al., 2011). For example, using fMRI it could be shown that improvements in motor performance following practice are associated with changes in the activation of M1 movement representations (Hlustik et al., 2004; Xiong et al., 2009). Likewise, the connectivity between regions engaged in motor performance dynamically changes due to experience in healthy subjects (Wu et al., 2008) or due to recovery processes in, e.g., stroke patients (Rehme et al., 2011). Using TMS, it was observed that motor representations of the hand area increased in healthy subjects while learning a skilled motor task with their hand (Pascual-Leone et al., 2005). Moreover, non-invasive brain stimulation techniques like TMS are capable of inducing cortical plasticity in humans.

1.3 Transcranial magnetic stimulation

TMS was first described in 1985 by Anthony Barker and colleagues as a non-invasive, pain-free tool to stimulate the human cortex. When TMS is applied over the motor cortex, it can produce a muscle twitch or interfere with the execution of movements. Today, TMS is used to modulate pathological networks via repetitive TMS (rTMS) or to probe physiological properties of neuronal tissue. Using stereotaxic frameless neuronavigation (Figure 3) a precise stimulation of the underlying neuronal tissue can be achieved. The TMS coil can be co-registered to the individual anatomy of a subject using a structural MR scan via facial and cranial landmarks or using individual/probabilistic fMRI data (Sparing et al., 2008).

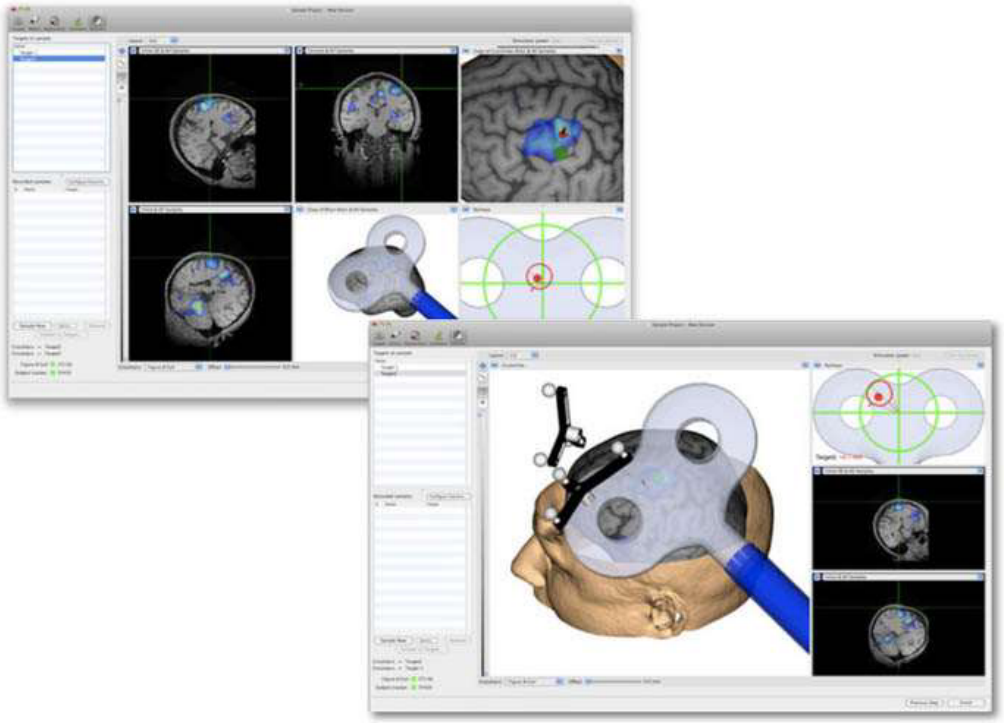

(BrainSight, Rogue Research Inc, https://www.rogue-research.com)

Figure 3: Stereotaxic frameless neuronavigation. A precise stimulation of neuronal tissue can be achieved by a co-registration of the subjects' head and an individual, structural MR scan via specified landmarks. The screenshot of the BrainSight software (Rogue Research Inc., Montreal, Canada) shows a 3D reconstruction of the subjects head based on an individual MR scan. Movements of the subjects' head and the TMS coil are tracked by an infrared camera system via markers mounted on the subjects' head and the coil. Stimulation points/ targets can be saved for a reliable stimulation within and between sessions.

1.3.1 Principles of transcranial magnetic stimulation

TMS is based on Faraday´s law of electromagnetic induction, saying that electric energy can induce a magnetic field and vice versa (Faraday, 1832). The TMS coil is positioned tangentially to the subjects head and a strong magnetic pulse of short duration (~ 2 Tesla, 50-100 µs), which is induced via the electric current, is applied (Figure 4). The magnetic field can pass the skull unhindered and induce an electric field in the underlying tissue. This may lead to the depolarization of pyramidal cells with monosynaptic, excitatory connections to the spinal cord motoneurons, thereby causing a peripheral muscle contraction, which is recordable in the form of a motor-evoked

potential (MEP) observed in the electromyography (EMG) of the contralateral target muscle. As the axons of the pyramidal cells are activated by differences in potentials along their length, the direction of the induced current is important, e.g., posterior-anterior direction perpendicular to the line of the sulcus for the hand area.

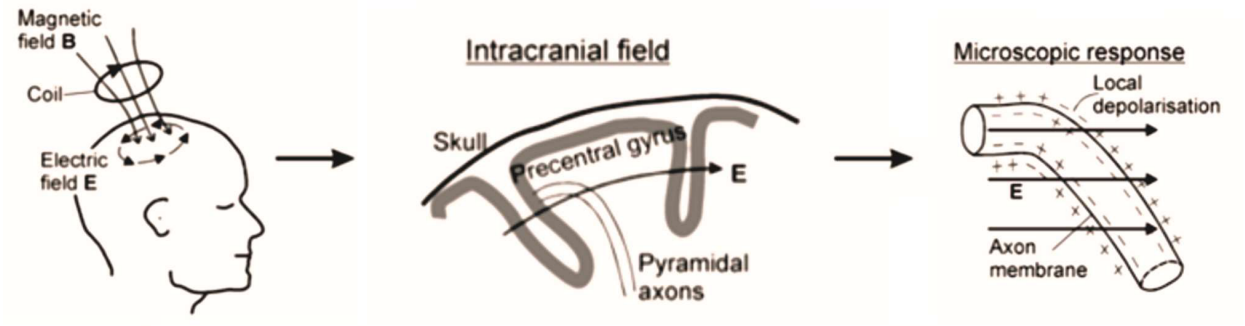

(adapted by Ilmoniemi et al., 1999)

Figure 4: Principles of TMS. The electric current in the coil induces a magnetic field B, which induces an electric field E in the brain. The intracranial field E runs in posterior-anterior direction parallel to the surface of the precentral gyrus when stimulating the motor cortex. At the microscopic level, the electric field E causes local depolarization of the axon membrane and thereby firing of the neurons.

Invasive recordings from the pyramidal tract in cats and non-human primates showed that a single electrical stimulus results in a series of high-frequent descending waves (Adrian and Moruzzi, 1939; Patton and Amassian, 1954; Amassian et al., 1987). The first wave derives from the direct excitation of the axons of fast-conducting pyramidal tract neurons, and is therefore termed “D-wave”. The later waves (1-1.5 ms) originate from indirect, trans-synaptic activations of pyramidal tract neurons and are therefore termed “I-waves” (Patton and Amassian, 1954). These findings have been replicated in conscious humans using an electrode implanted in the cervical epidural space for pain therapy (Di Lazzaro et al., 2005). There is evidence that low intensity TMS inducing posterior-anterior (PA) currents evokes I-waves with a latency about 1 ms longer than the D-wave (I1-wave) (Day et al., 1989; Di Lazzaro et al., 1998a; Di Lazzaro et al., 1998b). When increasing stimulus intensity or applying anterior-posterior (AP) TMS, later I-waves appear (Di Lazzaro et al., 1998a; Di Lazzaro et al., 1998b; Di Lazzaro et al., 2012). A further increase in intensities leads to the recruitment

of D-waves, which can most easily be evoked by TMS with a latero-medial (LM) induced current. Therefore, it is thought that TMS excites the pyramidal cells either directly at the axon membrane or indirectly via transsynaptic input from interneurons (Di Lazzaro et al., 1998a).

1.3.2 Repetitive transcranial magnetic stimulation

In recent years, several rTMS protocols have been introduced which are capable of enhancing or suppressing cortical excitability beyond the stimulation period. These changes probably represent lasting changes in synaptic transmission, i.e., the induction of neural plasticity. It is widely assumed that changes in cortical excitability derive from the induction of long-term potentiation (LTP)- or long-term depression (LTD)-like mechanisms as observed in in-vitro experiments after electrical stimulation of hippocampal rat tissue (Malenka and Bear, 2004). Whether facilitatory or inhibitory effects are induced depends on the frequency applied: rTMS at low frequencies (≤ 1 Hz) causes a decrease of MEP amplitudes, whereas rTMS at high frequencies (≥ 5 Hz) increases MEP amplitudes, reflecting long-lasting changes in cortical excitability (Ridding and Rothwell, 2007; Di Lazzaro et al., 2011). For example, 1 Hz rTMS applied over the motor cortex for about 25 min (1,500 stimuli in total) reduced MEP amplitudes for about 30 min (Touge et al., 2001), whereas 1,800 pulses of 5 Hz rTMS led to an increase in MEP amplitudes for up to 30 min (Peinemann et al., 2004). Hence, changes in MEP amplitudes following rTMS provide a measure of local cortical plasticity.

In 2005, Ying-Zu Huang and colleagues introduced a specific rTMS protocol known as theta-burst stimulation (TBS). It has been described to induce strong and long lasting effects for at least 15-60 min with the advantage of lower stimulation intensities and shorter time of stimulation compared to conventional rTMS protocols. TBS was developed on the basis of animal studies, which could show that electrical stimulation applied in bursts of 3-5 pulses at 50-100 Hz induce LTP or LTD when repeated at 5 Hz (theta rhythm) (Larson and Lynch, 1986; Hess and Donoghue, 1996). Thereby, TBS resembles the naturally occurring firing pattern of neurons in the hippocampus or the motor cortex. Huang and colleagues (2005) were the first to apply a TBS protocol consisting of bursts of three pulses given at 50 Hz repeated at 5 Hz (600 pulses in total) using TMS in humans (Figure 5). When applied intermittently at an inter-stimulus

interval of 8 s TBS (intermittent TBS, iTBS) leads to LTP-like effects, whereas a continuous application of 40 s (continuous TBS, cTBS) leads to LTD-like effects (Huang et al., 2005). iTBS aftereffects manifest in an increase of MEP amplitudes of about 15 minutes (duration of stimulation: 191.84 s), whereas cTBS induces a decrease in MEP amplitudes for up to 60 minutes (duration of stimulation: 40.04 s). It has been proposed that cTBS preferentially reduces I1-waves, whereas iTBS and other rTMS protocols modulate late I-waves (Hamada et al., 2013). In contrast, D-waves are not modified by changes in cortical excitability.

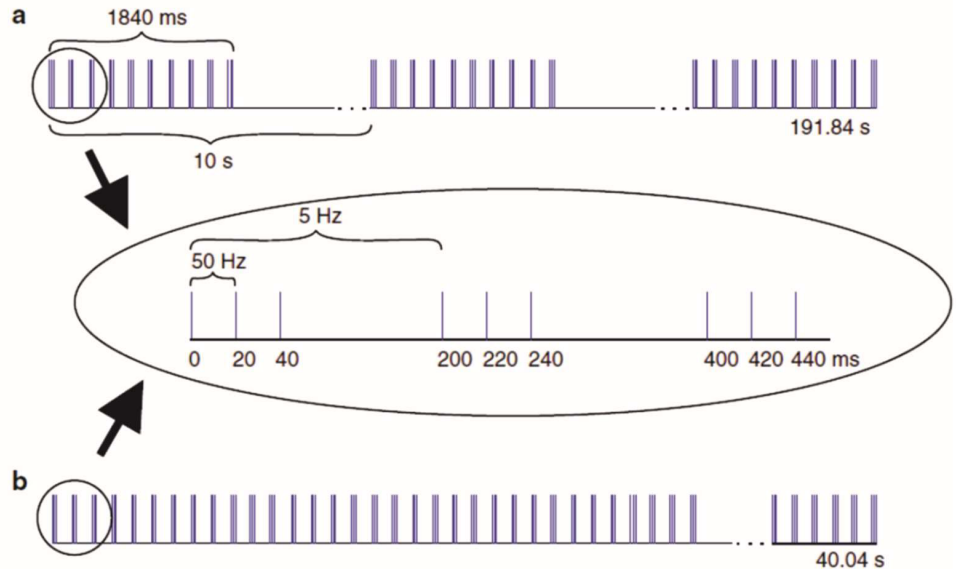

(Cárdenas-Morales et al., 2010)

Figure 5: Theta-burst stimulation (TBS). The basic elements of TBS are bursts of three pulses given at 50 Hz (inter-stimulus interval of 20 ms). Bursts are repeated at 5 Hz (inter-stimulus interval of 200 ms). **A** Intermittent TBS (iTBS). When TBS is applied for 2 s followed by a break of 8 s for 191.84 s in total it induces facilitation. **B** Continuous TBS (cTBS). 40.04 s of uninterrupted TBS induce inhibition. Usually, both iTBS and cTBS consist of 600 pulses.

1.3.3 Neurophysiological basis of rTMS/TBS effects

To date, the neurophysiological mechanisms underlying rTMS/TBS effects are still incompletely understood. As outlined above, changes in cortical excitability induced by rTMS/TBS may be due to changes at the level of synaptic transmission similar to LTP

and LTD as described in animals. However, direct evidence for this hypothesis is hard to obtain in human studies.

Animal studies recently demonstrated that rTMS changes the expression of the immediate early gene products c-Fos and zif268, which are markers of cellular activation (Aydin-Abidin et al., 2008; Funke and Benali, 2010). They also suggested that rTMS/TBS interferes with the cellular expression of various neuronal proteins reflecting the activity level of the γ-aminobutric acid (GABA)-ergic inhibitory system, like the GABA-synthesizing enzymes glutamate decarboxylase (GAD)65 and GAD67 as well as the calcium-binding proteins Parvalbumin, Calbindin and Calretinin (Trippe et al., 2009; Benali et al., 2011; Funke and Benali, 2011). Pharmacological studies in humans provided evidence that TBS aftereffects, at least partly, depend on the activity of glutamatergic N-Methyl-D-Aspartate (NMDA) receptors since LTP- and LTD-like effects can be blocked by administration of the NMDA receptor antagonist memantine (Huang et al., 2007). The NMDA receptor plays an important role in synaptic plasticity as they allow Ca^{2+} influx, which is critical for long-term plasticity changes (MacDermott et al., 1986). Therefore, it seems likely that rTMS induces LTD- or LTP-like processes.

Using fMRI, it could be shown that rTMS has not only an impact on the neuronal properties of the stimulated region but may also impact on the activity levels of remote but interconnected areas (Bestmann et al., 2003, 2004, 2005). A number of fMRI studies using different rTMS protocols proved that rTMS influences not only activity levels but also connectivity of the stimulated network (Grefkes et al., 2010; Vercammen et al., 2010; Eldaief et al., 2011; van der Werf et al., 2011), thereby suggesting another possible mechanism underlying rTMS effects at the systems level.

1.3.4 Inter-individual variability in the response to rTMS/TBS

A number of studies have recently reported a considerable amount of variability in the neurophysiological and behavioral response to TBS and other rTMS protocols with one third to one half of the subjects not responding in the “canonical manner”, i.e., being non-responders (Martin et al., 2006; Hamada et al., 2013; López-Alonso et al., 2014). Non-responders show either no or even the opposite response than expected. Since an increasing number of studies reported a considerable amount of non-responders among their subjects, understanding the mechanisms underlying inter-subject

variability to TBS and other rTMS protocols appears mandatory (Vallence et al., 2013). Variability is supposed to depend on biological factors like age (Freitas et al., 2011), sex (Inghilleri et al., 2004) and genetic polymorphism of the brain derived neurotrophic factor (Kleim et al., 2006; Cheeran et al., 2008). Likewise, technical aspects such as the direction of current flow and the intensity of stimulation contribute to variability of rTMS responsiveness (Talelli et al., 2007). Furthermore, attention (Conte et al., 2007; Conte et al., 2008) and previous history of activation (Gentner et al., 2008; Iezzi et al., 2008) have been proposed as possible factors contributing to the variability of responses. Recently, Hamada and colleagues (2013) suggested that the activation of particular classes of interneurons, which may be indicated by the recruitment of late I-waves, accounts for about 50% of the variance in responses to TBS. They reported that the individual susceptibility to TBS is strongly related to the latency of MEPs evoked with anterior-posterior (AP) directed current relative to latero-medial (LM) current, which in turn is indicative for the efficiency of I-wave recruitment. Subjects with a high MEP-latency showed the “expected” response to TBS (responders, efficient I-wave recruitment), whereas subjects with a short MEP-latency exhibited the “opposite” effect (non-responders, non-efficient I-wave recruitment). Using fMRI, a recent study of our group could show that MEP-latencies are also strongly correlated with the functional connectivity between premotor areas and M1, giving indirect evidence that the connectivity within the motor system might underlie responsiveness to TBS (Volz et al., 2014). Whether or not motor network connectivity and susceptibility to TBS are directly related to each other needs to be investigated.

Another factor that can influence the induction of aftereffects induced by TBS are the number of pulses applied (Gentner et al., 2008; Gamboa et al., 2010; Gamboa et al., 2011). Different human studies already investigated the effect of multiple stimulation blocks on cortical excitability. Using different inter-stimulus intervals between two blocks of iTBS (1,200 pulses in total) of 0, 2, 5 and 20 min Gamboa and colleagues (2010, 2011) could not observe a further increase in cortical excitability over the whole group of subjects. Aftereffects were rather similar compared to a single block or even a suppression of aftereffects could be observed. In contrast, a recent animal study could show that multiple stimulation blocks separated by 15 min led to dose-dependent changes in the expression of various proteins reflecting the activity level of the GABAergic inhibitory system already after three blocks of iTBS, i.e., 1,800 pulses (Volz

et al., 2013). This raises the question whether similar aftereffects can be observed in humans when applying three iTBS blocks with an inter-stimulus interval of 15 min and whether multiple stimulation blocks can change the individual responsiveness to TBS.

1.4 Functional magnetic resonance imaging

fMRI is a non-invasive tool for measuring hemodynamic changes associated with enhanced neural activity, and became the mainstay of neuroimaging in neuroscience since its introduction in the early 1990s (Ogawa et al., 1990). fMRI can be used as a complementary method to study the effects of TMS on brain networks involved in specific functions.

1.4.1 Physical principles of MRI

MRI has been independently developed by different authors in 1973 (Lauterbur, 1973; Mansfield and Grannell, 1973). It is based on the absorption and emission of radio waves by tissue placed in magnetic fields. Hydrogen atoms in the brain, which are most commonly measured by means of MRI, possess electrical properties as well as the quantum mechanical property that they spin around their axis ("spin"). When hydrogen nuclei (protons) are placed in the magnetic field of an MR-scanner, they align with the magnetic field due to their magnetic dipole moment (MDM). Since spins have a weak preference to realign parallel instead of antiparallel with the magnetic field, a longitudinal magnetization (M_z) can be measured. In the next step, a brief, high frequent 90° radio frequency (RF) pulse is applied, which causes a tilt of the MDM´s of the hydrogen nuclei into the x-y plane (transversal magnetization, M_{xy}). As soon as the RF-pulse is terminated, the MDM´s return to their original lower energy state thereby releasing energy known as relaxation. This signal is detected by the receiving coils of the MRI scanner. Depending on the relaxation time a longitudinal relaxation T1 (0.5 - 5 s) and a transverse relaxation T2 or T2* (300 - 500 ms) can be separated. The longitudinal T1 relaxation is the time needed for transformation from M_{xy} back to M_z, whereas the transverse T2 relaxation describes the decay of the MDM´s in the x-y plane due to dephasing (spins start to rotate with different velocities). T1-weighted images are proper for high-resolution anatomical images, because the contrast between grey and white matter is high. In contrast, T2-weighted images are most

suitable for pathological scans as lesions appear very bright. T2* are used for fMRI, because of their sensitivity to local field inhomogeneities (Stöcker and Shah, 2006).

1.4.2 Physiological basis of fMRI

The most common indirect measure of neural activity relies on the blood oxygenation level dependent (BOLD) effect. Seiji Ogawa and colleagues first described the BOLD effect in 1990. It is based on hemodynamic changes in the deoxyhemoglobin concentration in the blood, and also depends on the cerebral blood flow (CBF) and blood volume (BV). Deoxyhemoglobin is paramagnetic (has a positive magnetic susceptibility) as the central ion atom is not shielded by any oxygen atoms and therefore causes an inhomogeneity in the magnetic field. In contrast, when an oxygen molecule is attached to hemoglobin (oxyhemoglobin) during transportation it is diamagnetic (has a negative magnetic susceptibility) and therefore has no effect on the magnetic field. Hence, increased levels of deoxyhemoglobin relative to oxyhemoglobin may cause field inhomogneities, which result in a decrease of the fMRI signal (Ogawa et al., 1990).

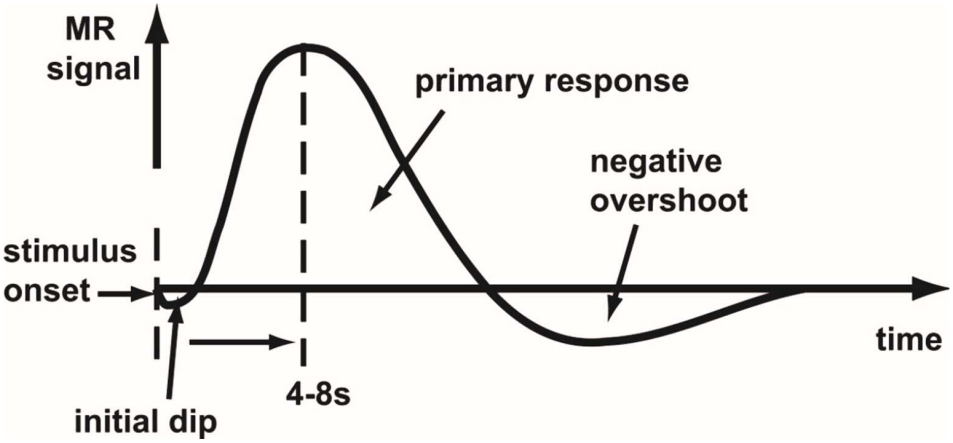

(Kornak et al., 2011)

Figure 6: Hemodynamic response function (HRF). The initial dip in the BOLD signal after stimulus onset (first dashed line) is followed by a large over-compensation in oxygenated blood delivery (max. 4-8 s after stimulus onset, second dashed line). The BOLD signal slowly decays followed by a negative undershoot before returning to baseline.

A mathematical model to describe the time course of the BOLD signal is the hemodynamic response function (HRF, Figure 6), which consists of three stages: the fMRI signal initially decreases due to the use of oxygen by the firing neurons (increased level of deoxyhemoglobin). Following this initial decrease, an oversupply of oxygenated blood due to a local enhancement of CBF and BV leads to an increase in the BOLD signal (Buxton et al., 1998). Finally, the deoxyhemoglobin level returns to normal and the BOLD signal decays with an undershoot (slightly below baseline levels) before reaching its original baseline (Heeger and Ress, 2002).

Although BOLD-fMRI is widely used, the relationship between the measured fMRI signal and the underlying neural activity is still poorly understood. By simultaneous intracortical recording of the neural signal and fMRI responses of the visual cortex in monkeys, Logothetis and colleagues (2001) could show that hemodynamic responses are better correlated with local field potentials (LFP) than with multi-unit responses. Therefore, the BOLD signal seems to reflect primarily the input and processing of neuronal information rather than its spiking output (Logothetis, 2002).

1.4.3 Task-based fMRI – effective connectivity

In task-based fMRI the BOLD signal during an active task (e.g., visually-triggered hand movements) is contrasted by a control-condition or baseline (Ogawa et al., 1990). Before statistical analysis, fMRI data need to be preprocessed in order to optimize sensitivity. As a first step, fMRI data are spatially realigned to a reference volume in order to correct for head motion induced shifts. Then the realigned fMRI data are co-registered with a structural image (usually T1-weighted). After the co-registration, fMRI data are spatially normalized to a standard template resulting in images with a common reference space (e.g., Montreal Neurological Institute [MNI] space). This procedure allows statistical group comparisons. In the last step of the preprocessing the images are spatially smoothed with a Gaussian kernel to increase the signal-to-noise ratio and to increase the power of statistical analysis (Smith, 2001). Next, a general linear model (GLM) is used for the statistical analysis (Kiebel and Holmes, 2007). Here, the experimental conditions are modeled using boxcar stimulus functions convolved with the HRF including covariates (e.g., head motion parameters to account for movement-

related variance). The estimated parameters are tested by F- or T-contrasts, resulting in a statistical map of activated voxels surviving a pre-defined statistical threshold.

Importantly, fMRI data cannot only be used to localize neural activity (BOLD signal), but to compute how activity in one region is related to the activity in another region. This is referred to as functional connectivity, i.e., the temporal correlations between spatially distinct neurophysiological events (Friston et al., 1993). However, functional connectivity provides no information about the directionality or causality of connectivity between two regions. Here, models of effective connectivity can be applied. Effective connectivity refers to the influence that one neural unit exerts over another (Friston et al., 2003). A frequently used method to estimate effective connectivity from neuroimaging data is dynamic causal modeling (DCM) where the brain is treated as an input-state-output system with one output per region (Friston et al., 2003; Stephan et al., 2010). In contrast to other approaches such as structural equation modeling (McIntosh and Gonzalez-Lima, 1994; Büchel and Friston, 1997) or multivariate autoregressive models (Goebel et al., 2003; Harrison et al., 2003), in DCM the input is treated as known, as opposed to unknown or stochastic (Friston et al., 2003). In DCM effective connectivity is estimated in a Bayesian fashion within a pre-defined network of anatomically and functionally plausible regions. DCM treats the nonlinear neural system as a bilinear model using the following bilinear differential equation:

$$\frac{dz}{dt} = Az + \sum_j u_j B^j z + Cu$$

$\frac{dz}{dt}$ denotes the change in neuronal activity z over time t, u is the experimental input and j refers to the j^{th} input (Friston et al., 2003; Stephan et al., 2007). Matrix A represents the fixed connectivity among the regions in the absence of an input. The matrices B^j encode the change in connectivity induced by the j^{th} input u_j, i.e., the external input modulating the coupling among regions (e.g., during learning or attention). Matrix C expresses the strength of direct influences of inputs on neuronal activity, i.e., the external inputs eliciting responses through direct influences on a specific region (e.g., sensory stimuli) (Stephan et al., 2007). A, B and C are matrices of unknown neural coupling parameters θ^n.

For fMRI data, the bilinear model is combined with an empirically validated hemodynamic forward model that translates neural activity into a measured signal

(BOLD response). The so-called “Balloon-Windkessel model” (Buxton et al., 1998; Friston et al., 2000) consists of five hemodynamic parameters θ^h describing the relations between the following five hemodynamic state variables: (i) neuronal activity, (ii) vasodilatory and activity-dependent signal, (iii) normalized blood flow, (iv) normalized venous volume and (v) normalized deoxyhemoglobin content (Friston et al., 2003; Stephan et al., 2007). These variables are not influenced by the state of other regions.

The neural and hemodynamic parameters are estimated from the measured BOLD data using a Bayesian approach so that the predicted BOLD response fits best to the observed BOLD response. Therefore, expectation maximization and a Laplace approximation are used (Friston, 2002). Afterwards, the model with the best model fit given the data can be determined out of many models using Bayesian model selection (Penny et al., 2004). The “winner model” is the model that can explain the measured data most precisely using the smallest number of parameters.

1.4.4 Resting-state fMRI - functional connectivity

A recently popular approach in neuroimaging is “resting-state” fMRI. In contrast to task-based fMRI, resting-state fMRI measures the spontaneous fluctuations in the BOLD signal, i.e., the “baseline” activity of the brain in the absence of a task (Biswal et al., 1995; Damoiseaux and Greicius, 2009; van den Heuvel and Hulshoff Pol, 2010). Subjects either lie with eyes closed in the scanner or have to fixate a crosshair, which is presented on a TFT screen visible through a mirror attached to the MR head coil. Additionally, subjects are instructed not to think about anything specific.

Resting-state fMRI data are often used to estimate functional connectivity, i.e., temporal correlations between spatially distinct neurophysiological events (Friston et al., 1993). One method to analyze functional connectivity (after preprocessing as described in 1.4.3) is a seed-to-seed network analysis where the time series information of different regions-of-interest (ROI) at defined coordinates are correlated by means of Pearson´s correlations. A more established approach is a ‘seed voxel – whole brain’ correlation. Here, the time-course of a seed region is correlated with the time-course of every other voxel in the brain, thus requiring less a-priori assumptions on putative target regions. The resulting resting-state map reflects the functional

connectivity of the seed-region (Damoiseaux and Greicius, 2009). Biswal and colleagues (1995) were the first to show that the resting-state BOLD time-series of the left and right M1 were highly correlated suggesting a functional connectivity even in the absence of an overt motor task. Interestingly, it could be shown that functional connectivity is positively correlated with anatomical connectivity as assessed via diffusion tensor imaging (DTI) (Koch et al., 2002). However, functional connectivity is not necessarily paralleled by anatomical connectivity since signal correlations between two regions could also be mediated by indirect anatomical connections (no direct connecting fibers present in DTI map). In contrast, functional connectivity is always high when anatomical connectivity is present (Koch et al., 2002). Until to date, different functionally linked resting-state networks have been identified like the primary sensorimotor network, the primary visual and extra-striate visual network and the so-called default mode network (Biswal et al., 1995; Beckmann et al., 2005; Salvador et al., 2005; Damoiseaux et al., 2006; De Luca et al., 2006).

1.5 Objectives

To date, TBS and other plasticity inducing protocols are widely used in both basic scientific research and for clinical applications. However, the mechanisms underlying excitability changes induced by TBS as well as the factors contributing to the high inter-individual variability observed in the response to TBS are still poorly understood. Therefore, the primary goal of the present thesis was to investigate the mechanisms underlying iTBS-induced cortical plasticity for the human motor system. Secondly, the studies of the present thesis aimed at understanding the factors associated with inter-individual variability in the response to iTBS. Moreover, the question was addressed whether iTBS aftereffects can be enhanced by increasing the stimulation dose.

Three studies were conducted to answer the following questions:

I. *Is there a relationship between iTBS-induced changes in M1 excitability and neural properties of the stimulated region? (study I)*
   Different studies suggested that the magnitude of rTMS aftereffects are associated with M1 activity and its connectivity with premotor areas (Ameli et al., 2009; Grefkes et al., 2010). Based on these findings we hypothesized that the individual susceptibility to iTBS will be related to M1 activity as well as M1

connectivity with premotor areas, thereby revealing a possible mechanism underlying iTBS aftereffect on the systems level.

II. *Are iTBS aftereffects dose-dependent at the local (cortical excitability) as well as at the systems level (functional connectivity)? (study II)*

Findings in rats suggested dose-dependent increases on the cellular level, suggesting accumulative effects following multiple blocks of iTBS (Volz et al., 2013). However, human studies thus far failed to demonstrate such additive aftereffects (Gamboa et al., 2010; Gamboa et al., 2011). We hypothesized that the application of three blocks of iTBS (same stimulation protocol as Volz and colleagues, 2013) leads to dose-dependent increases in cortical excitability, possibly revealing a further mechanism underlying iTBS aftereffects. Moreover, recent studies showed that rTMS is capable of modulating the connectivity of a given region within a network of brain areas (Grefkes et al., 2010; Vercammen et al., 2010; Eldaief et al., 2011; van der Werf et al., 2011; Watanabe et al., 2013). Therefore, our hypothesis was that iTBS induces changes after stimulation of M1 in the functional connectivity between M1 and distinct motor areas.

III. *Can responsiveness to iTBS be changed by increasing the dose or is responsiveness intrinsically determined? (study III)*

A growing number of studies reports that responsiveness to TBS is highly variable between subjects (Hamada et al., 2013; Hinder et al., 2014; López-Alonso et al., 2014). Hamada and colleagues (2013) suggested that responders and non-responders to TBS differ in their recruitment of interneuron networks, reflecting an intrinsic difference between subjects. Therefore, we hypothesized that iTBS will primarily modulate cortical excitability in responders after multiple blocks of iTBS.

IV. *Do responders and non-responders to iTBS (in terms of MEP increases) also differ in functional connectivity after stimulation? (study III)*

The recruitment of interneuron networks by TMS has been shown to be strongly related to the functional connectivity between M1 and the premotor cortex (Volz

et al., 2014), thereby implying a relationship between responsiveness to TBS and motor network connectivity. We, therefore, hypothesized that responders and non-responders to iTBS will differ in their functional connectivity before and after stimulation.

In study I (Cárdenas-Morales et al., 2014) resting-state functional connectivity, task-induced activation and task-related effective connectivity were assessed in 12 healthy, right-handed subjects. In the MR scanner, subjects underwent fMRI (i) under rest and (ii) while performing a simple hand motor task. On separate days, iTBS aftereffects on MEP amplitudes were tested for up to 25 min. Using a within-subject design each subject received a stimulation over the left M1 (M1-iTBS) and a control stimulation over the parieto-occipital vertex (sham-iTBS).

In study II (Nettekoven et al., 2014), dose-dependent effects on MEP-amplitudes and resting-state functional connectivity were tested after three serially applied blocks of iTBS. Blocks were separated by 15 min. Using a sham-controlled, within-subject design each subject (16, healthy, right-handed) participated in four sessions in total. At baseline and after each iTBS block resting-state fMRI (rs-fMRI) or MEP amplitudes were measured (i.e., rs-fMRI_M1-iTBS, rs-fMRI_sham-iTBS, MEPs_M1-iTBS, MEPs_sham-iTBS). Data were analyzed on a group level.

In study III (Nettekoven et al., under review), the data of study II were re-analyzed regarding the inter-individual variability between subjects. Responders and non-responders were classified according to their increase in MEP-amplitudes after the first block (>10%). This criterion resulted in a group of seven responders and nine non-responders. Differences between groups before stimulation as well as dose-dependent changes in resting-state functional connectivity and MEPs after iTBS within and between groups were investigated.

2. Publications

2.1 Network connectivity and individual responses to brain stimulation in the human motor system; Cárdenas-Morales L, Volz LJ, Michely J, Rehme AK, Pool EM, Nettekoven C, Eickhoff SB, Fink GR, Grefkes C.; Cerebral Cortex 2014 July; 24 (7): 1697-707

2.2 Dose-dependent effects of theta burst rTMS on cortical excitability and resting-state connectivity of the human motor system; Nettekoven C, Volz LJ, Kutscha M, Pool EM, Rehme AK, Eickhoff SB, Fink GR, Grefkes C.; Journal of Neuroscience 2014 May 14; 34 (20): 6849-59

2.3 Inter-individual variability in cortical excitability and motor network connectivity following multiple blocks of rTMS; Nettekoven C, Volz LJ, Kutscha M, Pool EM, Rehme AK, Eickhoff SB, Fink GR, Grefkes C.; under review

2.1 Network connectivity and individual responses to brain stimulation in the human motor system

Cárdenas-Morales L, Volz LJ, Michely J, Rehme AK, Pool EM, Nettekoven C, Eickhoff SB, Fink GR, Grefkes C.

Cerebral Cortex 2014 Jul; 24 (7):1697-707

Cerebral Cortex July 2014;24:1697–1707
doi:10.1093/cercor/bht023
Advance Access publication February 8, 2013

Network Connectivity and Individual Responses to Brain Stimulation in the Human Motor System

Lizbeth Cárdenas-Morales[1,2], Lukas J. Volz[1,2], Jochen Michely[1,2], Anne K. Rehme[1], Eva-Maria Pool[1], Charlotte Nettekoven[1], Simon B. Eickhoff[3,4], Gereon R. Fink[2,3] and Christian Grefkes[1,2]

[1]Neuromodulation and Neurorehabilitation, Max Planck Institute for Neurological Research, 50931 Cologne, Germany, [2]Department of Neurology, Cologne University Hospital, 50924 Cologne, Germany, [3]Institute of Neurosciences and Medicine (INM-1, INM-3), 52425 Juelich Research Centre, Juelich, Germany and [4]Institute for Clinical Neuroscience and Medical Psychology, Heinrich-Heine University, 40225 Düsseldorf, Germany

Address correspondence to Dr Christian Grefkes, Department of Neurology, Uniklinik Köln, Kerpener Straße 62, 50924 Köln, Germany. Email: christian.grefkes@uk-koeln.deL.C.-M. and L.J.V.contributed equally to the manuscript (shared first-authorship).

The mechanisms driving cortical plasticity in response to brain stimulation are still incompletely understood. We here explored whether neural activity and connectivity in the motor system relate to the magnitude of cortical plasticity induced by repetitive transcranial magnetic stimulation (rTMS). Twelve right-handed volunteers underwent functional magnetic resonance imaging during rest and while performing a simple hand motor task. Resting-state functional connectivity, task-induced activation, and task-related effective connectivity were assessed for a network of key motor areas. We then investigated the effects of intermittent theta-burst stimulation (iTBS) on motor-evoked potentials (MEP) for up to 25 min after stimulation over left primary motor cortex (M1) or parieto-occipital vertex (for control). ITBS-induced increases in MEP amplitudes correlated negatively with movement-related fMRI activity in left M1. Control iTBS had no effect on M1 excitability. Subjects with better response to M1-iTBS featured stronger preinterventional effective connectivity between left premotor areas and left M1. In contrast, resting-state connectivity did not predict iTBS aftereffects. Plasticity-related changes in M1 following brain stimulation seem to depend not only on local factors but also on interconnected brain regions. Predominantly activity-dependent properties of the cortical motor system are indicative of excitability changes following induction of cortical plasticity with rTMS.

Keywords: brain stimulation, neuromodulation, plasticity, repetitive TMS

Introduction

Fundamental processes of the brain like learning and acquisition of new motor skills depend on neuronal plasticity in a number of spatially distributed but interconnected brain regions. Methodological advances in neuroimaging and non-invasive brain stimulation—such as repetitive transcranial magnetic stimulation (rTMS)—have substantially furthered our knowledge on cortical plasticity and underlying mechanisms (for reviews, see, e.g., Censor and Cohen 2011; Dayan and Cohen 2011). Intermittent theta-burst stimulation (iTBS) is a specific type of rTMS that induces changes in cortical excitability beyond the stimulation period (Huang et al. 2005). When applied to the primary motor cortex (M1) iTBS increases the amplitudes of motor-evoked potentials (MEPs) subsequently induced by single-pulse TMS for up to 20 min (Huang et al. 2005; for a review, see Cárdenas-Morales et al. 2010).

It is widely assumed that long-term potentiation (LTP)- and long-term depression (LTD)-like processes induced by iTBS and other rTMS protocols (Huang et al. 2005, 2007), similar to what has been observed for in vitro stimulation of cortical synapses (Tsumoto 1992), may play an important role in the evolution of these stimulation aftereffects (Thickbroom 2007). There is, however, a considerable amount of interindividual variability in the response to iTBS (and also other rTMS protocols) which seems to depend on biological factors like age (Freitas et al. 2011) and genetic polymorphisms of the brain-derived neurotrophic factor (Kleim et al. 2006; Cheeran et al. 2008), but also on technical aspects such as the direction of current flow, the intensity of stimulation and the number of pulses applied (Talelli et al. 2007; Gentner et al. 2008; Gamboa et al. 2010). Recently, Hamada et al. (2012) showed that the activation of particular classes of interneurons by iTBS—as indicated by the recruitment of late indirect waves (I-waves)—accounts for parts of individual differences in stimulation aftereffects. Interestingly, these late I-waves were demonstrated to depend on influences exerted by premotor areas, and imply a crucial role of interneuron networks in human cortical plasticity (Shimazu et al. 2004; Lemon 2008). Therefore, the question arises whether remote areas might also influence the susceptibility to plasticity-inducing stimulation protocols like iTBS. Further support for this hypothesis derives from patient studies, linking decreased functional connectivity between premotor and primary motor cortex with higher susceptibility to rTMS in patients with dystonia (Quartarone et al. 2003; Koch et al. 2008; Huang et al. 2010). Moreover, rTMS does not only induce regional changes at the stimulation site (e.g., M1), but also in spatially remote parts of the brain (Bestmann et al. 2003, 2005; Esser et al. 2006; Suppa et al. 2008; Cárdenas-Morales et al. 2011). Consequently, it appears reasonable to assume that the physiological changes following an intervention also depend on how efficient the stimulated area (e.g., M1) is integrated into a given functional network, for example, the cortical motor system.

In the present study, we addressed the issue of the physiological mechanisms underlying motocortical plasticity from a system-level perspective using neuroimaging and models of connectivity (Friston 1994). We scanned a group of healthy subjects with functional magnetic resonance imaging (fMRI) during rest and while performing a simple hand motor task in order to test the hypothesis that the plasticity effects induced by iTBS on motocortical excitability are related to activity and connectivity of the motor system. Connectivity was tested prior to iTBS for a network consisting of key motor areas. Then, in 2 separate sessions, iTBS was either applied to the dominant (left) motor cortex or to a control stimulation site

over parieto-occipital cortex (Herwig et al. 2007; Herwig et al. 2010). MEPs were recorded for a period up to 25-min post-stimulation. We correlated changes in MEP amplitudes following iTBS of M1 (or control) to BOLD activity, functional resting-state, and dynamic causal modeling of effective connectivity within the cortical motor system. Previous studies using rTMS showed that the magnitude of intervention effects is related to M1 activity and its connectivity to premotor areas (Ameli et al. 2009; Grefkes et al. 2010; Wang et al. 2011). We, hence, hypothesized that individual patterns of neural activity in M1 and connectivity between M1 and other relevant motor areas indicate the susceptibility to a plasticity-enhancing stimulation protocol like iTBS applied over M1. Given the relationship between ventral premotor cortex (vPMC), late I-waves, and iTBS response (Shimazu et al. 2004; Lemon 2008; Hamada et al. 2012), we further reasoned that subjects showing strong connectivity of this area with M1 would show especially high magnitudes of changes in cortical excitability following stimulation with iTBS.

Materials and Methods

Subjects

Twelve healthy, right-handed volunteers (mean age: 39 ± 11 years; 5 females) were recruited. Exclusion criteria were a history of brain injury, neurologic, or psychiatric disease, the presence of any major medical illness, or an intake of any medication during the time of the study. All participants gave their written informed consent for the experiments, and were paid for participation. The project adhered to the Declaration of Helsinki and was approved by the Ethics Committee of the University of Cologne.

Experimental Design

The within-subject design comprised three different sessions performed on different days. In the first session, subjects underwent fMRI measurements during rest and during performance of a simple hand motor task. In the second and third sessions, either iTBS over the dominant (left) M1 or over parieto-occipital vertex (Pz, for control) was carried out in a randomized order with electrophysiological monitoring before and after intervention. The intersession interval was 2–3 days.

Functional MRI

All subjects first underwent resting-state fMRI followed by an fMRI while subjects performed an active motor task. MR images were acquired on a Siemens Trio 3.0 T scanner (Siemens Medical Solutions, Erlangen, Germany). Both paradigms were measured using a gradient echo-planar imaging (EPI) sequence with the following parameters: TR = 2200 ms, TE = 30 ms, FOV = 200 mm, 33 slices, voxel size: $3.1 \times 3.1 \times 3.1$ mm^3, 20% distance factor, flip angle = 90°, resting-state fMRI: 184 volumes, motor task fMRI: 283 volumes. The slices covered the whole brain extending from the vertex to lower parts of the cerebellum. In addition, high-resolution T_1-weighted structural images were acquired (TR = 2250 ms, TE = 3.93 ms, FOV = 256 mm, 176 sagittal slices, voxel size = $1.0 \times 1.0 \times 1.0$ mm^3).

For the resting-state paradigm, subjects were instructed to remain motionless and to fixate a red cross on a black screen during scanning. The fixation cross was presented on a shielded TFT screen at the rear end of the scanner, which was visible via a mirror mounted to the MR head coil. The resting-state session lasted about 7 min, as it has been shown that longer scanning times provide no significant improvement of signal-to-noise but promote fatigue of the subjects (Van Dijk et al. 2010). Preventing fatigue was also the reason for scanning the subjects with open eyes. The subjects were monitored by means of an MR compatible infrared camera attached to the end of the scanner.

The fMRI motor task consisted of visually cued hand movements with thumb abductions. Written instructions were displayed on the screen for 1 s indicating whether the left or the right hand had to be moved in the upcoming block of trials. Subjects were instructed to perform the movements for 14 s with maximum amplitude at a frequency of 1 Hz as indicated by a blinking circle until a black screen indicated to rest for the following 15 s. Subjects were trained outside and inside the scanner until they reached stable performance. Overall, the motor task used in the present study had only a few degrees of freedom, with a predefined movement amplitude and low movement frequency, so that subjects were readily able to perform the task with high stability after a few (2–3) practice trials. Note that the motor task activated the same muscles as used for TMS recordings (the left hand movements were necessary for localizing the motor areas of interest in the right hemisphere, which were also part of the connectivity model as described further below).

fMRI Preprocessing

FMRI data were analyzed using Statistical Parametric Mapping (SPM8; Wellcome Department of Imaging Neuroscience, London, UK, http://www.fil.ion.ucl.ac.uk). The first 4 volumes of each session ("dummy" images) were discarded from further analysis. The resting-state and the motor task EPI volumes were then realigned to the mean image of each time series and coregistered with the structural T_1-weighted image. For the group analyses, all images were spatially normalized to the standard template of the Montreal Neurological Institute (MNI, Canada) using the unified segmentation approach (Ashburner and Friston 2005). Finally, data were smoothed using an isotropic Gaussian kernel of 8-mm full-width at half-maximum.

For the resting-state data, variance that could be explained by known confounds was removed from the smoothed image time series. Confound regressors included the tissue-class-specific global signal intensities and their squared values, the 6 head motion parameters from realignment, their squared values as well as their first-order derivatives (Jakobs et al. 2012; Reetz et al. 2012). Data were band-pass filtered between 0.01 and 0.08 Hz.

Statistical Analysis: fMRI Motor Task Data

For the hand motor task, statistical analysis was performed in the framework of the general linear model (GLM). The experimental conditions were modeled using boxcar stimulus functions convolved with a canonical hemodynamic response function. The time series in each voxel were high-pass filtered at 1/128 Hz. The 6-head motion parameters, as assessed by the realignment algorithm, were treated as covariates to remove movement-related variance from the image time series. Simple main effects for each experimental condition were calculated for every subject by applying appropriate baseline contrasts. Voxels were identified as significant on the single-subject level if their t-values passed a height threshold of $T > 4.7$, corresponding to $P < 0.05$ (family-wise error [FWE] corrected for multiple comparisons at voxel level).

For fMRI group analyses, the parameter estimates of the experimental conditions were compared between subjects ($n = 12$) in a second-level GLM with the factor hand (levels "right" and "left"). For correlation analyses between movement-related BOLD activity and iTBS aftereffects (see below), the contrast images "right-hand movements versus rest" were entered into an SPM multiple regression analysis with the individual strength of the iTBS aftereffects on cortical excitability as covariate (see TMS Data Analysis section). As all TMS parameters were derived from the left motor hand area, we had a strong anatomical hypothesis with regard to the location of significant effects in left M1. We hence performed a small volume correction (SVC) using an 8-mm sphere centered at the hand knob formation (Yousry et al. 1997) of the precentral gyrus (MNI coordinates (x, y, z): −40, −20, 52).

Dynamic Causal Modeling

We used dynamic causal modeling (DCM; Friston et al. 2003) to estimate effective connectivity among key motor areas activated by the

fMRI motor task. DCM uses a bilinear model (Friston et al. 2003), where the changes in neuronal states over time are modeled as

$$\frac{dx}{dt} = \left(A + \sum_{j=1}^{m} u_j B^{(j)}\right)x + Cu$$

where x is the state vector, A represents the endogenous (intrinsic) connectivity, $B(j)$ represent the task-dependent modulations of the modeled region driven by the input function u (here: 0 or 1 due to the boxcar function of the block design employed in the fMRI experiment), and C represents the influence of direct inputs to the system. As becomes evident from this formulation, the endogenous connectivity (DCM-A matrix) is always present during the experiment and hence represents the task-independent component of interregional coupling. The task-dependent modulations represented in the B matrix, however, only contribute to the changes in neuronal states when the respective task is performed, that is, when the value input function is 1 (not, however, in the baseline condition). The bilinear model also indicates that endogenous connectivity should not be influenced or even driven by task-related activity. Rather, the latter will be independently modeled in addition to it. This, however, does not exclude that the coupling parameters correlate between DCM-A and DCM-B.

As DCMs are computed on the single-subject level, we extracted the BOLD time series (first eigenvariate) from 8 volumes of interest (VOIs) at subject-specific coordinates within 8-mm spheres around individually defined activation maxima in the normalized SPMs. The contrast "right hand movement versus rest" was used to localize the VOIs in the left hemisphere while the contrast "left hand movement versus rest" served to extract right hemispheric VOIs. All VOIs were defined by functional and anatomical criteria based on the individual activation maps superimposed on the corresponding structural T_1 volume using a-priori-defined anatomical constraints: M1 on the rostral wall of the central sulcus at the "hand knob" formation (Yousry et al. 1997), supplementary motor area (SMA) on the medial wall within the interhemispheric fissure between the paracentral lobule (posterior landmark) and the coronal plane running through the anterior commissure (Picard and Strick 2001), and vPMC close to the inferior precentral gyrus and pars opercularis (Rizzolatti et al. 2002). Also other areas constitute important nodes in the motor system. For example, the dorsal premotor cortex (dPMC) situated in superior precentral sulcus is a key region in movement planning, especially with respect to visually guided reaching movements (Rizzolatti and Luppino 2001; Prado et al. 2005). However, in DCM, the stability of model estimation limits the number of areas that can be included into a model (Penny et al. 2004; Stephan et al. 2009). As monkey studies showed that neurons in vPMC (areas F4/F5) are engaged in movements of the hands and fingers while neurons in dPMC rather code movements of the arm based on visual and somatosensory information (Dum and Strick 1992; Rizzolatti et al. 1998), we decided to include vPMC into our model as the fMRI task primarily addressed finger movements (which activated vPMC rather than dPMC, see Fig. 2). As subjects were requested to move their hands according to the frequency of the visual pacing cue, activity within the cortical motor system was assumed to be driven by the visual system. Strongest activity within the visual cortex was found at the occipital poles corresponding to the foveal representations in the primary visual cortex (V1), which was selected as sensory input region for DCM (Grefkes, Eickhoff et al. 2008). The individual coordinates for all VOIs are given in Table 1.

Connectivity Models

On the basis of published data on anatomical connectivity in macaque monkeys, we assumed endogenous connections between SMA and ipsilateral and contralateral M1 (Rouiller et al. 1994), between SMA and ipsilateral (Luppino et al. 1993) as well as contralateral vPMC (Boussaoud et al. 2005), between vPMC and both ipsi- and contralateral M1 (Rouiller et al. 1994), as well as homotopic transcallosal connections among M1–M1 (Rouiller et al. 1994), SMA–SMA (McGuire et al. 1991), and vPMC–vPMC (Boussaoud et al. 2005). Evidently, the condition-specific modulations of interregional coupling do not necessarily affect all possible anatomical connections. We, therefore, constructed 7 alternative models (see Supplementary Fig. 1) of connectivity representing biologically plausible hypotheses on interregional coupling. The models varied in complexity and numbers of connections ranging from sparsely (e.g., model 1) to fully connected models (e.g., model 7). We then used Bayesian model selection (Penny et al. 2004) to identify the model yielding the highest evidence given the data using a random effects approach (Stephan et al. 2009). Note that we did not employ model selection for the resting-state data as here coupling parameters (i.e., time-series correlations) are independently computed for each pair of connection (in contrast to DCM where the estimation of coupling parameters depends on model structure). The coupling parameters of the most likely generative model were tested for statistical significance by means of 1-sample t-tests for each experimental session (false discovery rate [FDR] corrected for multiple comparisons, $P < 0.05$) (Benjamini and Hochberg 1995). Correlation analyses between iTBS aftereffects and significant DCM coupling parameters were computed using Statistical Program of the Social Sciences (SPSS 19, Chicago, 2009), and finally FDR corrected for multiple comparisons.

Statistical Analysis: fMRI Resting-State Data

For the resting-state analysis, times series information (first eigenvariates) of the motor VOIs were extracted from the normalized EPIs at the very same coordinates as used in the DCM analysis. A seed-to-seed network analysis was computed by means of linear Pearson's correlations between resting-state time courses of all 6 motor VOIs ($P < 0.05$, FDR corrected). Correlation coefficients were converted to Fisher's Z-scores using the formula $Z = (1/2) \times \ln(1 + r)/(1 - r) = \operatorname{artanh}(r)$ to yield approximately normally distributed data in the resting-state connectivity matrix. This network analysis was complemented by a seed-based whole-brain group analysis consisting of correlations

Table 1
Local maxima of fMRI BOLD-signal of each subject used as VOIs for DCM

Subject	V1_L	V1_R	SMA_L	SMA_R	vPMC_L	vPMC_R	M1_L	M1_R
1	−8 −96 −6	12 −96 −8	−6 −7 65	4 −7 56	−56 −4 28	54 14 26	−30 −26 62	32 −22 64
2	−4 −98 0	14 −98 −2	−8 −6 56	4 0 62	−46 2 42	52 10 32	−38 −24 60	34 −18 60
3	−10 −96 −20	18 −98 −10	−6 −8 70	10 0 60	−54 −6 42	58 −8 40	−32 −22 60	36 −20 60
4	−12 −92 −10	16 −98 −4	−6 −8 50	6 −6 66	−54 −16 38	56 −10 48	−34 −26 62	34 −18 58
5	−12 −96 −14	20 −96 −2	−4 −6 50	10 −2 58	−54 6 16	52 8 36	−36 −26 56	40 −26 52
6	−16 −94 −12	22 −92 −10	−6 −6 56	8 −6 60	−56 −2 40	58 4 38	−32 −26 56	32 −24 60
7	−4 −90 −10	22 −94 0	−4 −8 64	8 2 70	−42 −18 58	44 −10 60	−40 −24 58	40 −18 60
8	−10 −98 −10	18 −96 −2	−4 −8 54	6 −8 72	−58 4 34	56 0 46	−38 −22 48	34 −20 63
9	−10 −92 −14	14 −98 −10	−2 −6 60	6 2 56	−42 −8 36	46 4 40	−40 −18 58	36 −22 56
10	−10 −100 −8	12 −94 −8	−4 −4 56	8 2 58	−40 4 34	52 6 40	−34 −24 56	38 −24 54
11	−10 −96 −14	10 −94 −12	−4 0 54	4 4 62	−48 −6 48	56 4 44	−36 −24 58	32 −24 68
12	−10 −92 −14	14 −92 −10	−4 −4 58	8 4 54	−48 −6 46	54 −8 42	−36 −26 58	36 −24 56
Mean	−9 −95 −11	16 −95 −6	−5 −6 58	7 −1 61	−50 −4 38	53 1 41	−35 −20 57	35 −21 59
SD	3 3 5	4 2 4	2 2 6	2 4 5	6 8 10	4 8 8	3 3 3	2 2 4

between seed voxel time courses in stimulated left M1 and time courses of every other voxel in the brain (Eickhoff and Grefkes 2011; zu Eulenburg et al. 2012).

Transcranial Magnetic Stimulation

Single-pulse TMS was delivered using a monophasic Magstim 200^2 stimulator (Magstim Co., Whitland, Dyfed, UK). MEP amplitudes were measured from the right abductor pollicis brevis (APB) muscle using Ag/AgCl surface electrodes (Tyco Healthcare, Neustadt, Germany) with a belly-tendon montage. The EMG signal was amplified, filtered (0.5 Hz high-pass and 30–300 Hz band-pass) and digitized with a Powerlab 26T and LabChart software package version 5 (ADInstruments, Ltd., Dunedin, New Zealand). The position of the electrodes was photographed in a standard montage, and used as reference for the second iTBS session to minimize intersession variability.

The coil was positioned over the hand area of M1, tangentially to the scalp with the handle-pointing posterior. The "motor hotspot" over left M1 was defined as the location where MEPs could be evoked with highest amplitude and shortest latencies. The coil position was marked on the skull using a water-proof pen, and photographed as anatomical reference for the second iTBS session. The resting motor threshold (RMT) was defined as the lowest stimulus intensity that elicited at least five responses ≥50 μV within 10 consecutive single-pulses with the target muscle at rest (Rossini et al. 1994; Ziemann et al. 1996; Rothwell et al. 1999).

Theta Burst Stimulation

iTBS was delivered over the left M1 using a Magstim SuperRapid2 stimulator with a figure-of-eight coil (70-mm standard coil, Magstim Co., Whitland, Dyfed, UK). In line with other groups (Huang et al. 2005; Hamada et al. 2012) we did not use the SuperRapid2 stimulator for MEP acquisition as this stimulator can only induce biphasic waveforms of the TMS pulse. However, biphasic pulses induce a complex pattern of activation in the stimulated cortex exciting different neuronal populations during the different phases of the pulse, which results in less homogenous MEPs than those evoked by monophasic pulses (Terao and Ugawa 2002; Di Lazzaro et al. 2004). We, therefore, used the Magstim 200^2 stimulator to evoke MEPs with monophasic waveforms (Huang et al. 2005; Hamada et al. 2012). Note that the efficiency of iTBS in increasing cortical excitability was demonstrated not to dependent of the waveform (bi/monophasic) of the TMS pulse (Zafar et al. 2008).

iTBS consisted of 3 pulses delivered at a frequency of 50 Hz every 200 ms during 2 s (10 bursts) and repeated every 10 s for a total duration of 191 s (600 pulses) (Huang et al. 2005). We first determined the motor hotspot for the SuperRapid2-coil (posterior–anterior-oriented current) followed by the assessment of the RMT (RMTs were usually higher for the SuperRapid2 than for the Magstim 2002 stimulator). Then, iTBS was delivered at 70% RMT. Note that this is a slight modification with respect to the original iTBS protocol, which uses 80% active motor threshold (AMT, Huang et al. 2005). However, we assumed similar iTBS response as 70% RMT is usually in a similar range of absolute stimulator output intensities like 80% AMT (Chen et al. 1998; Gentner et al. 2008; Sarfeld et al. 2012). Control stimulation was delivered over the parieto-occipital vertex (Pz) using the same stimulator output intensity as for M1 stimulation. To reduce possible cortical stimulation effects in the control condition, the coil was angled at 45°, touching the skull not with the centre but with the rim opposite the handle. In this position, the coil–cortex distance is essentially larger such that the electromagnetic field, if at all reaching the cortex, is substantially weaker and far outside the target range (Herwig et al. 2007; Herwig et al. 2010).

Motor hotspots were defined for both stimulators and marked on the skull by means of a waterproof pen. MEP amplitudes evoked by monophasic single-pulse TMS (Magstim 200^2 stimulator) were evaluated before and after the delivery of iTBS.

Subjects were comfortably seated in an adjustable armchair with headrest. Baseline corticospinal excitability (in terms of MEPs) was assessed by measuring the amplitudes of 36 MEPs in the right APB muscle at rest as response to single-pulse TMS (posterior–anterior oriented current) applied with an intensity of 120% RMT at a frequency of 0.2 Hz. After iTBS, batches of MEPs to 12 single TMS pulses were recorded every 5 min for 25 min (120 RMT, 0.2 Hz) from the identical position as those evoked before stimulation (Huang et al. 2005).

TMS Data Analysis

In line with Huang et al. (2005), we analyzed iTBS aftereffects by means of a 2-way-repeated measures analysis of variance (ANOVA) of MEP amplitudes normalized to baseline assessments with the factors "intervention" (2 levels: M1-iTBS vs control-iTBS) and "time" (5 levels: "5 min," "10 min," "15 min," "20 min," "25 min"), followed up by *t*-tests comparing baseline and MEP amplitudes after different points in time testing for the temporal maximum of stimulation aftereffects.

For correlation analyses with neural activity and connectivity (BOLD signal, DCM, and resting-state parameters), we used 2 parameters as index for the strength of the iTBS aftereffects. 1) MEP amplitudes after 10 min (i.e., the point of time when strongest and most significant differences were observed between M1 and sham stimulation) and 2) the maximum MEP response (change in MEP amplitude relative to baseline) over the entire 25-min recording session. This means that we performed all correlation analyses twice, that is, for the 10-min post-iTBS values and for the maximum iTBS response over the whole session.

Statistical Correction for Multiple Comparisons

To obtain comparable statistical results, the same approach—FDR correction for multiple correlations—was used for all analyses performed in this study. This represents a trade-off between statistical sensitivity (given the large number of comparisons) and adjustment of *P* values required by multiple testing. However, for the main findings, we, in addition, also present Bonferroni corrected *P*-values in order to show the statistical robustness of the results.

Results

TMS and iTBS were well tolerated and no subject reported relevant side effects. Two participants with high motor thresholds reported mild headache after the experiment.

iTBS Aftereffects on Electrophysiological Parameters

Mean RMT was 44.5 ± 8.3% for iTBS and 43.0 ± 8.0% of maximal stimulator output for control stimulation. Baseline MEP amplitudes were not significantly different between M1-iTBS (0.69 ± 0.46 mV) and control-iTBS (0.80 ± 0.37 mV) (Student's *t*-test; $P = 0.259$). When testing for an intervention effect on normalized MEP amplitudes, a 2-way-repeated measures ANOVA showed a significant main effect for "intervention" ($F_{1,10} = 7.10$, $P = 0.022$) but not for "time" (Fig. 1). Although no significant interaction effect was evident ($P = 0.13$), which implied that iTBS over M1 induced a lasting increase in MEP amplitude, we used Student's *t*-tests to identify the point of time with maximal difference between sham and M1 stimulation (as in Huang et al. 2005). We found that M1-iTBS yielded the maximum effect, that is, largest and most significant differences in normalized MEP amplitudes between M1 and sham stimulation at 10 min following stimulation (5 min: $P = 0.047$, 10 min: $P = 0.022$, 15 min: $P = 0.059$). Hence, iTBS applied over M1 with 70% RMT significantly enhanced cortical excitability compared with both baseline and control stimulation (over Pz). No significant correlations were evident for iTBS aftereffects and electrophysiological baseline parameters (RMT: $r = -0.121$, $P = 0.708$; baseline MEP amplitudes: for sham- ($r = -0.162$, $P = 0.616$) and M1 stimulation ($r = -0.162$, $P = 0.614$).

fMRI BOLD Data and iTBS Aftereffects

All subjects were readily able to perform the task with the requested frequency and movement amplitude after a few seconds of training due to the relative simplicity of the motor task. Training was performed for the first 3 blocks of trials in order to control for habituation effects (scanner environment, position of the hands, etc.).

The fMRI group analysis showed that compared with no-movement (baseline), right-hand movements were associated with enhanced BOLD activity in a left-lateralized network comprising left M1, SMA, bilateral vPMC, bilateral primary, and higher visual areas (V1–V5), as well as subcortical regions like left thalamus, left putamen, and right anterior cerebellum (see Fig. 2*A*; $P < 0.05$, FWE corrected at the voxel level). Movements of the left hand yielded a similar, yet mirror-reversed network of activity.

In order to test whether the fMRI BOLD signal during movements of the right hand was related to the iTBS aftereffect on MEP amplitudes, we performed an SPM multiple regression analysis of the respective individual contrast images and the relative increase of MEP amplitudes (percentage compared with baseline) after 10 min (referring to the moment of strongest iTBS aftereffects upon M1 stimulation, see above). This analysis showed a negative correlation between iTBS aftereffects and the BOLD signal in a cluster of voxels at the motor hand knob (see Fig. 2*B*; local maximum at MNI coordinates (x, y, z): −40, −20, 52; $T = 2.84$, $P = 0.048$; small volume corrected on the voxel level): Subjects showing stronger M1-iTBS aftereffects were those with less preinterventional task-related neural activity in the stimulated area. Furthermore, when plotting this cluster of voxels correlating with iTBS aftereffects together with the peak activation cluster for movements of the respective hand, we observed that the local activation maxima did not overlap but lay adjacent to each other (see Supplementary Fig. 3). This means that those subjects who had more extended activation clusters around the group local maximum were those with less response to iTBS.

When correlating the imaging data with the maximum iTBS aftereffect over the 25-min recording session, we only found a trend toward significance in the same M1 cluster ($P < 0.1$). No further correlations between neural activation within other motor regions than M1- and iTBS-effects were evident. The equivalent correlation with the MEP data from the control-iTBS session did not yield any significant result.

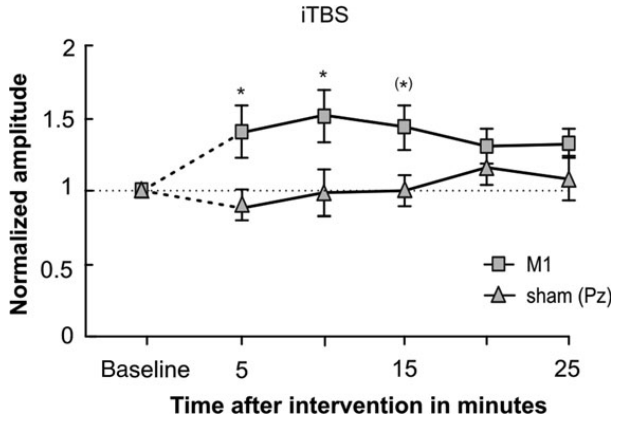

Figure 1. Changes in MEP amplitude following real- (squares) and sham-iTBS (triangles), normalized to prestimulation MEP amplitudes. Asterisk indicates significant aftereffect following real-iTBS compared with sham; $P < 0.05$; Student's t-test.

Resting-State Connectivity and iTBS Aftereffects

The group analysis showed that during the resting-state, interregional coupling among the motor VOIs was predominantly significant for interhemispheric connections, that is, between SMA-SMA, vPMC-vPMC, M1-M1; left SMA-right vPMC; right SMA-left vPMC and left SMA-right M1 ($P < 0.05$, FDR corrected). The analysis further revealed significant intrahemispheric resting-state coupling between SMA and vPMC in both hemispheres, as well as a significant connection between left SMA-left M1 (see Fig. 3*B*). More importantly, there was no significant correlation between any of the resting-state parameters and iTBS aftereffects ($P > 0.1$, for all comparisons). Likewise, correlations between individual left M1 seed voxel maps and iTBS aftereffect sizes did not show significant effects. Hence, in our sample of subjects, we did not find a significant relationship between resting-state coupling of M1 and iTBS aftereffects.

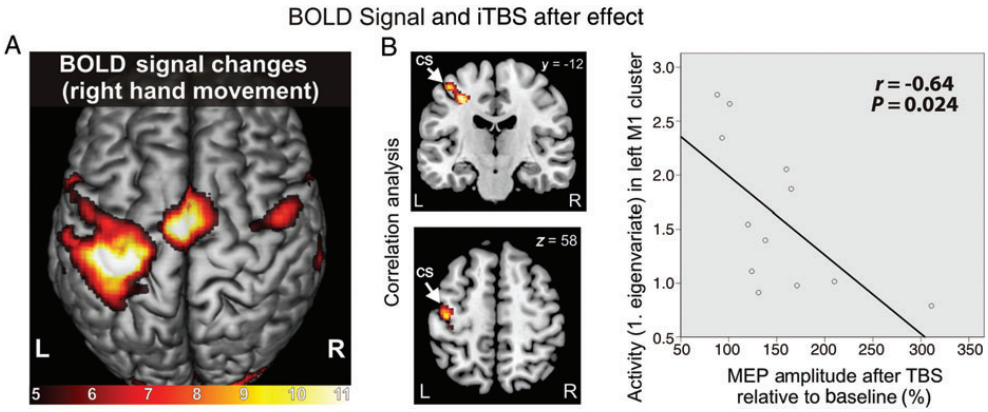

Figure 2. (*A*) BOLD activation changes during the movement of the right hand ($P < 0.05$; FWE corrected at voxel level; color bar represents t-values). Activation clusters were surface-rendered onto canonical brain. (*B*) SPM regression analysis: cluster of neural activation at the hand knob area negatively correlated with iTBS aftereffects (changes in MEP amplitude 10-min post-stimulation; $r = -0.64$, $P < 0.05$, SVC corrected on the voxel level). CS, central sulcus; L, left; R, right.

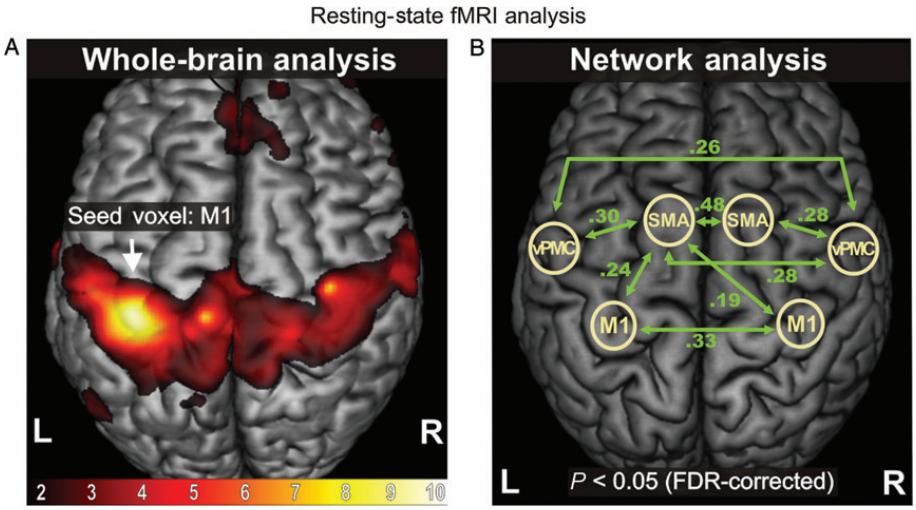

Figure 3. Resting-state fMRI analysis. (*A*) Seed-based whole-brain group analysis (seed region: left M1; MNI coordinates −36 −24 58, that is, the local maximum of the group analysis in Fig. 2*A*). Correlated fMRI time courses were not only found in the vicinity of the seed voxel, but also in homotopic regions in the contralateral hemisphere (voxel threshold: $P < 0.05$; color bar represents *t*-values). However, these correlations did not predict the iTBS aftereffects. (*B*) Network analysis testing for correlated resting-state activity in key regions of the motor system. Coordinates were derived from the motor task data of each individual subjects. We found strongly correlated (linear Pearson's correlations; $P < 0.05$, FDR corrected) BOLD times courses especially for interhemispheric connections as well as for intrahemispheric coupling between left SMA and M1, as well as left SMA and right M1 (correlation coefficients given as Fisher's *z*-scores). M1, primary motor cortex; SMA, supplementary motor area; vPMC, ventral premotor cortex.

DCM Connectivity and iTBS Aftereffects

We tested 7 alternative models of interregional connectivity (see Supplementary Fig. 1). These models varied in complexity and numbers of connections ranging from sparsely (e.g., model 1) to fully connected models (e.g., model 7). The experimental input (C matrix) was set to bilateral V1 for all models, as visual cues were used to trigger the movement frequency during the fMRI motor task. We assumed connections between bilateral V1 and all nodes of our network. It is essential to note that coupling parameters obtained from DCM refer to functional interactions, but do not necessarily reflect direct axonal connections. For example, the relay of visual information toward the premotor regions, e.g., via parietal regions that were not explicitly modeled in the DCM should be implicitly reflected in the derived rate constants of our model for effective connectivity within the cortical motor system. The model selection procedure identified model 7 (see Supplementary Fig. 1) with fully connected VOIs as the most likely generative model given the data.

Endogenous Coupling

Endogenous coupling (DCM-A matrix) refers to the coupling of areas independent of the effect of condition, that is, whether subjects moved the left or right hand. Note that this is not equivalent to an analysis of the resting-state as the whole times series information including the movement conditions are used to estimate endogenous connectivity. Therefore, endogenous coupling represents the constant component of connectivity in the activated motor system.

Overall, endogenous connectivity between the motor areas of interest was symmetrically organized across hemispheres ($P < 0.05$, FDR corrected for multiple comparisons). Endogenous coupling within the left or right hemisphere was positive for the interaction between the SMA, vPMC, and M1 with strongest effects for connections targeting M1. A negative coupling was found for interhemispheric connections among both M1, indicating an inhibitory connection among bilateral M1 (see Supplementary Fig. 2).

There were significant ($P < 0.05$, FDR corrected) positive correlations between iTBS aftereffects and endogenous coupling parameters from left SMA to left vPMC ($r = 0.81$, $P = 0.021$), from left vPMC to left M1 ($r = 0.78$, $P = 0.028$), and from left M1 to left vPMC ($r = 0.74$, $P = 0.048$). After Bonferroni correction, the connection from left SMA to left vPMC remained significant ($r = 0.81$, $P = 0.043$), while the coupling from left vPMC to left M1 showed a trend of significance ($r = 0.78$, $P = 0.083$). Hence, in contrast to the resting-state data, the iTBS-effect on excitability of left M1 was predicted by a stronger preinterventional, endogenous coupling of premotor areas with left M1. There were no significant correlations between endogenous coupling parameters and control-iTBS aftereffects.

Hand Movement-Specific Coupling

The modulation of interregional coupling induced by moving the right hand featured increases in the promoting influences of left vPMC and left SMA with left M1, but also inhibition of right M1 (see Fig. 4; $P < 0.05$, FDR corrected). Movements of the left hand were associated with a similar yet mirror-reversed modulation of coupling. The DCM-A and DCM-B matrices yielded a weak but significant correlation ($r = 0.473$, $P = 0.008$). This means that subjects with higher intrinsic/endogenous coupling parameters also showed a stronger modulation of these connections during movements of the right hand.

For correlations with iTBS aftereffects, we only considered coupling parameters estimated for data recorded during movements of the right hand, as MEPs were recorded from the right APB muscle. Here, we found significant correlations (FDR corrected for multiple comparisons) for couplings from left SMA to left vPMC ($r = 0.85$, $P = 0.004$), from left vPMC to left SMA ($r = 0.79$, $P = 0.010$), from left vPMC to left M1

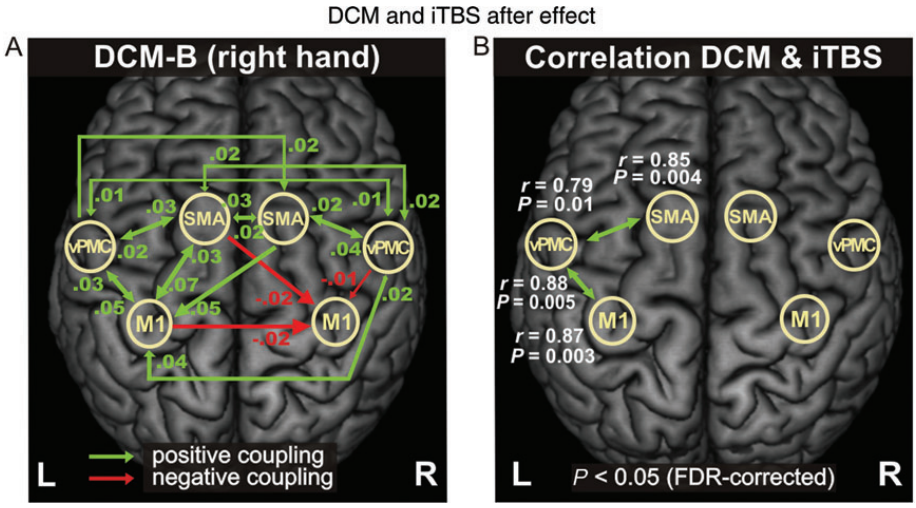

Figure 4. (*A*) Effective connectivity during movements of the right hand as estimated by dynamic causal modeling (DCM-B; green arrows represent positive coupling, red arrows indicate negative coupling). Strongest coupling estimates were found for interactions targeting left M1, while neural activity in right M1 was inhibited by both intra- and interhemispheric interactions ($P < 0.05$, FDR corrected for multiple comparisons) (*B*) Significant correlations of DCM coupling parameters with iTBS aftereffects ($P < 0.05$, FDR corrected). Here, high preinterventional coupling estimates between left vPMC and left SMA as well as between left vPMC and M1 predicted stronger iTBS aftereffects after 10 min. Note that VOIs were identical to those used for the resting-state analysis (Fig. 3). Abbreviations as in Figure 3.

($r = 0.87$, $P = 0.003$), and from left M1 to left vPMC ($r = 0.88$, $P = 0.005$). All of these connections remained significant after Bonferroni correction for multiple comparisons (SMA-vPMC: $P = 0.013$; vPMC-M1: $P = 0.006$; M1-vPMC: $P = 0.005$), except the coupling from left vPMC to left SMA ($P = 0.072$), which showed a statistical trend. That is, greater M1-iTBS aftereffects most likely occurred in subjects with stronger excitatory couplings between left SMA and vPMC as well as between left vPMC and M1. Of note, all significant effects were found for connections within the stimulated hemisphere although also coupling parameters of the nonstimulated (i.e., right) hemisphere were considered in the analysis. The same connections also significantly correlated when using the maximum effect across the 25 recording sessions as covariate ($P < 0.05$, for all comparisons). Control-iTBS aftereffects did not yield any significant correlations.

Discussion

ITBS applied over left M1 was well tolerated and resulted in significant enhancement of cortical excitability for up to 10 min with a strong statistical trend for 15 min. Two prestimulation settings correlated with individual iTBS susceptibility as indexed by higher poststimulation MEPs: 1) a relatively focal and low level of movement induced BOLD-activity in the left stimulated M1 and 2) strong intrahemispheric excitatory couplings between left SMA and left vPMC, and from left vPMC driving the stimulated (left) M1. In contrast, individual iTBS aftereffects were not predicted by functional connectivity of these areas during resting-state. Our data hence strongly suggest that predominantly activity-dependent properties of the cortical motor system, especially among M1, vPMC, and SMA, are indicative of excitability changes following induction of cortical plasticity with iTBS.

Modulating Cortical Excitability with iTBS

The cellular and neurophysiological mechanisms underlying iTBS-effects to date remain poorly understood (Thickbroom 2007; Cárdenas-Morales et al. 2010). One hypothesis is that rTMS protocols like iTBS induce synaptic plasticity changes, comparable with LTP—like effects, similar to what has been observed for the stimulation of preparations of synaptic connections in vitro (Tsumoto 1992). Neuropharmacological studies showed that the response to iTBS is—at least partially—dependent on NMDA-receptor activity (Huang et al. 2007; Teo et al. 2007), resembling LTP-like effects observed in animal studies (Hrabetova and Sacktor 1997). Another mechanism possibly involved in the evolution of iTBS aftereffects lies in the alteration of the cortical inhibitory system, as suggested by human electrophysiological (Di Lazzaro et al. 2008) and animal studies (Benali et al. 2011; Funke and Benali 2011). However, the individual responses to iTBS have been shown to be relatively variable (Ridding and Ziemann 2010) which is relevant when using iTBS to manipulate cortical excitability. Hamada et al. (2012) found that about 50% of variability regarding the individual susceptibility to iTBS could be explained by which forms of I-waves (early/late; depending on different MEP latencies upon different coil orientations) can be recruited in a given subject. These I-waves evolve depending on which types of interneurons are affected by the stimulation (Hamada et al. 2012). Such an interpretation is supported by recent findings in animal models which showed that iTBS interferes with the activity of distinct subgroups of inhibitory interneurons in the cortex of the rat (Funke and Benali 2011) as indicated by changes in the expression of activity-dependent proteins like the calcium-binding proteins Parvalbumin and Calbindin.

Neural Activation and iTBS Aftereffects

We found that both fMRI activities at the stimulation site as well as strong connectivity within the motor network of the stimulated hemisphere are indicative of a better response to iTBS. Although a simple fMRI motor task was used in this study subtle variation in task performance between subjects (e.g., differences in force, timing, or velocity) might have

increased the experimental variance (i.e., "noise"). Therefore, it might well be that also activity and connectivity of other areas are related to plasticity-inducing effects, albeit to a weaker degree than the significant findings in the present study (representing the most robust effects). However, as the main focus of the present study was to investigate the role of connectivity in stimulation aftereffects, we rather preferred a simple motor task with robust BOLD activation patterns, as for DCM a reliable definition of the regions of interest is mandatory in the individual SPMs of each and every subject.

ITBS applied over left M1 compared with control stimulation was demonstrated to decrease BOLD activity in M1 during a right hand choice-reaction task (button-press task upon visual cue) (Cárdenas-Morales et al. 2011). These findings probably reflect increased efficacy of neural signal transmission resulting in less neural activity required to accomplish the motor task. In line with this assumption, we found a negative correlation between changes of MEP amplitudes following iTBS and larger clusters of movement-related M1 stimulation prior to stimulation. Our data hence suggest that subjects with more focused M1 BOLD activity (possibly reflecting that less neural resources were needed to perform the task) were more responsive to iTBS. In healthy subjects, extended motor system activity is typically observed during learning of a new motor skill, which focuses during consolidation (Toni et al. 1998; Floyer-Lea and Matthews 2004; Park et al. 2010). In patient populations with motor impairments, we usually observe more extended, that is, less focal activity in motor areas, which focuses during the process of motor recovery (Chollet et al. 1991; Ward et al. 2003; Eickhoff et al. 2008; Grefkes, Nowak et al. 2008). Hence, more extended activity and less premotor–M1 connectivity are indicative for lower levels of motor performance and/or more effort to perform a given motor task. Accordingly, a more focal pattern of task-induced BOLD activity in M1 reflects a more efficient cortical motor network, which might have more capacity to respond to a plasticity-enhancing intervention. We thus speculate that subjects who showed a strong response to iTBS had "a more efficient" intrinsic motor network architecture with less need to recruit larger parts of M1 when moving the hand (i.e., more focused M1 cluster, cf., Supplementary Fig. 3) which in turn might have enabled them to recruit these "inactive" portions of M1 cortex following stimulation.

Connectivity and iTBS Aftereffects

Focally applied interventions like rTMS do not only have effects on the stimulated region, but may also affect activity in interconnected regions remote from the stimulation site (Bestmann et al. 2003, 2005; Suppa et al. 2008; Cárdenas-Morales et al. 2011). Likewise, the response to rTMS applied over M1 can be modulated by prior stimulation (priming) of remote areas as demonstrated for contralateral M1 (Ragert et al. 2009) and ipsilateral SMA (Hamada et al. 2009). Our data show that certain aspects of the connectivity state of the stimulated brain region are related to the individual amount of change in cortical excitability following iTBS and therefore possibly contribute to the evolution of cortical plasticity within the cortical motor network.

In the current study, we found no significant correlations between resting-state connectivity and iTBS-effects neither for seed-to-seed voxel analyses nor for M1-functional connectivity maps. This finding suggests that resting-state properties of the motor system have (if at all) only little predictive value for iTBS aftereffects. One potential caveat to this null result is that fMRI and TMS measurements were not assessed in the same session, and hence connectivity might have changed from the time of the resting-state measurements to the actual stimulation. Evidently, such short-term changes would not be reflected in the current analysis. However, earlier studies found a moderate to high test–retest reliability of functional resting-state connectivity (Shehzad et al. 2009; Van Dijk et al. 2010), making this scenario less likely. DCM applied to fMRI data has also been shown to be highly reliable between sessions (Schuyler et al. 2010). Moreover, the fact that fMRI activity and DCM connectivity pattern recorded at the same session in which the resting-state data were acquired were highly correlated with iTBS aftereffects further implies a relative stability of the data. Furthermore, other groups found evidence that resting-state assessments of brain activity are only poorly correlated with TBS susceptibility, for example, when compared with electroencephalography (EEG) recordings (McAllister et al. 2011). These data well match our resting-state fMRI results which also were nonpredictive for iTBS aftereffects. Our finding that stronger active-state connectivity between motor areas indicated a better response to iTBS aftereffects resembles data reported for the auditory system where stronger DCM connectivity of the primary auditory cortex predicted a better response to rTMS (Andoh and Zatorre 2011). Interestingly, in the present study also endogenous coupling among the motor areas (DCM-A) in the stimulated hemisphere was related to iTBS aftereffects albeit not as strong as observed for the additional effect induced by movements of the right hand. While it may seem puzzling at first that endogenous coupling in DCM is related to iTBS aftereffects whereas the "endogenous" resting-state connectivity is not, this apparent discrepancy is readily resolved when considering that, in these 2 cases, the term "endogenous" has vastly different meanings. In DCM, endogenous connectivity represents the constant part of connectivity in the activated motor system, which also includes the entire task set and—in contrast to resting-state scans—is specific to a particular fMRI experiment (Friston et al. 2003). Therefore, a possible interpretation is that the biological factors facilitating the coupling of motors areas in the activated motor system might also enable a higher susceptibility to plasticity-enhancing interventions like iTBS. For example, lesions to gray or white matter were demonstrated to reduce endogenous coupling between premotor areas and M1 concurrent to reduced motor performance in stroke patients (Grefkes, Nowak et al. 2008; Grefkes et al. 2010; Rehme et al. 2011; Wang et al. 2011). Both the lateral premotor cortex and the SMA region have dense axonal connections with M1, and both areas are known to be critical for motor planning and control (Jenkins et al. 2000; Schubotz and von Cramon 2003; Hoshi and Tanji 2004, 2007). Therefore, one explanation for our finding is that higher coupling of M1 with premotor areas reflects stronger activity-dependent synaptic transmission, which might impact on the susceptibility of neuronal excitability to iTBS.

Premotor Connectivity and iTBS Aftereffects

A more specific interpretation is possible for the significant correlation between the excitatory coupling from left vPMC to

left M1 and iTBS aftereffects: Hamada et al. (2012) found that individual aftereffects of iTBS might depend on individual differences in the recruitment of cortical neurons simulated with TMS. Subjects in whom late I-waves (estimated by latency differences of MEPs computed for different coil orientations) were recruited showed high susceptibility to iTBS. Late I-waves are a part of the MEP generated by stimulation of M1, possibly reflecting the input of complex oligosynaptic circuits to corticospinal neurons located in M1 (Hamada et al. 2012). These late I-waves have been shown to be enhanced following iTBS (Di Lazzaro et al. 2008). Electrophysiological studies in macaques demonstrated that late I-waves are strongly influenced by input from neurons located in vPMC (Shimazu et al. 2004; Lemon 2008). This relationship fits well with our data, which showed that effective connectivity between vPMC and M1 was a strong predictor for iTBS aftereffects. However, whether or not I-waves are related to connectivity parameters assessed with fMRI remains to be explored in future studies.

Furthermore, an alternative line of interpretation of our findings is that not only vPMC and M1, but the entire motor system is engaged in the aftereffects following M1 stimulation. Given the finding that the iTBS-effects correlated with connectivity among M1, vPMC, and SMA not only for the feedforward, but also for the feedback directions, we hypothesize that this connection pattern represents the network's ability to successfully propagate activity between cortical motor regions. TMS experiments performed during fMRI acquisition showed that M1 stimulation does not only induce BOLD activity in the stimulated region but also in interconnected motor regions like SMA and premotor cortex (Bestmann et al. 2003). This fits perfectly with our findings that plasticity-enhancing stimulation effects were associated with the connectivity strength among these regions. Therefore, an interesting (but speculative) interpretation of these relationships is that the whole system including the SMA and premotor cortex rather than a single area only might contribute to intervention effects. Support for this hypothesis is found in a study published by Ameli et al. (2009) who could show that stroke patients with lesions affecting the premotor cortex but sparing the M1 hand knob region are less responsive to excitability enhancing 10-Hz rTMS. Such effects might, for example, result from disrupted connectivity of the stimulation site, which would nicely fit the interpretation of the present data. Hence, the individual ability to strongly interconnect important cortical motor regions might underlie the induction of cortical plasticity within the cortical motor network (as indicated by the correlation with the individual changes in cortical excitability following iTBS).

Esser et al. (2006) demonstrated changes in premotor cortex activity after iTBS applied to M1 using high-density EEG. In the present study, we did not assess fMRI after iTBS as the primary objective of the study was to investigate the relationship between connectivity and variability in motor cortex plasticity induced by noninvasive brain stimulation. Other studies have already demonstrated that rTMS may interfere with connectivity not only at the stimulation site, but also between remote areas (Grefkes et al. 2010). However, the effects of iTBS on motor system connectivity remains to be elucidated in future studies.

Conclusions

iTBS aftereffects on M1 excitability are robustly predicted by a low level of BOLD activity at the stimulation site as well as strong effective connectivity among premotor areas, and a strong excitatory coupling from vPMC to M1. In contrast, there was no association with connectivity measured at rest. Importantly, our data confirm that cortical plasticity as induced by iTBS not only depends on local features of the stimulated cortex but is also influenced by interactions with remote cortical areas. Here, our data suggest that especially the ventral premotor cortex plays a crucial role in modulating iTBS responses in M1. Furthermore, the task-dependent interplay of M1, vPMC, and SMA seems to be involved in changes in cortical excitability and therefore cortical plasticity within the human motor network.

Supplementary Material

Supplementary material can be found at: http://www.cercor.oxfordjournals.org/.

Funding

C.G. was supported by a grant provided by the German Research Foundation (Deutsche Forschungsgemeinschaft, GR 3285/2-1).

Notes

We thank Dr. Marc Tittgemeyer and the MR staff for technical support. We also thank Dr. Masashi Hamada from the Sobell Department of Motor Neuroscience for valuable discussions. *Conflict of Interest*: None declared.

References

Ameli M, Grefkes C, Kemper F, Riegg FP, Rehme AK, Karbe H, Fink GR, Nowak DA. 2009. Differential effects of high-frequency repetitive transcranial magnetic stimulation over ipsilesional primary motor cortex in cortical and subcortical middle cerebral artery stroke. Ann Neurol. 66:298–309.

Andoh J, Zatorre RJ. 2011. Interhemispheric connectivity influences the degree of modulation of TMS-induced effects during auditory processing. Front Psychol. 2:161.

Ashburner J, Friston KJ. 2005. Unified segmentation. Neuroimage. 26:839–851.

Benali A, Trippe J, Weiler E, Mix A, Petrasch-Parwez E, Girzalsky W, Eysel UT, Erdmann R, Funke K. 2011. Theta-burst transcranial magnetic stimulation alters cortical inhibition. J Neurosci. 31:1193–1203.

Benjamini Y, Hochberg Y. 1995. Controlling the false discovery rate: a practical and powerful approach to multiple testing. J R Stat Soc Ser B (Methodological). 57:289–300.

Bestmann S, Baudewig J, Siebner HR, Rothwell JC, Frahm J. 2005. BOLD MRI responses to repetitive TMS over human dorsal premotor cortex. Neuroimage. 28:22–29.

Bestmann S, Baudewig J, Siebner HR, Rothwell JC, Frahm J. 2003. Subthreshold high-frequency TMS of human primary motor cortex modulates interconnected frontal motor areas as detected by interleaved fMRI-TMS. Neuroimage. 20:1685–1696.

Boussaoud D, Tanne-Gariepy J, Wannier T, Rouiller EM. 2005. Callosal connections of dorsal versus ventral premotor areas in the macaque monkey: a multiple retrograde tracing study. BMC Neurosci. 6:67.

Cárdenas-Morales L, Gron G, Kammer T. 2011. Exploring the aftereffects of theta burst magnetic stimulation on the human motor

cortex: a functional imaging study. Hum Brain Mapp. 32: 1948–1960.
Cárdenas-Morales L, Nowak DA, Kammer T, Wolf RC, Schonfeldt-Lecuona C. 2010. Mechanisms and applications of theta-burst rTMS on the human motor cortex. Brain Topogr. 22:294–306.
Censor N, Cohen LG. 2011. Using repetitive transcranial magnetic stimulation to study the underlying neural mechanisms of human motor learning and memory. J Physiol. 589:21–28.
Cheeran B, Talelli P, Mori F, Koch G, Suppa A, Edwards M, Houlden H, Bhatia K, Greenwood R, Rothwell JC. 2008. A common polymorphism in the brain-derived neurotrophic factor gene (BDNF) modulates human cortical plasticity and the response to rTMS. J Physiol. 586:5717–5725.
Chen R, Tam A, Butefisch C, Corwell B, Ziemann U, Rothwell JC, Cohen LG. 1998. Intracortical inhibition and facilitation in different representations of the human motor cortex. J Neurophysiol. 80:2870–2881.
Chollet F, DiPiero V, Wise RJ, Brooks DJ, Dolan RJ, Frackowiak RS. 1991. The functional anatomy of motor recovery after stroke in humans: a study with positron emission tomography. Ann Neurol. 29:63–71.
Dayan E, Cohen LG. 2011. Neuroplasticity subserving motor skill learning. Neuron. 72:443–454.
Di Lazzaro V, Oliviero A, Pilato F, Saturno E, Dileone M, Mazzone P, Insola A, Tonali PA, Rothwell JC. 2004. The physiological basis of transcranial motor cortex stimulation in conscious humans. Clin Neurophysiol. 115:255–266.
Di Lazzaro V, Pilato F, Dileone M, Profice P, Oliviero A, Mazzone P, Insola A, Ranieri F, Meglio M, Tonali PA et al. 2008. The physiological basis of the effects of intermittent theta burst stimulation of the human motor cortex. J Physiol. 586:3871–3879.
Dum RP, Strick PL. 1992. Medial wall motor areas and skeletomotor control. Curr Opin Neurobiol. 2:836–839.
Eickhoff SB, Dafotakis M, Grefkes C, Shah NJ, Zilles K, Piza-Katzer H. 2008. Central adaptation following heterotopic hand replantation probed by fMRI and effective connectivity analysis. Exp Neurol. 212:132–144.
Eickhoff SB, Grefkes C. 2011. Approaches for the integrated analysis of structure, function and connectivity of the human brain. Clin EEG Neurosci. 42:107–121.
Esser SK, Huber R, Massimini M, Peterson MJ, Ferrarelli F, Tononi G. 2006. A direct demonstration of cortical LTP in humans: a combined TMS/EEG study. Brain Res Bull. 69:86–94.
Floyer-Lea A, Matthews PM. 2004. Changing brain networks for visuomotor control with increased movement automaticity. J Neurophysiol. 92:2405–2412.
Freitas C, Perez J, Knobel M, Tormos JM, Oberman L, Eldaief M, Bashir S, Vernet M, Pena-Gomez C, Pascual-Leone A. 2011. Changes in cortical plasticity across the lifespan. Front Aging Neurosci. 3:5.
Friston KJ. 1994. Functional and effective connectivity in neuroimaging: a synthesis. Hum Brain Mapp. 2:56–78.
Friston KJ, Harrison L, Penny W. 2003. Dynamic causal modelling. Neuroimage. 19:1273–1302.
Funke K, Benali A. 2011. Modulation of cortical inhibition by rTMS-findings obtained from animal models. J Physiol. 589: 4423–4435.
Gamboa OL, Antal A, Moliadze V, Paulus W. 2010. Simply longer is not better: reversal of theta burst after-effect with prolonged stimulation. Exp Brain Res. 204:181–187.
Gentner R, Wankerl K, Reinsberger C, Zeller D, Classen J. 2008. Depression of human corticospinal excitability induced by magnetic theta-burst stimulation: evidence of rapid polarity-reversing metaplasticity. Cereb Cortex. 18:2046–2053.
Grefkes C, Eickhoff SB, Nowak DA, Dafotakis M, Fink GR. 2008. Dynamic intra- and interhemispheric interactions during unilateral and bilateral hand movements assessed with fMRI and DCM. Neuroimage. 41:1382–1394.
Grefkes C, Nowak DA, Eickhoff SB, Dafotakis M, Kust J, Karbe H, Fink GR. 2008. Cortical connectivity after subcortical stroke assessed with functional magnetic resonance imaging. Ann Neurol. 63:236–246.
Grefkes C, Nowak DA, Wang LE, Dafotakis M, Eickhoff SB, Fink GR. 2010. Modulating cortical connectivity in stroke patients by rTMS assessed with fMRI and dynamic causal modeling. Neuroimage. 50:233–242.
Hamada M, Hanajima R, Terao Y, Okabe S, Nakatani-Enomoto S, Furubayashi T, Matsumoto H, Shirota Y, Ohminami S, Ugawa Y. 2009. Primary motor cortical metaplasticity induced by priming over the supplementary motor area. J Physiol. 587:4845–4862.
Hamada M, Murase N, Hasan A, Balaratnam M, Rothwell JC. 2013. The Role of Interneuron Networks in Driving Human Motor Cortical Plasticity. Cereb Cortex. 23:1593–1605.
Herwig U, Cardenas-Morales L, Connemann BJ, Kammer T, Schonfeldt-Lecuona C. 2010. Sham or real-post hoc estimation of stimulation condition in a randomized transcranial magnetic stimulation trial. Neurosci Lett. 471:30–33.
Herwig U, Fallgatter AJ, Hoppner J, Eschweiler GW, Kron M, Hajak G, Padberg F, Naderi-Heiden A, Abler B, Eichhammer P et al. 2007. Antidepressant effects of augmentative transcranial magnetic stimulation: randomised multicentre trial. Br J Psychiatry. 191:441–448.
Hoshi E, Tanji J. 2004. Differential roles of neuronal activity in the supplementary and presupplementary motor areas: from information retrieval to motor planning and execution. J Neurophysiol. 92:3482–3499.
Hoshi E, Tanji J. 2007. Distinctions between dorsal and ventral premotor areas: anatomical connectivity and functional properties. Curr Opin Neurobiol. 17:234–242.
Hrabetova S, Sacktor TC. 1997. Long-term potentiation and long-term depression are induced through pharmacologically distinct NMDA receptors. Neurosci Lett. 226:107–110.
Huang YZ, Chen RS, Rothwell JC, Wen HY. 2007. The after-effect of human theta burst stimulation is NMDA receptor dependent. Clin Neurophysiol. 118:1028–1032.
Huang YZ, Edwards MJ, Rounis E, Bhatia KP, Rothwell JC. 2005. Theta burst stimulation of the human motor cortex. Neuron. 45:201–206.
Huang YZ, Rothwell JC, Lu CS, Wang J, Chen RS. 2010. Restoration of motor inhibition through an abnormal premotor-motor connection in dystonia. Mov Disord. 25:696–703.
Jakobs O, Langner R, Caspers S, Roski C, Cieslik EC, Zilles K, Laird AR, Fox PT, Eickhoff SB. 2012. Across-study and within-subject functional connectivity of a right temporo-parietal junction subregion involved in stimulus-context integration. Neuroimage. 60:2389–2398.
Jenkins IH, Jahanshahi M, Jueptner M, Passingham RE, Brooks DJ. 2000. Self-initiated versus externally triggered movements. II. The effect of movement predictability on regional cerebral blood flow. Brain. 123(Pt 6):1216–1228.
Kleim JA, Chan S, Pringle E, Schallert K, Procaccio V, Jimenez R, Cramer SC. 2006. BDNF val66met polymorphism is associated with modified experience-dependent plasticity in human motor cortex. Nat Neurosci. 9:735–737.
Koch G, Schneider S, Baumer T, Franca M, Munchau A, Cheeran B, Fernandez del Olmo M, Cordivari C, Rounis E, Caltagirone C et al. 2008. Altered dorsal premotor-motor interhemispheric pathway activity in focal arm dystonia. Mov Disord. 23:660–668.
Lemon RN. 2008. Descending pathways in motor control. Annu Rev Neurosci. 31:195–218.
Luppino G, Matelli M, Camarda R, Rizzolatti G. 1993. Corticocortical connections of area F3 (SMA-proper) and area F6 (pre-SMA) in the macaque monkey. J Comp Neurol. 338:114–140.
McAllister SM, Rothwell JC, Ridding MC. 2011. Cortical oscillatory activity and the induction of plasticity in the human motor cortex. Eur J Neurosci. 33:1916–1924.
McGuire PK, Bates JF, Goldman-Rakic PS. 1991. Interhemispheric integration: I. Symmetry and convergence of the corticocortical connections of the left and the right principal sulcus (PS) and the left and the right supplementary motor area (SMA) in the rhesus monkey. Cereb Cortex. 1:390–407.

Park JW, Kim YH, Jang SH, Chang WH, Park CH, Kim ST. 2010. Dynamic changes in the cortico-subcortical network during early motor learning. NeuroRehabilitation. 26:95–103.
Penny WD, Stephan KE, Mechelli A, Friston KJ. 2004. Comparing dynamic causal models. Neuroimage. 22:1157–1172.
Picard N, Strick PL. 2001. Imaging the premotor areas. Curr Opin Neurobiol. 11:663–672.
Prado J, Clavagnier S, Otzenberger H, Scheiber C, Kennedy H, Perenin MT. 2005. Two cortical systems for reaching in central and peripheral vision. Neuron. 48:849–858.
Quartarone A, Bagnato S, Rizzo V, Siebner HR, Dattola V, Scalfari A, Morgante F, Battaglia F, Romano M, Girlanda P. 2003. Abnormal associative plasticity of the human motor cortex in writer's cramp. Brain. 126:2586–2596.
Ragert P, Camus M, Vandermeeren Y, Dimyan MA, Cohen LG. 2009. Modulation of effects of intermittent theta burst stimulation applied over primary motor cortex (M1) by conditioning stimulation of the opposite M1. J Neurophysiol. 102:766–773.
Reetz K, Dogan I, Rolfs A, Binkofski F, Schulz JB, Laird AR, Fox PT, Eickhoff SB. 2012. Investigating function and connectivity of morphometric findings - Exemplified on cerebellar atrophy in spinocerebellar ataxia 17 (SCA17). Neuroimage. 62:1354–1366.
Rehme AK, Eickhoff SB, Wang LE, Fink GR, Grefkes C. 2011. Dynamic causal modeling of cortical activity from the acute to the chronic stage after stroke. Neuroimage. 55:1147–1158.
Ridding MC, Ziemann U. 2010. Determinants of the induction of cortical plasticity by non-invasive brain stimulation in healthy subjects. J Physiol. 588:2291–2304.
Rizzolatti G, Fogassi L, Gallese V. 2002. Motor and cognitive functions of the ventral premotor cortex. Curr Opin Neurobiol. 12:149–154.
Rizzolatti G, Luppino G. 2001. The cortical motor system. Neuron. 31:889–901.
Rizzolatti G, Luppino G, Matelli M. 1998. The organization of the cortical motor system: new concepts. Electroencephalogr Clin Neurophysiol. 106:283–296.
Rossini PM, Barker AT, Berardelli A, Caramia MD, Caruso G, Cracco RQ, Dimitrijevic MR, Hallett M, Katayama Y, Lucking CH. 1994. Non-invasive electrical and magnetic stimulation of the brain, spinal cord and roots: basic principles and procedures for routine clinical application. Report of an IFCN committee. Electroencephalogr Clin Neurophysiol. 91:79–92.
Rothwell JC, Hallett M, Berardelli A, Eisen A, Rossini P, Paulus W. 1999. Magnetic stimulation: motor evoked potentials. The International Federation of Clinical Neurophysiology. Electroencephalogr Clin Neurophysiol Suppl. 52:97–103.
Rouiller EM, Babalian A, Kazennikov O, Moret V, Yu XH, Wiesendanger M. 1994. Transcallosal connections of the distal forelimb representations of the primary and supplementary motor cortical areas in macaque monkeys. Exp Brain Res. 102:227–243.
Sarfeld AS, Diekhoff S, Wang LE, Liuzzi G, Uludag K, Eickhoff SB, Fink GR, Grefkes C. 2012. Convergence of human brain mapping tools: neuronavigated TMS parameters and fMRI activity in the hand motor area. Hum Brain Mapp. 33(5):1107–23.
Schubotz RI, von Cramon DY. 2003. Functional-anatomical concepts of human premotor cortex: evidence from fMRI and PET studies. Neuroimage. 20(Suppl 1):S120–S131.
Schuyler B, Ollinger JM, Oakes TR, Johnstone T, Davidson RJ. 2010. Dynamic causal modeling applied to fMRI data shows high reliability. Neuroimage. 49:603–611.
Shehzad Z, Kelly AM, Reiss PT, Gee DG, Gotimer K, Uddin LQ, Lee SH, Margulies DS, Roy AK, Biswal BB et al. 2009. The resting brain: unconstrained yet reliable. Cereb Cortex. 19:2209–2229.
Shimazu H, Maier MA, Cerri G, Kirkwood PA, Lemon RN. 2004. Macaque ventral premotor cortex exerts powerful facilitation of motor cortex outputs to upper limb motoneurons. J Neurosci. 24:1200–1211.
Stephan KE, Penny WD, Daunizeau J, Moran RJ, Friston KJ. 2009. Bayesian model selection for group studies. Neuroimage. 46:1004–1017.
Suppa A, Ortu E, Zafar N, Deriu F, Paulus W, Berardelli A, Rothwell JC. 2008. Theta burst stimulation induces after-effects on contralateral primary motor cortex excitability in humans. J Physiol. 586:4489–4500.
Talelli P, Cheeran BJ, Teo JT, Rothwell JC. 2007. Pattern-specific role of the current orientation used to deliver Theta Burst Stimulation. Clin Neurophysiol. 118:1815–1823.
Teo JT, Swayne OB, Rothwell JC. 2007. Further evidence for NMDA-dependence of the after-effects of human theta burst stimulation. Clin Neurophysiol. 118:1649–1651.
Terao Y, Ugawa Y. 2002. Basic mechanisms of TMS. J Clin Neurophysiol. 19:322–343.
Thickbroom GW. 2007. Transcranial magnetic stimulation and synaptic plasticity: experimental framework and human models. Exp Brain Res. 180:583–593.
Toni I, Krams M, Turner R, Passingham RE. 1998. The time course of changes during motor sequence learning: a whole-brain fMRI study. Neuroimage. 8:50–61.
Tsumoto T. 1992. Long-term potentiation and long-term depression in the neocortex. Prog Neurobiol. 39:209–228.
Van Dijk KR, Hedden T, Venkataraman A, Evans KC, Lazar SW, Buckner RL. 2010. Intrinsic functional connectivity as a tool for human connectomics: theory, properties, and optimization. J Neurophysiol. 103:297–321.
Wang LE, Fink GR, Diekhoff S, Rehme AK, Eickhoff SB, Grefkes C. 2011. Noradrenergic enhancement improves motor network connectivity in stroke patients. Ann Neurol. 69:375–388.
Ward NS, Brown MM, Thompson AJ, Frackowiak RS. 2003. Neural correlates of motor recovery after stroke: a longitudinal fMRI study. Brain. 126:2476–2496.
Yousry TA, Schmid UD, Alkadhi H, Schmidt D, Peraud A, Buettner A, Winkler P. 1997. Localization of the motor hand area to a knob on the precentral gyrus. A new landmark. Brain. 120(Pt 1): 141–157.
Zafar N, Paulus W, Sommer M. 2008. Comparative assessment of best conventional with best theta burst repetitive transcranial magnetic stimulation protocols on human motor cortex excitability. Clin Neurophysiol. 119:1393–1399.
Ziemann U, Lonnecker S, Steinhoff BJ, Paulus W. 1996. The effect of lorazepam on the motor cortical excitability in man. Exp Brain Res. 109:127–135.
zu Eulenburg P, Caspers S, Roski C, Eickhoff SB. 2012. Meta-analytical definition and functional connectivity of the human vestibular cortex. Neuroimage. 60:162–169.

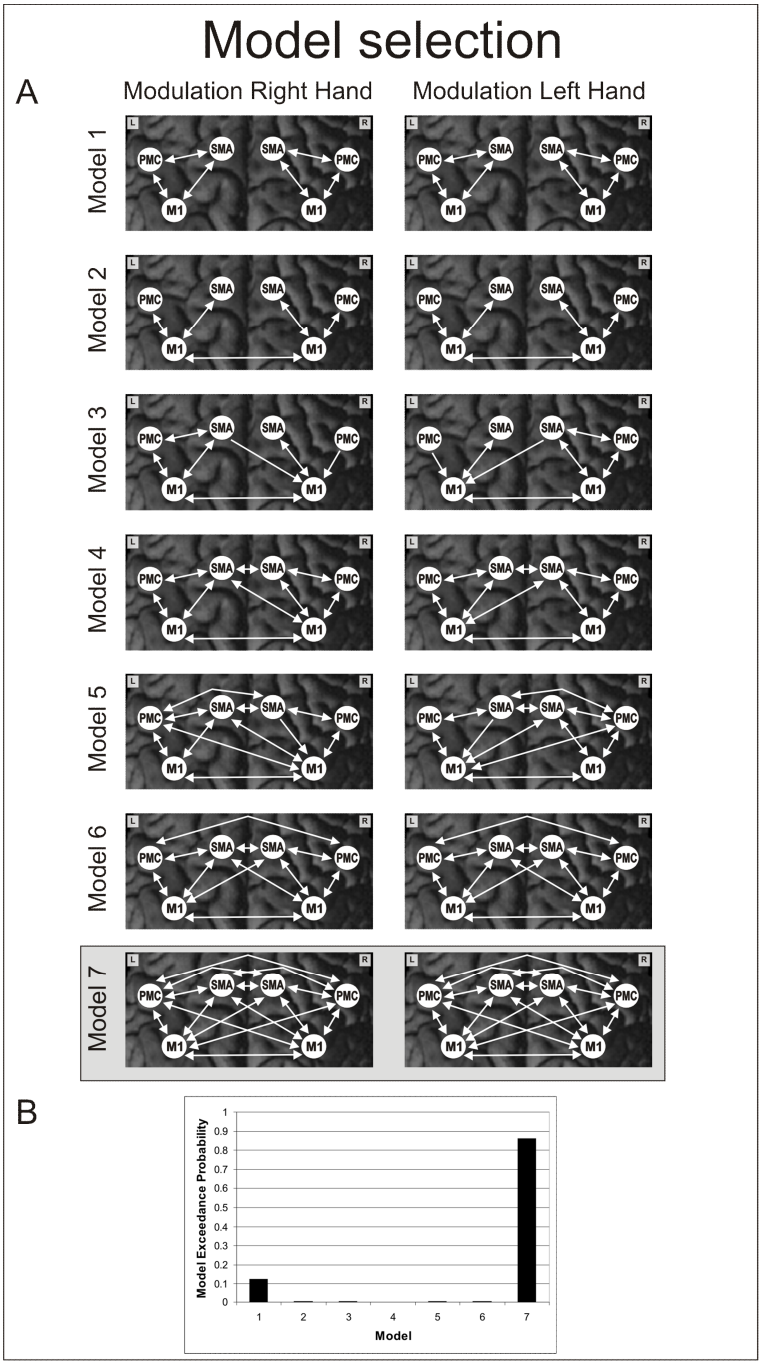

Suppl. Fig. 1. Cárdenas-Morales et al.

Suppl. Figure 1: Bayesian model selection. (A) Alternative connectivity models tested with DCM. All models are based on the same endogenous coupling matrix (i.e., a fully connected model). The seven models were tested against each other using Bayesian model selection (BMS) random effects analysis [Penny et al. 2004; Stephan et al. 2009]. The "winning model" (model 7) is highlighted by a gray box. Visual input provided by the right and left V1 into premotor regions are not shown in the figure. (B) Model exceedance probability for all 7 models, identifying model 7 as the "winning model", representing the best fit given the data.

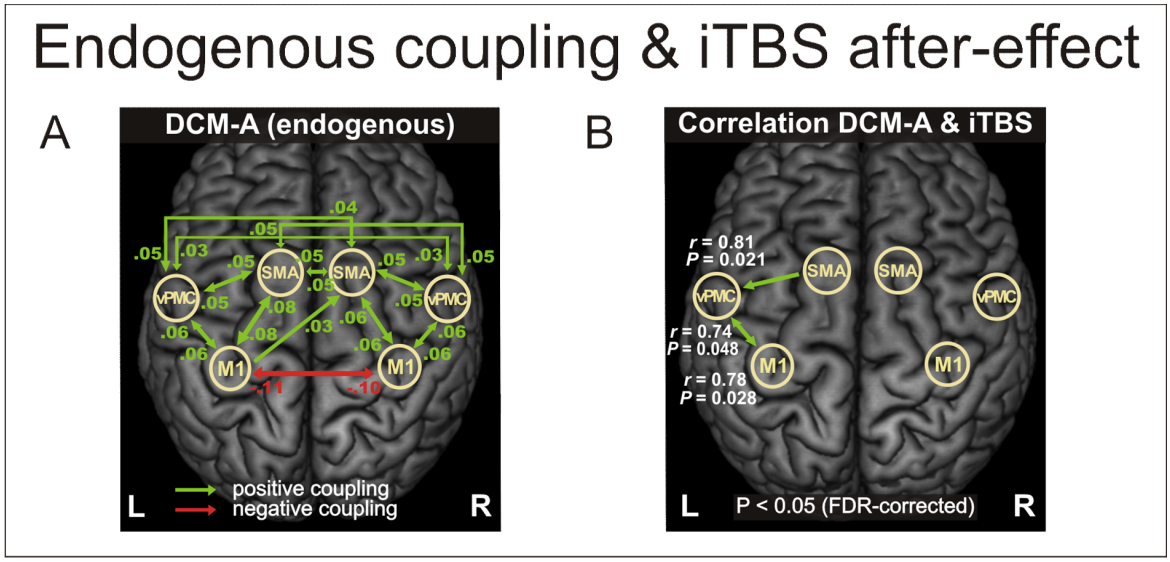

Suppl. Fig. 2. Cárdenas-Morales et al.

Suppl. Figure 2: (A) Endogenous coupling (DCM-A) of cortical motor regions as estimated by DCM ($P < 0.05$, FDR corrected). Coupling parameters suggest symmetrically organized endogenous connectivity in both hemispheres. (B) Correlation analysis between DCM-A coupling parameters and iTBS after-effect ($P < 0.05$, FDR corrected), showing similar but slightly weaker correlations compared to task-dependent connectivity (DCM-B, cf. Fig. 4). M1, primary motor cortex; SMA, supplementary motor area; vPMC, ventral premotor cortex.

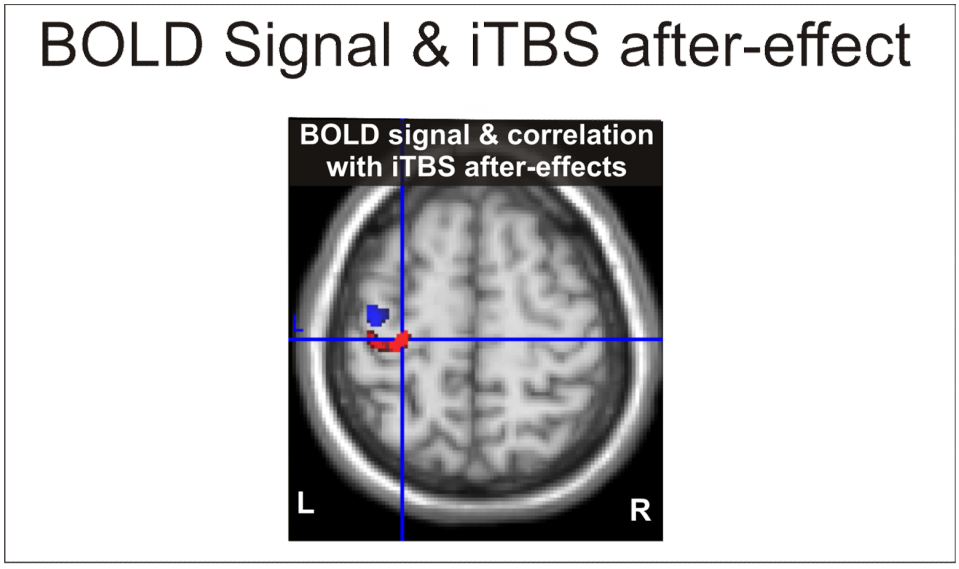

Suppl. Fig. 3. Cárdenas-Morales et al.

Suppl. Figure 3: BOLD signal and iTBS after-effect. The red cluster shows the peak voxel activity across all subjects during movement of the right hand (local maximum: -30, -24, 57). The blue cluster represents the voxels featuring the highest negative correlation between BOLD signal and individual iTBS-responses (local maximum: -40, -20, 52). Thus, subjects which showed less response to iTBS had a spatially more extended activation pattern during the motor task compared to subjects with high susceptibility to iTBS.

2.2 Dose-dependent effects of theta burst rTMS on cortical excitability and resting-state connectivity of the human motor system

Nettekoven C, Volz LJ, Kutscha M, Pool EM, Rehme AK, Eickhoff SB, Fink GR, Grefkes C

Journal of Neuroscience 2014 May 14; 34 (20): 6849-59

Development/Plasticity/Repair

Dose-Dependent Effects of Theta Burst rTMS on Cortical Excitability and Resting-State Connectivity of the Human Motor System

Charlotte Nettekoven,[1] Lukas J. Volz,[1,2] Martha Kutscha,[1] Eva-Maria Pool,[1] Anne K. Rehme,[1] Simon B. Eickhoff,[3,4] Gereon R. Fink,[2,3] and Christian Grefkes[1,2,3]

[1]Max Planck Institute for Neurological Research, 50931 Cologne, Germany, [2]Department of Neurology, Cologne University Hospital, 50924 Cologne, Germany, [3]Institute of Neuroscience and Medicine (INM-1, INM-3), Jülich Research Centre, 52428 Jülich, Germany, and [4]Institute of Clinical Neuroscience and Medical Psychology, Heinrich Heine University, 40225 Düsseldorf, Germany

Theta burst stimulation (TBS), a specific protocol of repetitive transcranial magnetic stimulation (rTMS), induces changes in cortical excitability that last beyond stimulation. TBS-induced aftereffects, however, vary between subjects, and the mechanisms underlying these aftereffects to date remain poorly understood. Therefore, the purpose of this study was to investigate whether increasing the number of pulses of intermittent TBS (iTBS) (1) increases cortical excitability as measured by motor-evoked potentials (MEPs) and (2) alters functional connectivity measured using resting-state fMRI, in a dose-dependent manner. Sixteen healthy, human subjects received three serially applied iTBS blocks of 600 pulses over the primary motor cortex (M1 stimulation) and the parieto-occipital vertex (sham stimulation) to test for dose-dependent iTBS effects on cortical excitability and functional connectivity (four sessions in total). iTBS over M1 increased MEP amplitudes compared with sham stimulation after each stimulation block. Although the increase in MEP amplitudes did not differ between the first and second block of M1 stimulation, we observed a significant increase after three blocks (1800 pulses). Furthermore, iTBS enhanced resting-state functional connectivity between the stimulated M1 and premotor regions in both hemispheres. Functional connectivity between M1 and ipsilateral dorsal premotor cortex further increased dose-dependently after 1800 pulses of iTBS over M1. However, no correlation between changes in MEP amplitudes and functional connectivity was detected. In summary, our data show that increasing the number of iTBS stimulation blocks results in dose-dependent effects at the local level (cortical excitability) as well as at a systems level (functional connectivity) with a dose-dependent enhancement of dorsal premotor cortex-M1 connectivity.

Key words: **functional connectivity; iTBS; neural plasticity; premotor cortex; resting-state fMRI; supplementary motor area**

Introduction

Neural plasticity describes the fundamental property of the brain to undergo structural and functional modifications after patterns of activity or stimulation (Pascual-Leone et al., 2005). Repetitive transcranial magnetic stimulation (rTMS) can be used to alter electrophysiological properties of cortical areas (Wassermann, 1998). Depending on stimulation frequency and pattern, rTMS may enhance or suppress cortical excitability with effects extending beyond the stimulation period (Pascual-Leone et al., 1998). However, responses to rTMS vary considerably between subjects, and the mechanisms underlying excitability changes remain poorly understood (Ridding and Ziemann, 2010; Hamada et al., 2013).

Intermittent theta burst stimulation (iTBS) is a specific rTMS protocol that effectively increases cortical excitability of the targeted brain region after a relatively short stimulation period (Huang et al., 2005; Di Lazzaro et al., 2008; Gamboa et al., 2010, 2011; Cárdenas-Morales et al., 2013). Neuropharmacological studies suggest that the response to iTBS, at least in part, depends on NMDA-receptor activity (Huang et al., 2007; Teo et al., 2007). Data obtained in rats imply that iTBS interferes with the cellular expression of various neuronal proteins reflecting the activity level of the GABAergic inhibitory system (Benali et al., 2011; Funke and Benali, 2011). Moreover, the application of multiple iTBS blocks has a dose-dependent effect on the expression of these proteins in rodents (Volz et al., 2013). In contrast, studies in humans thus far failed to demonstrate additive aftereffects of multiple iTBS blocks on motor–cortical excitability (Gamboa et al., 2010, 2011).

Received Nov. 27, 2013; revised April 7, 2014; accepted April 10, 2014.

Author contributions: C.N., L.J.V., G.R.F., and C.G. designed research; C.N., M.K., and E.-M.P. performed research; A.K.R., S.B.E., and C.G. contributed unpublished reagents/analytic tools; C.N., L.J.V., M.K., E.-M.P., A.K.R., and C.G. analyzed data; C.N., L.J.V., S.B.E., G.R.F., and C.G. wrote the paper.

This work was supported by Deutsche Forschungsgemeinschaft Grants GR 3285/2-1, GR3285/5-1, and KFO219-TP8 to C.G., National Institutes of Health Grant R01-MH074457-01A1 to S.B.E., Deutsche Forschungsgemeinschaft Grants EI 816/4-1 and LA 3071/3-1, the Helmholtz Initiative on Systems Biology, and the European EFT program (Human Brain Project). G.R.F. was supported by the Marga and Walter Boll Stiftung. We thank our volunteers and Dr. Marc Tittgemeyer and the MR staff of the Max Planck Institute for Neurological Research for support.

The authors declare no competing financial interests.

Correspondence should be addressed to Dr. Christian Grefkes, Department of Neurology, Uniklinik Köln, Kerpener Straße 62, 50924 Köln, Germany. E-mail: Christian.Grefkes@uk-koeln.de.

DOI:10.1523/JNEUROSCI.4993-13.2014

 0270-6474/14/346849-11$15.00/0

Importantly, rTMS not only influences neuronal properties of the stimulated region but may also impact on the activity levels of remote but interconnected areas (Bestmann et al., 2003, 2004, 2005). Studies using different kinds of rTMS protocols provide converging evidence that rTMS can be used to modulate connectivity of a given region within a network of brain areas (Grefkes et al., 2010; Vercammen et al., 2010; Eldaief et al., 2011; van der Werf et al., 2010; Watanabe et al., 2014). The wealth of studies using rTMS to modulate human cortical excitability is contrasted by the dearth of data regarding dose-dependent effects of rTMS or iTBS on both local neural activity under the stimulated area and on remote effects.

In the current study, we thus addressed the question whether a repeated iTBS application in humans exerts dose-dependent effects on (1) regional, cortical excitability in the primary motor cortex (M1) and/or (2) motor–network connectivity of the stimulated site (here, M1). To this end, we used a multimodal approach, where each of three serially applied iTBS blocks was followed by the assessment of (1) motor-evoked potentials (MEPs, corticospinal excitability) or (2) resting-state fMRI (functional connectivity) on separate days. Based on previous findings (Gamboa et al., 2010, 2011; Volz et al., 2013), we hypothesized that iTBS increases cortical excitability in a dose-dependent way. Moreover, we hypothesized that iTBS induces changes in resting-state functional connectivity (rsFC) between the stimulated M1 and other regions of the (cortical) motor network (Vercammen et al., 2010; Eldaief et al., 2011; van der Werf et al., 2010).

Materials and Methods

Subjects

We included 16 healthy, right-handed subjects (7 males, mean ± SD age: 27 ± 3 years) with no history of neurological or psychiatric diseases. All subjects provided informed written consent. Right-handedness was verified using the Edinburgh Handedness Inventory (Oldfield, 1971). The study was performed according to the Declaration of Helsinki (1969, last revision 2008) and approved by the local ethics committee.

Experimental design

Main experiment. We used a single-blind, vertex stimulation controlled crossover within-subject design to test for the effects of multiple serially applied iTBS blocks on (1) cortical excitability and (2) functional connectivity. The experimental design is illustrated in Figure 1. Each subject participated in two MEP sessions (to assess cortical excitability) and two fMRI sessions (to assess cortical connectivity) on different days (main experiment, Fig. 1*A*). Sessions were separated by at least 1 week to avoid carryover effects. To test for dose-dependent effects, subjects received three iTBS applications with 600 pulses per application (see below) interrupted by a stimulation break of 15 min (compare Volz et al., 2013) in each session. In

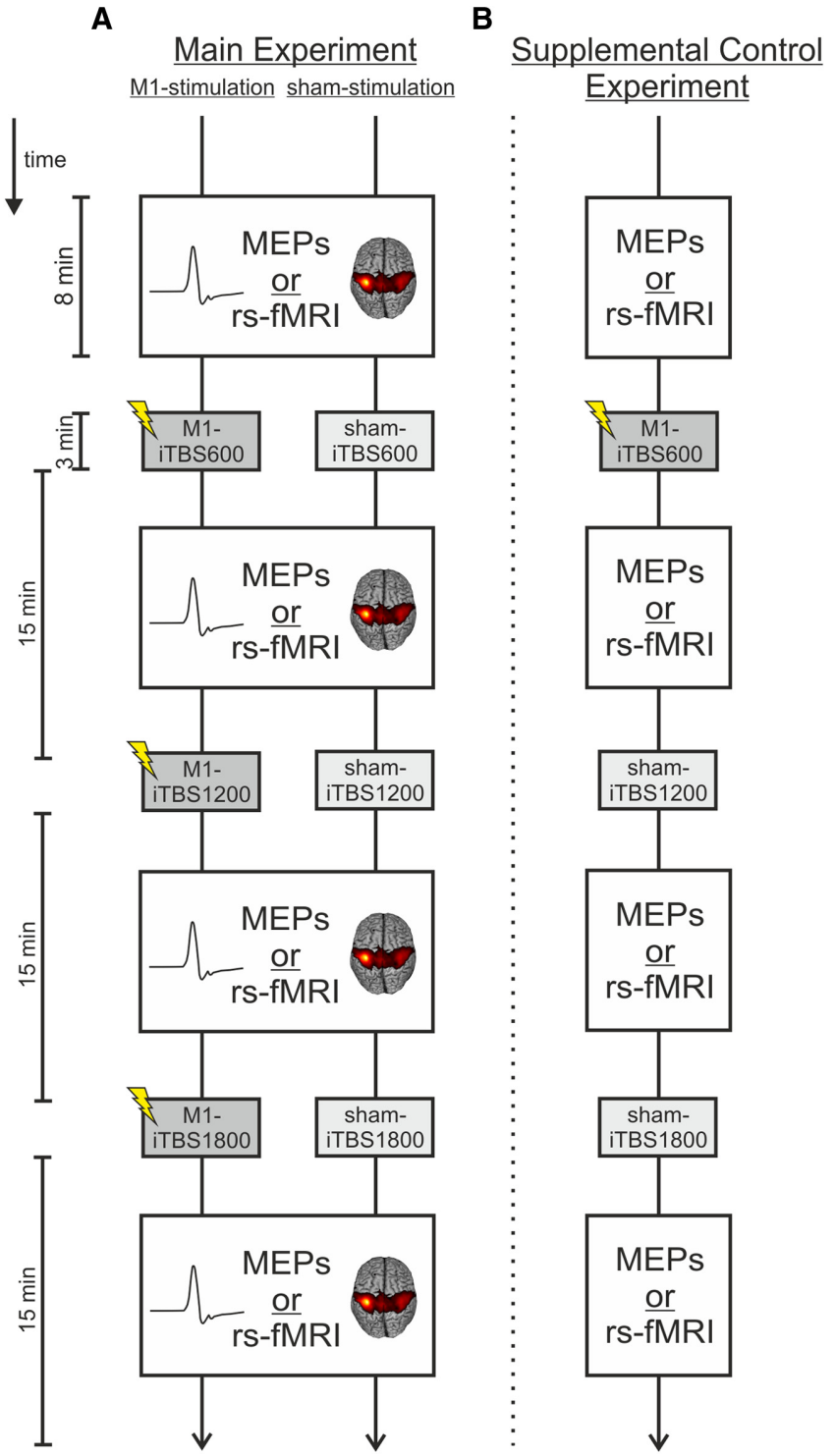

Figure 1. Experimental design. ***A***, Main experiment. Subjects took part in two MEP sessions (M1-iTBS_MEPs, sham-iTBS_MEPs) and two resting-state fMRI sessions (M1-iTBS_rs-fMRI, sham-iTBS_rs-fMRI) on four separate days. Using a within-subject design, each subject received three serially applied iTBS blocks over M1 (M1 stimulation) and over the parieto-occipital vertex (sham stimulation), each followed by the assessment of MEPs or resting-state fMRI. ***B***, Supplemental control experiment. In a second experiment, a subgroup of 6 subjects additionally received one stimulation over M1 followed by two stimulations over the parieto-occipital vertex (supplemental control stimulation) to test for the specificity of additive aftereffects after serial iTBS over M1.

two of the four sessions, subjects were stimulated over M1 of the dominant (left) hemisphere (M1 stimulation). In the other two sessions, stimulation was applied over the parieto-occipital vertex (sham stimulation). Thus, each subject underwent the following four sessions: M1-iTBS_MEPs, sham-iTBS_MEPs, M1-iTBS_rs-fMRI, and sham-iTBS_rs-fMRI. In the MEP sessions, MEPs were measured at baseline and after each iTBS block. Likewise, in the fMRI sessions, resting-state fMRI time series were acquired at baseline and after each iTBS block. Importantly, MEP and resting-state fMRI measurements were performed within a similar time frame: both recordings were started ~3 min after the end of iTBS applications, and lasted ~8 min (controlled by a stopwatch). The order of M1 and sham stimulation was randomized between subjects.

Supplemental control experiment. Six participants from the main experiment were tested in a control experiment to test for the specificity of putative aftereffects after serial iTBS over M1 (Fig. 1*B*). Stimulation aftereffects were again tested with MEPs and resting-state fMRI on separate days. In contrast to the main experiment, subjects now received only one iTBS block over M1 followed by two sham stimulation blocks over the vertex (supplemental control experiment, Fig. 1*B*). Data from the main experiment (3 × M1 stimulation) were replotted for this subgroup of subjects ($n = 6$). This allowed us to differentiate dose-dependent changes in MEP amplitudes and rsFC after three consecutive M1-iTBS blocks from stimulation effects resulting from the first M1-iTBS block and consecutive changes over time.

Neuronavigated transcranial magnetic stimulation

The position of the TMS coil was tracked and recorded using the neuronavigation system "BrainSight2" (Rogue Research). For neuronavigation, the head of the subject was coregistered with an individual high-resolution anatomical MR image (voxel size: $1.0 \times 1.0 \times 1.0\ mm^3$, FOV = 256 mm, 176 sagittal slices, TR = 2250 ms, TE = 3.93 ms) via anatomical landmarks (e.g., nasion and crus helicis) before the hotspot search.

MEP amplitudes of the abductor pollicis brevis (APB) muscle were measured using Ag/AgCl surface electrodes (Tyco Healthcare) in a belly-tendon montage. The EMG signal was amplified, filtered (0.5 Hz high pass and 30–300 Hz bandpass), and digitized with a Powerlab 26T device and the LabChart software package version 5 (AD Instruments).

For the initial positioning of the TMS coil, the M1 "hand knob" formation was used as an anatomical landmark (Yousry et al., 1997). The coil was positioned tangentially to the scalp with the handle pointing posterolaterally. The stimulation "hotspot" for iTBS and MEP acquisition was defined as the location where MEPs with highest amplitude and lowest latency could be evoked. Then, the resting motor threshold (RMT) was defined using an algorithm provided by the TMS Motor Threshold Assessment Tool 2.0 (http://www.clinicalresearcher.org/software.htm). The software defines the RMT in 12 steps using maximum likelihood calculations based on positive (peak-to-peak amplitude of at least 50 μV) or negative MEP responses as marked by the investigator via button press. The RMT was assessed at baseline and after the third iTBS application on each of the four sessions.

Theta burst stimulation

We used the iTBS protocol described by Huang et al. (2005). Accordingly, iTBS consisted of three pulses delivered at a frequency of 50 Hz (1 burst) applied every 200 ms for 2 s (10 bursts), repeated every 10 s for a total duration of 191 s (600 pulses). As previously described and evaluated, iTBS was delivered at 70% of the RMT (Gentner et al., 2008; Sarfeld et al., 2012; Cárdenas-Morales et al., 2013). This is a slight modification to the original iTBS protocol according to which iTBS has been applied at 80% of the individual active motor threshold (AMT) (Huang et al., 2005). Our intention was to prevent voluntary preactivation of the target muscle, which may impact on TBS aftereffects (Gentner et al., 2008; Huang et al., 2008) but is necessary to assess the AMT. Evidence suggests that 70% RMT reflects a comparable range of absolute stimulator output intensities compared with 80% AMT (Chen et al., 1998; Sarfeld et al., 2012). Furthermore, previous studies already applied TBS with 70% of the RMT and reported aftereffects that are in perfect accordance to results using a stimulation intensity of 80% AMT (Gentner et al., 2008; Cárdenas-Morales et al., 2013).

We applied iTBS either over the left, dominant M1 (i.e., the "hotspot") or over the parieto-occipital vertex as sham stimulation (Herwig et al., 2007, 2010). For sham stimulation, the same stimulator output intensity was used as for M1 stimulation. To reduce possible cortical stimulation effects in the sham condition, the coil was held at 45°, touching the skull not with the center but with the rim opposite the handle. In this position, the coil–cortex distance is substantially larger such that the electromagnetic field, if at all reaching the cortex, is substantially weaker and far outside the target range (Herwig et al., 2007, 2010).

On each of the 4 d, iTBS was repeated three times (either 3 × M1 stimulation or 3 × sham stimulation over the vertex) separated by 15 min, leading to a total of 1800 pulses (i.e., iTBS600, iTBS1200, iTBS1800; Figure 1*A*). This protocol was previously shown to evoke additive iTBS aftereffects at the cellular level in rats (Volz et al., 2013). Use of the neuronavigation system warranted a reliable positioning of the TMS stimulation site across all sessions and subjects. iTBS was delivered using a Magstim SuperRapid 2 with a figure-of-eight coil (70 mm standard coil, Magstim).

MEPs

Motor cortex excitability was assessed via MEPs recorded from the APB. Neuronavigated single-pulse TMS was applied over the same location as used for iTBS (motor–cortical representation of the APB at the M1 "hand knob" formation) using a monophasic Magstim 200^2 stimulator (Magstim). In line with other groups (Huang et al., 2005; Hamada et al., 2013), we used different stimulators for MEP acquisition and delivery of iTBS for the following reason: The SuperRapid2 stimulator, which we used for high-frequency (burst) stimulation (i.e., iTBS), induces MEPs with biphasic waveforms exciting different neuronal populations during the different phases of the pulse. In contrast, the monophasic waveform of the Magstim 200^2 stimulator, which we used for MEP acquisition, results in more homogeneous MEPs and hence represents the standard way of assessing electrophysiological properties of M1 (Terao and Ugawa, 2002; Di Lazzaro et al., 2004). iTBS-induced changes in cortical excitability are comparable, regardless of the waveform (mono/bisphasic) used to evoke MEPs via single-pulse TMS (Zafar et al., 2008).

At baseline and after each iTBS application (three blocks separated by 15 min), a stimulus–response curve of MEPs evoked with 90%–150% of the RMT was assessed in steps of 10%. TMS pulses were applied at ~0.1–0.2 Hz (acquisition time, ~8 min). Two blocks of five pulses were recorded in a randomized order for each intensity, except for 120%, which was assessed in six blocks at five pulses (because 120% represents the commonly used stimulation intensity, see e.g., Kobayashi et al., 2004; Cárdenas-Morales et al., 2013), adding up to a total number of 90 MEPs. Ten MEPs per intensity have been shown to result in reliable stimulus–response curves (Carroll et al., 2001).

Data analysis (MEPs)

For each subject and session (M1 stimulation, sham stimulation), MEP amplitudes acquired after iTBS were normalized to baseline values (i.e., MEPs acquired before the first iTBS application in the respective session) of the respective intensity. This means that after normalization all MEPs for a given intensity of the stimulus–response curve were close to 1.0 (i.e., 100%) in case that there was no difference in MEP amplitudes after iTBS. We used normalized MEP amplitudes to assess changes in cortical excitability rather than absolute MEP amplitudes to account for variance in RMTs at different stimulation days (i.e., M1 and sham stimulation). Normalized MEP amplitudes were then entered into a three-way repeated-measures ANOVA with the factors intervention (2 levels: M1-iTBS, sham-iTBS), dose (3 levels: iTBS600, iTBS1200, iTBS1800), and intensity (7 levels: 90–150% of the RMT) using SPSS version 21 (Statistical Package for the Social Sciences, IBM). In case of significant main or interaction effects, *post hoc* Student's *t* tests were performed to compare the aftereffects of the two types of stimulation and the different doses applied. Given the clear directional hypothesis that iTBS would increase MEP amplitudes (Huang et al., 2005, 2007; Di Lazzaro et al., 2008; Cárdenas-Morales et al., 2013), we used one-tailed *post hoc t* tests ($p \leq 0.05$).

Finally, stimulus–response curves were plotted for each subject using the absolute MEP amplitudes. The steepness of the curves was computed

by means of linear regression analyses, and R^2 values were calculated to assess the quality of fit using SPSS. Stimulation-induced changes were again tested by a repeated-measures ANOVA.

MRI

The experimental procedures (iTBS applications) of the fMRI sessions were equivalent to those of the MEP sessions (Fig. 1*A*). Instead of MEP acquisition, however, resting-state fMRI time series were acquired at baseline and after each block of iTBS. Before the baseline fMRI measurements, the "hotspot" and RMT were assessed using the neuronavigation setup described above. Subjects were transported in an MR-compatible wheelchair into the scanner room between each resting-state fMRI and iTBS block to avoid any further movement and to obtain comparable conditions for the resting-state scans.

The fMRI sessions started with a baseline resting-state scan (duration ~8 min) where subjects were instructed to lie motionless in the scanner with open eyes fixating a red cross, which was presented on a TFT screen visible through a mirror attached to the MR head coil. After completion of the resting-state time-series, subjects were asked to perform an active motor task, which served as a functional localizer for determining coordinates of M1 and other motor related regions for subsequent analyses (see below). This "activity" condition was acquired after the resting state scan (i.e., resting-state connectivity estimates were not systematically influenced by prior motor activity).

After completion of the baseline fMRI session, subjects were transported from the scanner to the anteroom of the MR console (again sitting in the MR wheelchair without moving their right arm). After coregistration with the neuronavigation system (lasting 1–2 min), three blocks of iTBS were applied separated by 15 min (controlled by a stopwatch). Each of the three iTBS blocks was followed by another 8 min resting-state fMRI. Hence, the time protocol in the fMRI sessions was identical to the one used in the MEP sessions (Fig. 1).

Localizer task. We used a simple motor task as a functional localizer to identify the location of core motor regions for the subsequent resting-state analysis. The localizer task consisted of rhythmic thumb abductions and adductions with the right or left hand activating the same muscle as used for TMS recordings (APB). Left hand movements were necessary to also localize motor regions of the hemisphere contralateral to stimulation. Written instructions displayed for 2 s indicated movements of the left or right thumb for the following block of trials. Abduction–adduction movements were triggered by a blinking circle at the frequency of 1.0 Hz for 15 s until a black screen indicated to rest for 15 s. Six blocks for each hand resulted in an acquisition time of ~7 min. Motor performance was visually controlled during the whole assessment by the experimenter.

Image acquisition and preprocessing (task and resting-state fMRI)

fMRI images were aquired on a Siemens Trio 3.0 T scanner (Siemens Medical Solutions) using a gradient echo planar imaging (EPI) sequence with following parameters: TR = 2070 ms, TE = 30 ms, FOV = 200 mm, 31 slices, voxel size: 3.1 × 3.1 × 3.1 mm^3, 20% distance factor, flip angle = 90°, resting-state: 225 volumes (3 dummy images), localizer task: 202 volumes (3 dummy images). Acquisition planes and slice orientation were identical for the four fMRI assessments (i.e., 1 × baseline, 3 × post iTBS sessions) in both the M1 and sham stimulation condition. The slices covered the whole brain extending from the vertex to the lower parts of the cerebellum.

fMRI data were analyzed using Statistical Parametric Mapping (SPM8, http://www.fil.ion.ucl.ac.uk/spm/). The first three volumes ("dummy" images) of each session were discarded from further analyses to allow for magnetic field saturation. All remaining EPI volumes were realigned to the mean image of each time series and coregistered with the structural T1-weighted image. In a next step, all images were spatially normalized to the standard template of the MNI using the unified segmentation approach (Ashburner and Friston, 2005) and smoothed using an isotropic Gaussian kernel of 8 mm full-width at half-maximum.

Statistical analysis: functional localizer task

In the functional localizer task, the two experimental conditions (movements of the left or right thumb) were modeled using boxcar stimulus functions convolved with a canonical hemodynamic response function. The time series of each voxel were high-pass filtered at 1/128 Hz. The six head motion parameters, as assessed by the realignment algorithm, were treated as covariates to remove movement-related variance from the image time series. Simple main effects for each experimental condition were calculated for each subject by applying appropriate baseline contrasts. Voxels were identified as significant on the single-subject level if their *T*-values passed a height threshold of $p \leq 0.001$ ($T = 3.14$). The individual M1 coordinates of the stimulated hemisphere were then used as seed regions for the resting-state whole-brain analysis (see below). For the group analysis, the parameter estimates of all conditions (main effect right thumb movements, main effect left thumb movements) were subsequently entered into a full factorial ANOVA. Voxels were considered significant when passing a height threshold of $p \leq 0.05$, family-wise error (FWE)-corrected ($T = 5.72$).

Table 1. Single-subject coordinates of left primary motor cortex (M1) derived from the respective motor task baseline conjunction of both assessment days[a]

	MNI coordinates		
Subject	*x*	*y*	*z*
1	−34.5	−25.5	57
2	−40.5	−24	61.5
3	−40.5	−22.5	64.5
4	−37.5	−16.5	54
5	−30	−31.5	70.5
6	−40.5	−19.5	63
7	−42	−16.5	58.5
8	−31.5	−24	70.5
9	−33	−27	49.5
10	−40.5	−22.5	48
11	−42	−21	48
12	−39	−24	54
13	−43.5	−21	60
14	−43.5	−21	63
15	−36	−30	57
16	−34.5	−28.5	60
Mean	−37	−24	56.4
SD	4.9	3.2	5.4

[a]Single-subject coordinates were used as seed regions for the resting-state whole-brain analysis.

Statistical analysis: resting-state fMRI

For the statistical analysis of the resting-state data, variance that could be explained by known confounds was removed from the smoothed fMRI time-series. Confound regressors included the tissue-class-specific global signal intensities and their squared values, the six head motion parameters, their squared values, and their first-order derivatives (Jakobs et al., 2012; Reetz et al., 2012; Satterthwaite et al., 2013). A bandpass filter was used to preserve only frequencies between 0.01 and 0.08 Hz in the time-series data.

First, a seed-based whole-brain group analysis was computed: the time course within a sphere of 10 mm-diameter centered on the seed voxel (here, left M1, single-subject coordinates derived from localizer task; Table 1) was correlated with the time course of every other voxel in the brain by means of linear Pearson's correlation (Eickhoff and Grefkes, 2011; zu Eulenburg et al., 2012). Correlation coefficients were converted to Fisher's *z*-scores using the formula $z = (1/2) \times \ln(1 + r)/(1 - r) = \text{atanh}(r)$ to yield approximately normally distributed data.

To determine changes in functional connectivity after iTBS, individual baseline functional connectivity maps were subtracted from the respective maps after iTBS for each subject. For group level analysis, the individual subtraction maps were subsequently entered into a "flexible factorial" general linear model analysis in SPM8 with the factors subject and intervention (2 levels: M1-iTBS and sham-iTBS) and dose (3 levels: iTBS600, iTBS1200, and iTBS1800). Then, differential contrast were computed between (1) M1 and sham stimulation for iTBS600, iTBS1200, and iTBS1800, as well as (2) between the different doses applied (i.e., iTBS1800/iTBS1200, iTBS1800/iTBS600, and iTBS1200/iTBS600) for both stimulation conditions. The resting-state maps were masked by

Table 2. Single-subject coordinates of left primary visual cortex (V1)

	MNI coordinates		
Subjects	*x*	*y*	*z*
1	−10.5	−94.5	−9
2	0	−94.5	−16.5
3	−16.5	−103.5	−4.5
4	−9	−100.5	−12
5	−18	−88.5	−9
6	−19.5	−99	−15
7	−16.5	−105	−9
8	−16.5	−99	−12
9	−16.5	−100.5	−6
10	−15	−102	1.5
11	−13.5	−102	−6
12	−18	−102	−9
13	−18	−102	−9
14	−16.5	−102	−10.5
15	−15	−96	−3
16	−12	−105	−12
Mean	−18.6	−101.3	−10
SD	6.8	3.1	3.9

cytoarchitectonic probability maps of frontoparietal sensorimotor areas (Brodmann areas 6, 4 a/b, 3 a/b, 2, and 1) to focus inference on rsFC within the cortical sensorimotor network as provided by the SPM Anatomy Toolbox (Eickhoff et al., 2005). The statistical threshold was set to $p \leq 0.05$, family-wise error (FWE)-corrected at the cluster level.

Finally, to test whether iTBS applied over M1 also had influences on functional connectivity of nonmotor networks, an additional group analysis was performed for the visual network using an equivalent procedure as for the M1 maps. Accordingly, seed-based whole-brain connectivity maps were computed using the left primary visual cortex (V1) as seed region (Table 2; individual coordinates were derived from the localizer task). Like the M1 maps, visual resting-state connectivity maps were subsequently masked by the respective cytoarchitectonic probability maps as provided by the SPM Anatomy Toolbox (Eickhoff et al., 2005).

ROI analysis

As we hypothesized that rsFC would increase dose-dependently between M1 and distinct motor regions, we performed small-volume corrections in different ROIs for following contrasts: iTBS1800 versus iTBS600, iTBS1800 versus iTBS1200, and iTBS1200 versus iTBS600. Based on previous studies, reporting altered neural activity or rsFC after rTMS in distinct motor regions (Bestmann et al., 2004; Watanabe et al., 2014), we chose the following ROIs (group MNI coordinates, *x y z*): bilateral supplementary motor area (SMA, left: −4.5, −9, 64.5, right: 6, −3, 69), bilateral dorsal premotor cortex (dPMC, left: −31.5, −9, 60, right: 36, −9, 60), and right contralateral M1 (30, −28, 57). Connectivity estimates in these regions were FWE-corrected on the voxel level ($p < 0.05$) using 10 mm spheres centered around the respective ROI coordinate.

Correlation between MEP amplitudes and rsFC

Finally, we tested for correlations between dose-dependent changes observed at the electrophysiological level (i.e., MEPs) and changes at the systems level (i.e., rsFC). Therefore, contrast images (iTBS1800 vs iTBS1200; iTBS1800 vs iTBS600) were entered into SPM multiple regression analyses, including differences in normalized MEP amplitudes (iTBS1800 vs iTBS1200; iTBS1800 vs iTBS600) as covariates.

Results

iTBS aftereffects on electrophysiological parameters

Main experiment

Resting motor thresholds did not differ between M1 (32.3 ± 6.3% maximal stimulator output [MSO]) and sham stimulation (33.4 ± 7.3% MSO) ($p = 0.164$). Furthermore, iTBS had no effect on the RMT after the third iTBS block compared with baseline (M1 stimulation: 32.5 ± 6.8% MSO, $p = 0.78$; sham stimulation: 33.7 ± 6.2% MSO, $p = 0.74$). MEP amplitudes acquired at baseline were also not significantly different for M1 compared with sham stimulation ($p > 0.3$ for each comparison).

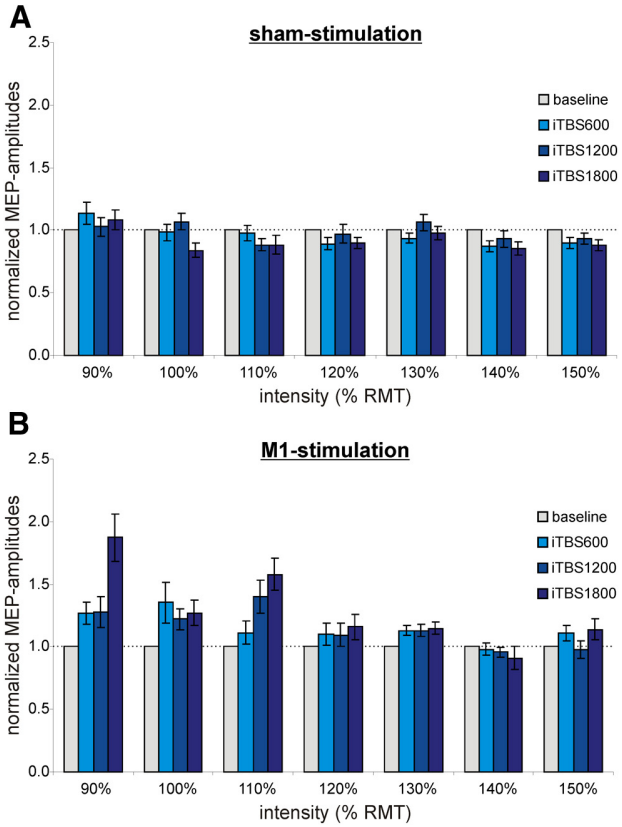

Figure 2. Main experiment: MEP amplitudes normalized to baseline (gray) at different stimulation intensities relative to the RMT. ***A***, sham stimulation. ***B***, M1 stimulation. Dose-dependent iTBS aftereffects seem to be more pronounced at near-threshold stimulation intensities (90%–110% of the RMT) compared with higher stimulation intensities (120%–150% of the RMT).

A three-way repeated-measures ANOVA testing for iTBS aftereffects on normalized MEP amplitudes revealed a significant main effect of the factor intervention (two levels: M1-iTBS, sham-iTBS; $F_{(1,15)} = 8.78$, $p = 0.010$) and an interaction effect for intervention (two levels: M1-iTBS, sham-iTBS) × dose (three levels: iTBS600, iTBS1200, iTBS1800) ($F_{(2,30)} = 5.61$, $p = 0.009$). The interaction effect indicated that there was a dose-dependent effect on MEP amplitudes depending on whether subjects received M1-iTBS or sham-iTBS. In contrast, there were no significant effects of the factor intensity (seven levels: 90%–150% RMT, $p \geq 0.05$ for each comparison). However, the interaction effect of the factors intervention × dose × intensity showed a statistical trend ($F_{(12,180)} = 1.60$, $p = 0.095$). When plotting the normalized MEP amplitudes for the different intensities (Fig. 2), dose-dependent iTBS aftereffects tended to be more pronounced at low-stimulation intensities (90%–110% RMT) compared with higher-stimulation intensities (120%–150% RMT).

To further explore what drives the significant interaction effect intervention × dose, we performed *post hoc t* tests on MEPs averaged across intensities for a given block of iTBS. This analysis showed that averaged MEP amplitudes were significantly higher after M1-iTBS compared with sham-iTBS for all doses: iTBS600 ($p = 0.019$), iTBS1200 ($p = 0.040$), and iTBS1800 ($p = 0.002$) (Fig. 3). Furthermore, aftereffects of M1-iTBS were significantly enhanced for iTBS1800 compared with iTBS1200 ($p = 0.042$) and iTBS600 ($p = 0.024$), whereas there was no significant difference between

iTBS600 and iTBS1200 ($p = 0.390$). In the sham condition, MEPs decreased after iTBS1800 compared with iTBS1200 ($p = 0.023$) (Fig. 3). There was no significant difference between iTBS600 and iTBS1200 as well as iTBS1800 after sham stimulation.

In addition, to test whether increases in MEP amplitudes after M1 stimulation were significantly different from baseline, we computed one-sample t tests on the respective differences for each stimulation session. We found that normalized MEP amplitudes after 600 ($p = 0.047$) and 1800 ($p = 0.013$) pulses of iTBS over M1 were significantly higher compared with baseline and that a strong statistical trend was evident after 1200 pulses of M1-iTBS ($p = 0.052$). When computing t tests on absolute MEP amplitudes, significant differences were also observed between baseline MEPs and iTBS1800 ($p < 0.01$), whereas differences between baseline and iTBS600 and iTBS1200 did not pass the statistical thresholds. This result can be explained by the large amount of between-subject variance in absolute MEP amplitudes at baseline (range: 0.2–2.2 mV), highlighting the importance of normalization for detecting stimulation aftereffects (Huang et al., 2005, 2008; Gentner et al., 2008).

Averaged R^2 values indicated a good fit of the stimulus–response curves to the linear regression models (M1 stimulation: $R^2 = 0.86 \pm 0.02$, sham stimulation: $R^2 = 0.87 \pm 0.03$). To test whether stimulation over M1 altered the steepness of the stimulus–response curves, the slopes of the individual stimulus–response curves were entered into a repeated-measures ANOVA. However, this analysis did not show a significant effect of the factor dose (4 levels: baseline, iTBS600, iTBS1200, and iTBS1800), indicating that increasing the number of iTBS pulses had no effect on the slope of the stimulus–response curves.

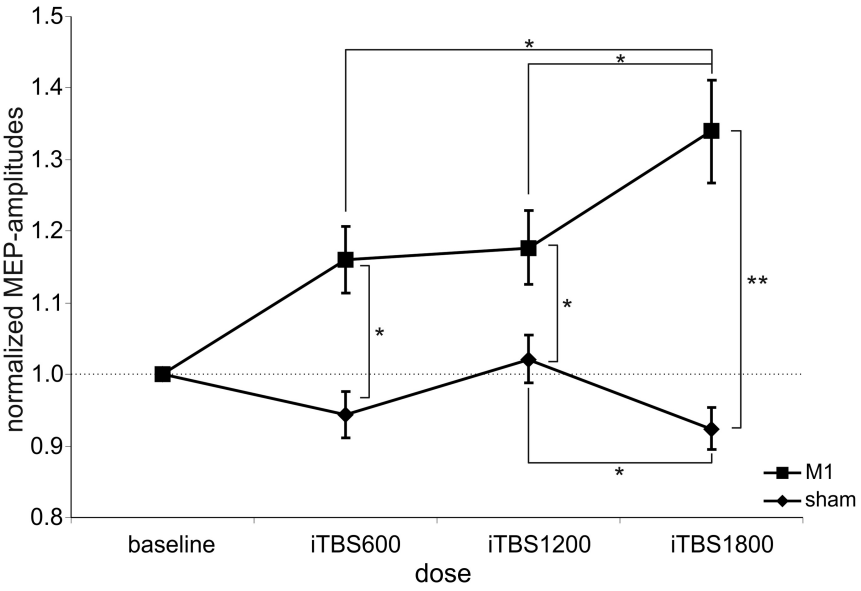

Figure 3. Main experiment: M1 versus sham stimulation. Changes in MEP amplitudes after M1 (squares) and sham stimulation (diamonds), normalized to baseline MEP amplitudes. Significant aftereffects after M1-iTBS compared with sham-iTBS or within stimulation conditions: *$p \leq 0.05$ (Student's t test); **$p \leq 0.001$ (Student's t test). M1-iTBS led to a significant increase in MEP amplitudes after iTBS600, iTBS1200, and iTBS1800 compared with sham stimulation and baseline. The increase after M1-iTBS1800 was significantly higher than that after M1-iTBS600 and M1-iTBS1200, whereas after sham-iTBS MEP amplitudes significantly decreased between iTBS1200 and iTBS1800.

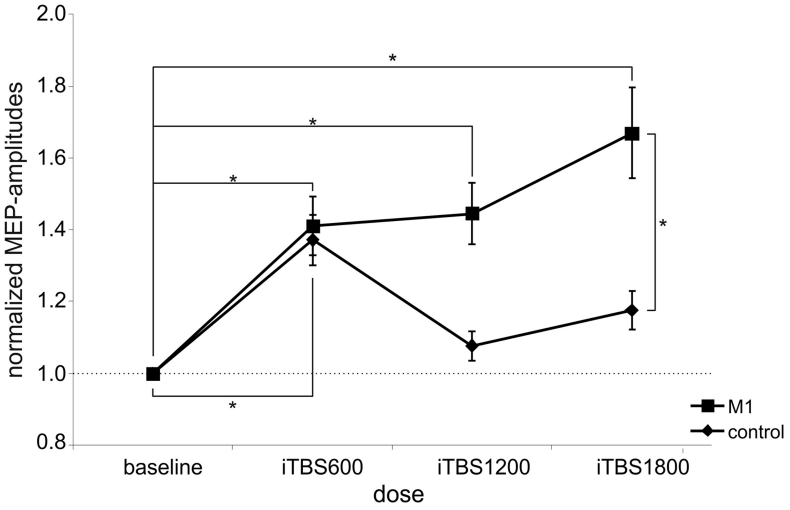

Figure 4. Supplemental control experiment: M1 versus supplemental control stimulation. Changes in MEP amplitudes after M1 (squares) and supplemental control stimulation (diamonds), normalized to baseline MEP amplitudes. *Significant aftereffects after M1-iTBS compared with supplemental control stimulation or baseline ($p \leq 0.05$, Student's t test). One stimulation over M1 in the supplemental control experiment led to comparable results as obtained after M1-iTBS600 in the main experiment. After three blocks of iTBS over M1 (M1-iTBS1800), MEP amplitudes were significantly higher compared with one M1 stimulation followed by two stimulations over the parieto-occipital vertex.

Supplemental control experiment

Six subjects, who also participated in the main experiment, were invited to a second experiment in which they received only one iTBS block over M1 followed by two sham stimulations over the parieto-occipital vertex (supplemental control experiment; Fig. 1*B*). Here, we found a significant increase in MEP amplitudes compared with baseline after the first stimulation block ($p = 0.018$, Student's t test; Fig. 4). Likewise, when replotting data from the main experiment, MEP amplitudes were significantly increased after one iTBS block over M1 compared with baseline for the same subjects ($n = 6$, $p = 0.024$). Accordingly, there was no significant difference between the main experiment and the control experiment after the first iTBS block ($p = 0.445$). As expected, in the control experiment, MEP amplitudes decreased after the second block of iTBS (now applied over the vertex for control; $p = 0.069$, iTBS1200 compared with iTBS600) and were no longer significantly different from baseline. Still, there was no significant difference between the main experiment and the control experiment after two iTBS blocks ($p = 0.104$). However, when directly comparing MEP amplitudes after three stimulation blocks between the main experiment and the control experiment, we found significantly higher amplitudes after three iTBS blocks over M1 compared with one iTBS block over M1 followed by two

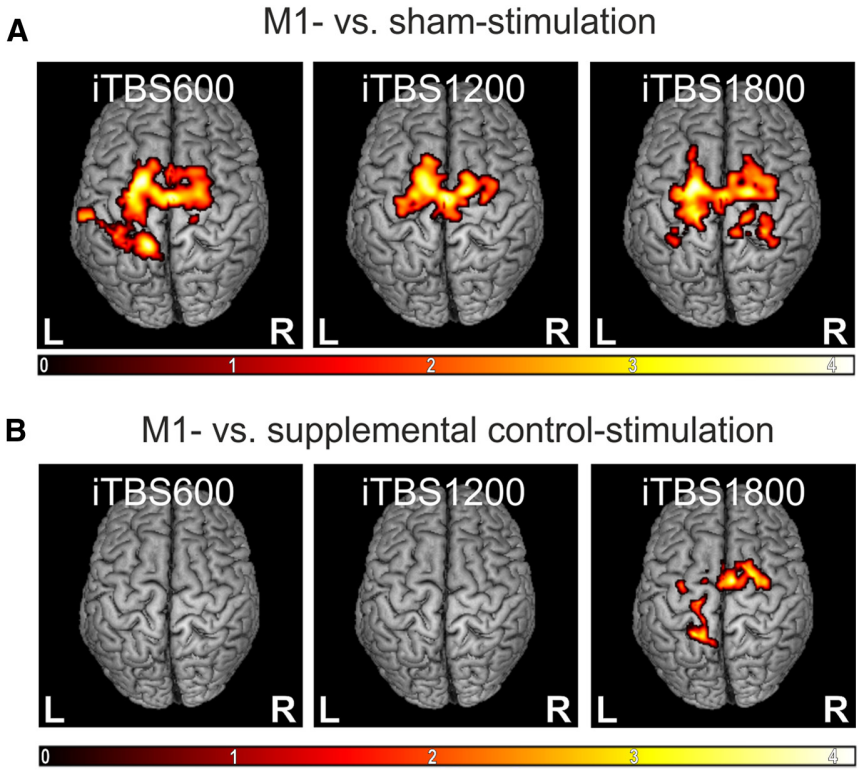

Figure 5. Changes in rsFC. M1 compared with sham stimulation, normalized to baseline values. Color bar represents *t* values. Only clusters surviving a cluster level FWE correction ($p \leq 0.05$) are shown. ***A***, Main experiment. M1-iTBS led to significantly higher changes in rsFC of M1 with bilateral premotor areas (dPMC, SMA) after all doses as well as with somatosensory and superior parietal cortex. ***B***, Supplemental control experiment. iTBS1800 over M1 led to significantly higher correlations in the time courses between M1 and premotor areas (dPMC, SMA) as well as somatosensory/superior parietal cortex compared with a single M1-iTBS application followed by two sham stimulations over the vertex (supplemental control stimulation).

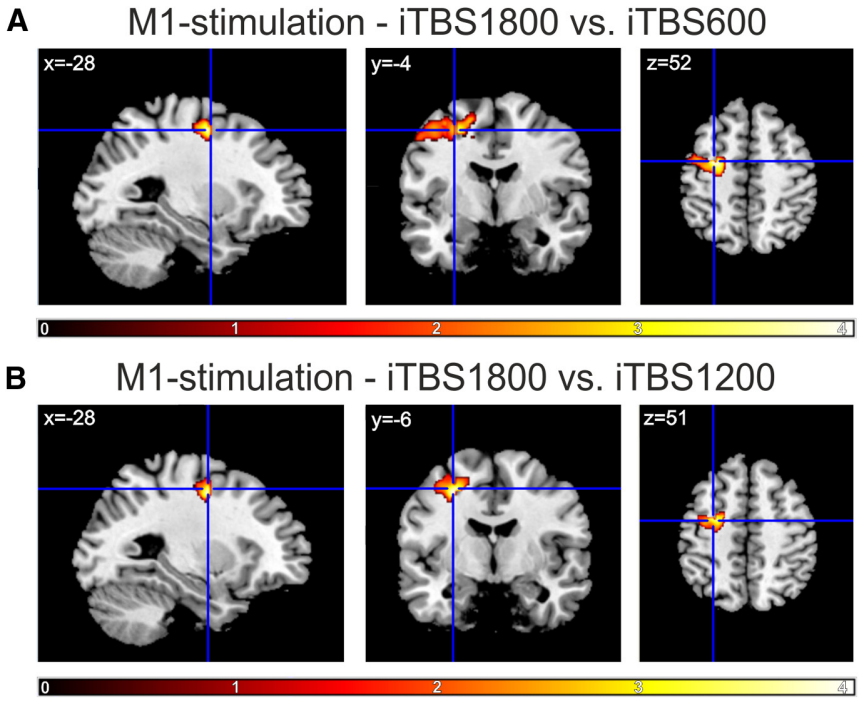

Figure 6. ROI analysis. Dose-dependent changes in rsFC. Contrasts between the increase in rsFC compared with baseline between iTBS1800 and (***A***) iTBS600 or (***B***) iTBS1200. Color bar represents *t* values. The cross indicates the coordinate where dose-dependent increases were found for ipsilateral dPMC-M1 rsFC. $p \leq 0.05$, small-volume FWE-corrected at the voxel level.

sham stimulations ($p = 0.050$). Therefore, our data suggest that aftereffects after iTBS1800 over M1 did not result from delayed effects induced by the first M1-iTBS block but indeed reflected additive effects resulting from repeated M1 stimulation.

iTBS aftereffects on rsFC

Main experiment

The seed-based whole-brain group analysis showed significant positive coupling of the stimulated M1 with a bihemispheric motor network comprising M1 and premotor areas as well as parts of the somatosensory and superior parietal cortex. Baseline measurements were not significantly different between M1 and sham stimulation sessions. Aftereffects of iTBS on M1 rsFC were tested by subtracting the individual baseline whole-brain images from images obtained after 600, 1200, and 1800 pulses. The flexible factorial analysis revealed that, compared with sham stimulation, iTBS over M1 was associated with a significantly stronger increase in rsFC between M1 and various sensorimotor regions. Local maxima were situated in bilateral SMA and dPMC (superior frontal sulcus) across all iTBS blocks and less consistently in parts of the somatosensory and superior parietal cortex ($p \leq 0.05$, cluster level FWE-corrected; Fig. 5*A*). In contrast, functional connectivity within the visual network was not influenced by iTBS over M1 or the vertex for either session. This finding indicates that iTBS over M1 did not lead to global (i.e., brainwide) changes in resting-state connectivity. Rather, stimulation effects remained within the stimulated M1 network.

We next tested for dose-dependent effects in *a priori* defined motor ROIs. We found significant effects for rsFC between the stimulated M1 and ipsilateral dPMC: the increase in M1-dPMC connectivity was significantly higher after iTBS1800 compared with iTBS600 and iTBS1200 ($p \leq 0.05$, small-volume FWE-corrected on the voxel level; Fig. 6). Furthermore, the increase in rsFC after M1-iTBS1800 was also significantly higher compared with sham stimulation (iTBS1800 vs iTBS600: $p = 0.027$, iTBS1800 vs iTBS1200: $p \leq 0.001$ small-volume FWE-corrected on the voxel level). No significant difference was found between iTBS600 and iTBS1200 within and between stimulation conditions. Hence, an additional increase in rsFC between M1 and ipsilateral dPMC was only evident after iTBS1800 compared with iTBS600 and iTBS1200, but not between iTBS600 and iTBS1200. No dose-dependent changes were observed for rsFC between the stim-

ulated M1 and contralateral dPMC as well as bilateral SMA and contralateral M1.

Supplemental control experiment

In the supplemental control experiment, six subjects received only one iTBS block over M1 followed by two sham stimulations over the parieto-occipital vertex. Here, the whole-brain group analysis revealed a stronger increase in connectivity between M1 and bilateral SMA, dPMC, and parts of the somatosensory and superior parietal cortex after 1800 pulses in the main experiment ($3 \times$ M1 stimulation) compared with 1800 pulses in the control experiment (one iTBS block over M1 followed by two sham stimulations) ($p = 0.048$, cluster level FWE-corrected; Fig. 5*B*). There was no significant difference between the main experiment (replotted data for $n = 6$) and the control experiment regarding iTBS600 and iTBS1200. Similar to our findings regarding MEP data, these results suggest that aftereffects after iTBS1800 over M1 did not result from delayed effects induced by the first M1-iTBS block but indeed reflected additive effects resulting from repeated M1 stimulation.

In summary, our data suggest that iTBS applied over M1 induced an increase of rsFC between the stimulated M1 and premotor areas compared with both baseline and sham stimulation. Furthermore, connectivity between M1 and the ipsilateral dPMC also depended on the number of stimuli applied.

Correlation between MEP amplitudes and rsFC

Increases in MEP amplitudes observed between M1-iTBS1800 and M1-iTBS600 or M1-iTBS1200 did not correlate with changes in rsFC within the sensorimotor network ($p > 0.05$, FWE-corrected for each correlation). This implies that changes in MEPs (representing changes at the local level) were not directly related to changes in connectivity of interconnected areas at the systems level after M1-iTBS.

Discussion

Summary of findings

In line with our hypotheses, we found that the application of three blocks of iTBS over M1 resulted in a significant increase of cortical excitability (as reflected by MEP amplitudes) compared with sham stimulation over the vertex. Importantly, an additive increase in MEP amplitudes was only observed after the third, but not the second block of iTBS. Furthermore, rsFC increased after iTBS between the stimulated M1 and premotor areas (i.e., dPMC and SMA), and with areas of the somatosensory and superior parietal cortex. Here, our data also revealed dose-specific changes after three blocks of iTBS between the stimulated M1 and ipsilateral dPMC. However, dose-dependent changes in excitability did not correlate with changes in motor network rsFC, suggesting that iTBS-induced aftereffects observed at the electrophysiological level and neural network level are based, at least in part, upon differential neurobiological mechanisms.

iTBS aftereffects on cortical excitability and their dose dependency

The application of rTMS offers the opportunity to noninvasively modulate motor–cortical excitability. Huang et al. (2005) introduced the iTBS protocol, which offers the advantage of enhancing cortical excitability for ~20 min using rather low stimulation intensities applied over a short period of time. Other groups have already aimed at amplifying iTBS aftereffects by increasing the number of iTBS stimuli. For example, Gamboa and colleagues (2010, 2011) doubled the number of pulses (2×600) but did not find a further increase of facilitatory aftereffects across different intersession intervals (0, 2, 5, 20 min), compared with 600 pulses. We observed a similar effect in the present study as there was no additional increase in MEP amplitudes after two blocks of iTBS (Fig. 3). Importantly, however, a third block of iTBS led to a further increase in MEP amplitudes. In contrast to earlier studies, we did not observe decreases in cortical excitability after repeated application of iTBS (Gamboa et al., 2010, 2011).

Homeostatic metaplasticity

One frequently used model for explaining the aftereffects of (multiple) rTMS sessions is the Bienenstock-Cooper-Munro (BCM) theory (Bienenstock et al., 1982). Accordingly, increased levels of postsynaptic activity (i.e., long-term potentiation [LTP]) after stimulation are assumed to favor the induction of long-term depression (LTD) by the next stimulation, thereby preventing an excessive buildup of LTD or LTP. Such activation history-dependent effects ("homeostatic metaplasticity") of neuronal ensembles might also underlie rTMS/iTBS aftereffects (Ziemann and Siebner, 2008). Hence, enhancing cortical excitability within the motor cortex via rTMS/iTBS might cause a concurrent increase in the threshold for inducing further synaptic plasticity (LTP-like effects). Such metaplastic effects might explain that two blocks of iTBS did not lead to a further increase of excitability (as observed in Gamboa et al., 2010, 2011 and also in the present study). However, the finding that 1800 pulses of iTBS caused an additional increase in cortical excitability can only be explained by overcoming the homeostatic threshold for inducing LTP-like synaptic plasticity after multiple stimulations.

Dose-dependent effects: cellular level

One potential biological mechanism underlying activation history-dependent effects of iTBS might lie in dose-dependent modifications of inhibitory systems (Di Lazzaro et al., 2005; Stagg et al., 2009; Funke and Benali, 2011). Hamada et al. (2013) suggested that individual differences in iTBS-induced plasticity arise from the distinct recruitment of inhibitory interneurons. Further support for the involvement of inhibitory cortical systems stems from animal studies reporting that TBS alters the expression-patterns of calcium-binding proteins parvalbumin and calbindin. The latter are likely to reflect activity changes within subgroups of GABAergic inhibitory interneurons in the rat cortex (Benali et al., 2011; Funke and Benali, 2011), which can be induced by iTBS and become most effective 20–40 min after iTBS (Hoppenrath and Funke, 2013). Furthermore, a recent study reported dose-specific aftereffects of multiple iTBS applications on the activity of distinct subgroups of interneurons of the rat cortex (Volz et al., 2013). Interestingly, the largest subgroup of these interneurons (i.e., parvalbumin-positive neurons) was significantly affected after ≥1800 pulses. Thus, a dose-dependent decrease of inhibitory interneuron activity could underlie the increase in cortical excitability after iTBS1800. Additionally, compensatory effects evoked by the first block of iTBS were shown to be attenuated after further stimulation. For example, the expression of GAD65, a marker reflecting the level of synaptic GABA secretion (Soghomonian and Martin, 1998), was initally increased after iTBS600, possibly compensating for less somatic activity (e.g., decrease of parvalbumin). However, GAD65 expression did not further increase after additional blocks of iTBS (Volz et al., 2013). Therefore, further LTP-like effects of the second iTBS block might have been prevented or even reversed into LTD-like effects, as suggested by the BCM rule

for homeostatic plasticity, e.g., resulting from saturation effects of LTP-promoting mechanisms or changes in inhibitory interneuron activity (e.g., GAD65 expression). Finally, the effects of a third iTBS block might also still be weakened because of homeostatic plasticity, but a simultaneous decrease in cortical inhibition (e.g., parvalbumin expression) might permit a further potentiation of facilitating aftereffects. Given the similarity in stimulation protocols and intersession interval (compare Figs. 1-3), such effects would nicely explain the dose-dependent findings of the present study.

Dose-dependent effects at near-threshold MEPs

Interestingly, we found that dose-dependent effects of iTBS seem to be more pronounced when evoking MEPs with near-threshold intensities (i.e., 90%–110%; Fig. 2). At high intensities, TMS directly activates the axons of corticospinal neurons (Di Lazzaro et al., 2008). Such "D-waves" are not modified by changes in cortical excitability (Di Lazzaro et al., 2012), explaining the relatively small effect of iTBS on high-intensity MEPs observed in the present study. In contrast, near-threshold TMS activates corticospinal neurons transsynaptically via axonal projections of interneurons. Therefore, a predominant effect of iTBS on near-threshold MEPs nicely fits our hypothesis on dose-dependent iTBS aftereffects possibly resulting from differential effects on distinct interneurons.

iTBS aftereffects on rsFC

Previous studies combining rTMS with resting-state fMRI already reported alterations of rsFC between the stimulated region and other brain regions after rTMS (Vercammen et al., 2010; Eldaief et al., 2011; van der Werf et al., 2010). Our data show that iTBS over M1 increases rsFC between the stimulated M1 and premotor areas (i.e., dPMC and SMA), as well as areas of the somatosensory and superior parietal cortex (Fig. 5). Importantly, this finding was specific for the stimulated motor network, as no changes were found in connectivity of the visual system. A similar anatomical selectivity has been reported in studies by showing that lesion-induced connectivity changes in one network do not spread over to other networks (Nomura et al., 2010; Sharma et al., 2009).

A possible explanation for iTBS-induced increases in rsFC might be the simultaneous induction of neural activity in the entire motor network during stimulation of M1. Previous studies frequently reported rTMS-induced changes in neural activity to be not exclusively local, but also to extend to remote, interconnected areas (Paus and Wolforth, 1998; Siebner et al., 2000; Bestmann et al., 2003, 2004, 2005; Suppa et al., 2008; Cárdenas-Morales et al., 2011). Activity changes in connected regions after iTBS might result from activity conduction by corticocortical fibers. The regions that showed increased M1-rsFC after iTBS (Fig. 5) are known to be densely connected to M1 (Stepniewska et al., 1993; Geyer et al., 2000). Such structural connections might facilitate coactivation of interconnected regions, thereby modulating the synchronicity of neural activity between interconnected areas. Support for this hypothesis stems from studies using repetitive applications of paired-associative stimulation protocols. Here, consecutive trials of paired-associative stimulation over M1 and posterior parietal cortex have been shown to increase functional connectivity between these two stimulation sites (Veniero et al., 2013). At a functional level, increased coherence of brain activity may represent an important neurophysiological mechanism enforcing communication between two areas that interact via concurrent input and output channels (Fries, 2005). Thus, an increase in coherence of brain activity after the simultaneous activation of interconnected brain areas by iTBS might underlie increased rsFC in our study.

However, our data revealed no direct correlation between individual changes in cortical excitability and rsFC. Thus, altered resting-state connectivity of the stimulated area does not seem to be linked to rTMS/iTBS-induced changes of excitability on the level of single subjects. The reason for this remains speculative (e.g., interindividual variability, different sessions, nonlinear aftereffects). However, it should be noted that numerous previous studies have also found absent (or only rather weak) correlations between rTMS-induced changes in excitability and aftereffects on the behavioral level (Ragert et al., 2008; Stefan et al., 2008; Zeller et al., 2012). This implies that, despite significant effects on the group level, the individual magnitude of aftereffects regarding cortical excitability cannot be reliably used to predict more "complex" (behavioral) rTMS aftereffects.

Limitations

We can currently only speculate about the cellular mechanisms underlying dose-dependent aftereffects. In humans, two noninvasive techniques have previously been used to assess cortical GABAergic inhibition (i.e., cortical GABA concentration via magnetic resonance spectroscopy) (Stagg et al., 2009) or GABA-dependent short-interval intracortical inhibition via double-pulse TMS (Kujirai et al., 1993). However, magnetic resonance spectroscopy or short-interval intracortical inhibition are not capable of differentiating between distinct subpopulations of GABAergic inhibitory interneurons. As outlined above, this information would be essential as animal studies reported opposing effects on somatic GABA concentration (e.g., reflected by decreased GAD67 levels) and synaptic GABA concentration (e.g., reflected by increased GAD65 levels) to underlie the evolution of dose-dependent iTBS effects.

It could well be that functional connectivity in the activated motor system (i.e., during a motor task) would have been a better predictor of excitability aftereffects (Cárdenas-Morales et al., 2013). However, for the scope of the present study (dose-dependent iTBS effects), resting-state measurements seem to be better suited as motor activity before iTBS has rather complex effects on stimulation-induced changes in excitability (Gentner et al., 2008; Silvanto and Pascual-Leone, 2008), which would have strongly biased the results.

Conclusions

In conclusion, our data suggest that the efficiency of iTBS in enhancing cortical excitability can be increased by applying a higher number of stimuli (i.e., 1800, but not 1200) compared with the conventional iTBS protocol in healthy subjects. Interestingly, we found that dose-dependent effects of iTBS seem to be more pronounced when evoking MEPs with near-threshold intensities, supporting the hypothesis of interneuron networks underlying iTBS aftereffects. Furthermore, we observed M1-iTBS to impact on rsFC within the motor system, i.e., increasing connectivity of the stimulated M1, particularly with premotor areas (i.e., dPMC, SMA). Here, rsFC between M1 and ipsilateral dPMC increased dose-dependently (after 1800 pulses). However, the significance of dose-dependent rTMS-induced changes in MEPs and rsFC regarding behavioral rTMS effects remains to be further elucidated to fully determine the neuromodulatory potential of iTBS1800 on motor function in health and disease.

References

Ashburner J, Friston KJ (2005) Unified segmentation. Neuroimage 26:839–851. CrossRef Medline

Benali A, Trippe J, Weiler E, Mix A, Petrasch-Parwez E, Girzalsky W, Eysel UT, Erdmann R, Funke K (2011) Theta burst transcranial magnetic stimulation alters cortical inhibition. J Neurosci 31:1193–1203. CrossRef Medline

Bestmann S, Baudewig J, Siebner HR, Rothwell JC, Frahm J (2003) Subthreshold high-frequency TMS of human primary motor cortex modulates interconnected frontal motor areas as detected by interleaved fMRI-TMS. Neuroimage 20:1685–1696. CrossRef Medline

Bestmann S, Baudewig J, Siebner HR, Rothwell JC, Frahm J (2004) Functional MRI of the immediate impact of transcranial magnetic stimulation on cortical and subcortical motor circuits. Eur J Neurosci 19:1950–1962. CrossRef Medline

Bestmann S, Baudewig J, Siebner HR, Rothwell JC, Frahm J (2005) BOLD MRI responses to repetitive TMS over human dorsal premotor cortex. Neuroimage 28:22–29. CrossRef Medline

Bienenstock EL, Cooper LN, Munro PW (1982) Theory for the development of neuron selectivity: orientation specificity and binocular interaction in visual cortex. J Neurosci 2:32–48. Medline

Cárdenas-Morales L, Grön G, Kammer T (2011) Exploring the aftereffects of theta burst magnetic stimulation on the human motor cortex: a functional imaging study. Hum Brain Mapp 32:1948–1960. CrossRef Medline

Cárdenas-Morales L, Volz LJ, Michely J, Rehme AK, Pool EM, Nettekoven C, Eickhoff SB, Fink GR, Grefkes C (2013) Network connectivity and individual responses to brain stimulation in the human motor system. Cereb Cortex. Advance online publication. Retrieved Feb. 8, 2013. doi: 10.1093/cercor/bht023. CrossRef Medline

Carroll TJ, Riek S, Carson RG (2001) Reliability of the input–output properties of the cortico-spinal pathway obtained from transcranial magnetic and electrical stimulation. J Neurosci Methods 112:193–202. CrossRef Medline

Chen R, Tam A, Bütefisch C, Corwell B, Ziemann U, Rothwell JC, Cohen LG (1998) Intracortical inhibition and facilitation in different representations of the human motor cortex. J Neurophysiol 80:2870–2881. Medline

Di Lazzaro V, Oliviero A, Pilato F, Saturno E, Dileone M, Mazzone P, Insola A, Tonali PA, Rothwell JC (2004) The physiological basis of transcranial motor cortex stimulation in conscious humans. Clin Neurophysiol 115:255–266. CrossRef Medline

Di Lazzaro V, Pilato F, Saturno E, Oliviero A, Dileone M, Mazzone P, Insola A, Tonali PA, Ranieri F, Huang YZ, Rothwell JC (2005) Theta burst repetitive transcranial magnetic stimulation suppresses specific excitatory circuits in the human motor cortex. J Physiol 565:945–950. CrossRef Medline

Di Lazzaro V, Pilato F, Dileone M, Profice P, Oliviero A, Mazzone P, Insola A, Ranieri F, Meglio M, Tonali PA, Rothwell JC (2008) The physiological basis of the effects of intermittent theta burst stimulation of the human motor cortex. J Physiol 586:3871–3879. CrossRef Medline

Di Lazzaro V, Profice P, Ranieri F, Capone F, Dileone M, Oliviero A, Pilato F (2012) I-wave origin and modulation. Brain Stimul 5:512–525. CrossRef Medline

Eickhoff SB, Grefkes C (2011) Approaches for the integrated analysis of structure, function and connectivity of the human brain. Clin EEG Neurosci 42:107–121. CrossRef Medline

Eickhoff SB, Stephan KE, Mohlberg H, Grefkes C, Fink GR, Amunts K, Zilles K (2005) A new SPM toolbox for combining probabilistic cytoarchitectonic maps and functional imaging data. Neuroimage 25:1325–1335. CrossRef Medline

Eldaief MC, Halko MA, Buckner RL, Pascual-Leone A (2011) Transcranial magnetic stimulation modulates the brain's intrinsic activity in a frequency-dependent manner. Proc Natl Acad Sci U S A 108:21229–21234. CrossRef Medline

Fries P (2005) A mechanism for cognitive dynamics: neuronal communication through neuronal coherence. Trends Cogn Sci 9:474–480. CrossRef Medline

Funke K, Benali A (2011) Modulation of cortical inhibition by rTMS: findings obtained from animal models. J Physiol 589:4423–4435. Medline

Gamboa OL, Antal A, Moliadze V, Paulus W (2010) Simply longer is not better: reversal of theta burst aftereffect with prolonged stimulation. Exp Brain Res 204:181–187. CrossRef Medline

Gamboa OL, Antal A, Laczo B, Moliadze V, Nitsche MA, Paulus W (2011) Impact of repetitive theta burst stimulation on motor cortex excitability. Brain Stimul 4:145–151. CrossRef Medline

Gentner R, Wankerl K, Reinsberger C, Zeller D, Classen J (2008) Depression of human corticospinal excitability induced by magnetic theta burst stimulation: evidence of rapid polarity-reversing metaplasticity. Cereb Cortex 18:2046–2053. CrossRef Medline

Geyer S, Matelli M, Luppino G, Zilles K (2000) Functional neuroanatomy of the primate isocortical motor system. Anat Embryol (Berl) 202:443–474. CrossRef Medline

Grefkes C, Nowak DA, Wang LE, Dafotakis M, Eickhoff SB, Fink GR (2010) Modulating cortical connectivity in stroke patients by rTMS assessed with fMRI and dynamic causal modeling. Neuroimage 50:233–242. CrossRef Medline

Hamada M, Murase N, Hasan A, Balaratnam M, Rothwell JC (2013) The role of interneuron networks in driving human motor cortical plasticity. Cereb Cortex 23:1593–1605. CrossRef Medline

Herwig U, Fallgatter AJ, Höppner J, Eschweiler GW, Kron M, Hajak G, Padberg F, Naderi-Heiden A, Abler B, Eichhammer P, Grossheinrich N, Hay B, Kammer T, Langguth B, Laske C, Plewnia C, Richter MM, Schulz M, Unterecker S, Zinke A, et al. (2007) Antidepressant effects of augmentative transcranial magnetic stimulation: randomised multicentre trial. Br J Psychiatry 191:441–448. CrossRef Medline

Herwig U, Cárdenas-Morales L, Connemann BJ, Kammer T, Schönfeldt-Lecuona C (2010) Sham or real: post hoc estimation of stimulation condition in a randomized transcranial magnetic stimulation trial. Neurosci Lett 471:30–33. CrossRef Medline

Hoppenrath K, Funke K (2013) Time-course of changes in neuronal activity markers following iTBS-TMS of the rat neocortex. Neurosci Lett 536:19–23. CrossRef Medline

Huang YZ, Edwards MJ, Rounis E, Bhatia KP, Rothwell JC (2005) Theta burst stimulation of the human motor cortex. Neuron 45:201–206. CrossRef Medline

Huang YZ, Chen RS, Rothwell JC, Wen HY (2007) The aftereffect of human theta burst stimulation is NMDA receptor dependent. Clin Neurophysiol 118:1028–1032. CrossRef Medline

Huang YZ, Rothwell JC, Edwards MJ, Chen RS (2008) Effect of physiological activity on an NMDA-dependent form of cortical plasticity in human. Cereb Cortex 18:563–570. CrossRef Medline

Jakobs O, Langner R, Caspers S, Roski C, Cieslik EC, Zilles K, Laird AR, Fox PT, Eickhoff SB (2012) Across-study and within-subject functional connectivity of a right temporo-parietal junction subregion involved in stimulus-context integration. Neuroimage 60:2389–2398. CrossRef Medline

Kobayashi M, Hutchinson S, Théoret H, Schlaug G, Pascual-Leone A (2004) Repetitive TMS of the motor cortex improves ipsilateral sequential simple finger movements. Neurology 62:91–98. CrossRef Medline

Kujirai T, Caramia MD, Rothwell JC, Day BL, Thompson PD, Ferbert A, Wroe S, Asselman P, Marsden CD (1993) Corticocortical inhibition in human motor cortex. J Physiol 471:501–519. Medline

Nomura EM, Gratton C, Visser RM, Kayser A, Perez F, D'Esposito M (2010) Double dissociation of two cognitive control networks in patients with focal brain lesions. Proc Natl Acad Sci U S A 107:12017–12022. CrossRef Medline

Oldfield RC (1971) The assessment and analysis of handedness: the Edinburgh inventory. Neuropsychologia 9:97–113. CrossRef Medline

Pascual-Leone A, Tormos JM, Keenan J, Tarazona F, Cañete C, Catalá MD (1998) Study and modulation of human cortical excitability with transcranial magnetic stimulation. J Clin Neurophysiol 15:333–343. CrossRef Medline

Pascual-Leone A, Amedi A, Fregni F, Merabet LB (2005) The plastic human brain cortex. Annu Rev Neurosci 28:377–401. CrossRef Medline

Paus T, Wolforth M (1998) Transcranial magnetic stimulation during PET: reaching and verifying the target site. Hum Brain Mapp 6:399–402. CrossRef Medline

Ragert P, Franzkowiak S, Schwenkreis P, Tegenthoff M, Dinse HR (2008) Improvement of tactile perception and enhancement of cortical excitability through intermittent theta burst rTMS over human primary somatosensory cortex. Exp Brain Res 184:1–11. CrossRef Medline

Reetz K, Dogan I, Rolfs A, Binkofski F, Schulz JB, Laird AR, Fox PT, Eickhoff SB (2012) Investigating function and connectivity of morphometric findings: exemplified on cerebellar atrophy in spinocerebellar ataxia 17 (SCA17). Neuroimage 62:1354–1366. CrossRef Medline

Ridding MC, Ziemann U (2010) Determinants of the induction of cortical plasticity by non-invasive brain stimulation in healthy subjects. J Physiol 588:2291–2304. CrossRef Medline

Sarfeld AS, Diekhoff S, Wang LE, Liuzzi G, Uludağ K, Eickhoff SB, Fink GR, Grefkes C (2012) Convergence of human brain mapping tools: neuronavigated TMS parameters and fMRI activity in the hand motor area. Hum Brain Mapp 33:1107–1123. CrossRef Medline

Satterthwaite TD, Elliott MA, Gerraty RT, Ruparel K, Loughead J, Calkins ME, Eickhoff SB, Hakonarson H, Gur RC, Gur RE, Wolf DH (2013) An improved framework for confound regression and filtering for control of motion artifact in the preprocessing of resting-state functional connectivity data. Neuroimage 64:240–256. CrossRef Medline

Sharma N, Baron JC, Rowe JB (2009) Motor imagery after stroke: relating outcome to motor network connectivity. Ann Neurol 66:604–616. CrossRef Medline

Siebner HR, Peller M, Willoch F, Minoshima S, Boecker H, Auer C, Drzezga A, Conrad B, Bartenstein P (2000) Lasting cortical activation after repetitive TMS of the motor cortex: a glucose metabolic study. Neurology 54:956–963. CrossRef Medline

Silvanto J, Pascual-Leone A (2008) State-dependency of transcranial magnetic stimulation. Brain Topogr 21:1–10. CrossRef Medline

Soghomonian JJ, Martin DL (1998) Two isoforms of glutamate decarboxylase: why? Trends Pharmacol Sci 19:500–505. CrossRef Medline

Stagg CJ, Wylezinska M, Matthews PM, Johansen-Berg H, Jezzard P, Rothwell JC, Bestmann S (2009) Neurochemical effects of theta burst stimulation as assessed by magnetic resonance spectroscopy. J Neurophysiol 101: 2872–2877. CrossRef Medline

Stefan K, Gentner R, Zeller D, Dang S, Classen J (2008) Theta burst stimulation: remote physiological and local behavioral aftereffects. Neuroimage 40:265–274. CrossRef Medline

Stepniewska I, Preuss TM, Kaas JH (1993) Architectonics, somatotopic organization, and ipsilateral cortical connections of the primary motor area (M1) of owl monkeys. J Comp Neurol 330:238–271. CrossRef Medline

Suppa A, Ortu E, Zafar N, Deriu F, Paulus W, Berardelli A, Rothwell JC (2008) Theta burst stimulation induces aftereffects on contralateral primary motor cortex excitability in humans. J Physiol 586:4489–4500. CrossRef Medline

Teo JT, Swayne OB, Rothwell JC (2007) Further evidence for NMDA dependence of the aftereffects of human theta burst stimulation. Clin Neurophysiol 118:1649–1651. CrossRef Medline

Terao Y, Ugawa Y (2002) Basic mechanisms of TMS. J Clin Neurophysiol 19:322–343. CrossRef Medline

van der Werf YD, Sanz-Arigita EJ, Menning S, van den Heuvel OA (2011) Modulating spontaneous brain activity using repetitive transcranial magnetic stimulation. BMC Neurosci 11:145. CrossRef Medline

Veniero D, Ponzo V, Koch G (2013) Paired associative stimulation enforces the communication between interconnected areas. J Neurosci 33:13773–13783. CrossRef Medline

Vercammen A, Knegtering H, Liemburg EJ, den Boer JA, Aleman A (2010) Functional connectivity of the temporo-parietal region in schizophrenia: effects of rTMS treatment of auditory hallucinations. J Psychiatr Res 44: 725–731. CrossRef Medline

Volz LJ, Benali A, Mix A, Neubacher U, Funke K (2013) Dose dependence of changes in cortical protein expression induced with repeated transcranial magnetic theta burst stimulation in the rat. Brain Stimul 6:598–606. CrossRef Medline

Wassermann EM (1998) Risk and safety of repetitive transcranial magnetic stimulation: report and suggested guidelines from the International Workshop on the Safety of Repetitive Transcranial Magnetic Stimulation, June 5–7, 1996. Electroencephalogr Clin Neurophysiol 108:1–16. CrossRef Medline

Watanabe T, Hanajima R, Shirota Y, Ohminami S, Tsutsumi R, Terao Y, Ugawa Y, Hirose S, Miyashita Y, Konishi S, Kunimatsu A, Ohtomo K (2014) Bidirectional effects on interhemispheric resting-state functional connectivity induced by excitatory and inhibitory repetitive transcranial magnetic stimulation. Hum Brain Mapp 35:1896–1905. CrossRef Medline

Yousry TA, Schmid UD, Alkadhi H, Schmidt D, Peraud A, Buettner A, Winkler P (1997) Localization of the motor hand area to a knob on the precentral gyrus: a new landmark. Brain 120:141–157. CrossRef Medline

Zafar N, Paulus W, Sommer M (2008) Comparative assessment of best conventional with best theta burst repetitive transcranial magnetic stimulation protocols on human motor cortex excitability. Clin Neurophysiol 119:1393–1399. CrossRef Medline

Zeller D, Dang SY, Weise D, Rieckmann P, Toyka KV, Classen J (2012) Excitability decreasing central motor plasticity is retained in multiple sclerosis patients. BMC Neurol 12:92. CrossRef Medline

Ziemann U, Siebner HR (2008) Modifying motor learning through gating and homeostatic metaplasticity. Brain Stimul 1:60–66. CrossRef Medline

zu Eulenburg P, Caspers S, Roski C, Eickhoff SB (2012) Meta-analytical definition and functional connectivity of the human vestibular cortex. Neuroimage 60:162–169. CrossRef Medline

2.3 Inter-individual variability in cortical excitability and motor network connectivity following multiple blocks of rTMS

Nettekoven C, Volz LJ, Kutscha M, Pool EM, Rehme AK, Eickhoff SB, Fink GR, Grefkes C

under review

Inter-individual variability in cortical excitability and motor network connectivity following multiple blocks of rTMS

NETTEKOVEN Charlotte[1,2], VOLZ Lukas J.[2], LEIMBACH Martha[2], POOL Eva-Maria[1,2], REHME Anne K.[1,2], EICKHOFF Simon B.[1,3], FINK Gereon R.[1,2], GREFKES Christian[1,2]

AFFILIATIONS

1. Institute of Neuroscience and Medicine (INM-1, INM-3), Juelich Research Centre, 52428 Juelich, Germany
2. Department of Neurology, Cologne University Hospital, 50924 Cologne, Germany
3. Institute of Clinical Neuroscience and Medical Psychology, Heinrich Heine University, 40225 Duesseldorf, Germany

CORRESPONDING AUTHOR

Name: Prof. Christian Grefkes, MD PhD
Address: Department of Neurology, Uniklinik Koeln, Kerpener Straße 62, 50924 Koeln, Germany
Telephone Number: +49 (0)221 478 87695
Email: Christian.Grefkes@uk-koeln.de

1

ABBREVIATIONS: AP – anterior-posterior, APB – abductor pollicis brevis, AMT – active motor threshold, ANOVA – analysis of variance, dPMC – dorsal premotor cortex, EPI – echo planar imaging, FD – framewise displacement, FDR – false discovery rate, fMRI – functional magnetic resonance imaging, FOV – field of view, FWE – family wise error, GLM – general linear model, iTBS – intermittent theta-burst stimulation, LM – latero-medial, MEP – motor-evoked potential, M1 – primary motor cortex, RMSE – root mean squared error, RMT – resting motor threshold, rsFC – resting-state functional connectivity, rTMS – repetitive transcranial magnetic stimulation, SMA – supplementary motor area, TBS – theta-burst stimulation, TE – echo time, TR – repetition time[1]

Abstract

The responsiveness to non-invasive neuromodulation protocols shows high inter-individual variability, the reasons of which remain poorly understood. We here tested whether the response to intermittent theta-burst stimulation (iTBS) – an effective repetitive transcranial magnetic stimulation (rTMS) protocol for increasing cortical excitability – depends on network properties of the cortical motor system. We furthermore investigated whether the responsiveness to iTBS is dose-dependent.

To this end, we used a sham-stimulation controlled, single-blinded within-subject design testing for the relationship between iTBS aftereffects and (i) motor-evoked potentials (MEPs) as well as (ii) resting-state functional connectivity (rsFC) in 16 healthy subjects. In each session, three blocks of iTBS were applied, separated by 15 min.

We found that non-responders (subjects not showing an MEP increase of ≥10% after one iTBS block) featured stronger rsFC between the stimulated primary motor cortex (M1) and premotor areas before stimulation (compared to responders). Increases in rsFC and MEPs after all three iTBS blocks as well as dose-dependent increases between blocks occurred exclusively in responders.

Our data suggest that responsiveness to iTBS at the local level (i.e., M1 excitability) depends upon the pre-interventional network connectivity of the stimulated region. Of note, increasing iTBS dose did not turn non-responders into responders. The finding that higher levels of pre-interventional connectivity precluded a response to iTBS is likely to reflect a ceiling effect underlying non-responsiveness to iTBS at the systems level.

Keywords: cortical plasticity, variability, dose-dependency, dPMC, SMA

1. Introduction

Theta-burst stimulation (TBS) is an effective repetitive transcranial magnetic stimulation (rTMS) protocol, which allows modulation of cortical excitability upon a rather short period of stimulation (Huang et al., 2005). However, a growing number of studies reports that the responsiveness to rTMS/TBS shows high inter-individual variability, sometimes even resulting in no overall alteration of cortical excitability (Hamada et al., 2013; Hinder et al., 2014; López-Alonso et al., 2014). Recent studies suggest that 50% - 73% of subjects are non-responders to rTMS/TBS (Hamada et al., 2013; Hinder et al., 2014).

To date, the reasons for this inter-individual variability remain poorly understood. Hamada and colleagues (2013) suggested that the differential recruitment of subtypes of cortical interneurons embedded in different cortico-cortical circuits may account for about 50% of the inter-individual variability. Based on a combined functional magnetic resonance imaging (fMRI)-TMS study, we recently demonstrated that the differential recruitment of these interneuron networks by TMS correlates with the functional connectivity between premotor areas and the primary motor cortex (M1) (Volz et al., 2014). This implies a relationship between responsiveness to TBS and motor network connectivity. Likewise, other studies suggested a tight relationship between rTMS-induced aftereffects and network connectivity of the stimulated region (Cardenas-Morales et al., 2014; Andoh and Zatorre, 2011, 2013; Downar et al., 2014; Salomons et al., 2014). For instance, the amount of pre-interventional premotor-M1 connectivity in the activated motor system strongly related to the individual susceptibility to cortical excitability enhancing intermittent TBS (iTBS) (Cárdenas-Morales et al., 2014).

Moreover, we demonstrated recently dose-dependent increases after iTBS in cortical excitability (motor-evoked potentials, MEPs) as well as in resting-state functional connectivity (rsFC) (Nettekoven et al., 2014). Thus, the question arises whether the group-level effect observed after the application of a higher iTBS dose stems from non-responders showing responsiveness after repeated stimulation, which would suggest that responsiveness is dose-dependent (i.e., a lacking MEP increase in the first block followed by MEP increases after additional blocks of stimulation). Alternatively, the group-level effect might be driven by an amplification of iTBS effects exclusively in responders, indicating that individual factors determine responsiveness (Hamada et al., 2013). Furthermore, it is still unclear whether

responders and non-responders also differ in their response to iTBS at the level of motor network connectivity, i.e., in the increase of rsFC after iTBS as well as in their rsFC at baseline.

We, therefore, analyzed changes in MEP size and rsFC after three blocks of iTBS applied over left M1 compared to control stimulation over the vertex in a cohort of 16 healthy subjects (Nettekoven et al., 2014). We assigned subjects to two groups: responders and non-responders. Assignment was based upon subjects´ increase in MEP amplitudes after one iTBS block. We hypothesized that (i) responders show decreased rsFC between premotor areas and M1 compared to non-responders at baseline (Volz et al., 2014) and that (ii) a higher dose of iTBS will primarily modulate cortical excitability and rsFC in responders rather than in non-responders (Hamada et al., 2013; Nettekoven et al., 2014).

2. Methods

2.1 Subjects

All data have previously been included in a publication on general dose-dependent effects of iTBS on MEPs and resting-state connectivity (Nettekoven et al., 2014). We here re-analyzed the entire data set with respect to individual responsiveness at the MEP level as well as fMRI network level, a question that we did not address in the original publication. Accordingly, data from 16 healthy, right-handed subjects were included (7 males, mean ± SD age: 27 ± 3 years, range: 23-35 years; no history of neurological or psychiatric diseases). Right-handedness was verified using the Edinburgh Handedness Inventory (Oldfield, 1971). All subjects provided informed written consent. The study was carried out according to the declaration of Helsinki (1969, last revision 2008) and had been approved by the local ethics committee.

2.2 Experimental design

A detailed description of the procedure has been previously published (Nettekoven et al., 2014). We here summarize the important steps. Figure 1 illustrates the experimental design. We used a single-blind, vertex-stimulation controlled, cross-over within-subject design to test for the effects of multiple serially applied iTBS blocks on (i) cortical excitability (MEP sessions) and (ii) rsFC (resting-state fMRI sessions) to further elucidate mechanisms underlying the individual responsiveness to iTBS. Each subject participated in two MEP sessions (A, B) and two resting-state

fMRI sessions (C, D). In two of the four sessions stimulation was applied over the left M1 (A: M1-iTBS_MEPs, C: M1-iTBS_rs-fMRI), and in the other two sessions over the parieto-occipital vertex (B: sham-iTBS_MEPs, D: sham-iTBS_rs-fMRI) (Herwig et al., 2010; Herwig et al., 2007). In each of the four sessions iTBS was repeated three times separated by 15 minutes, leading to a total of 1800 pulses (i.e., iTBS600, iTBS1200, iTBS1800) per session to examine the effect of dose (please cf. Nettekoven et al., 2014; Volz et al., 2013). Sessions were separated by at least one week to avoid carry-over effects. The order of M1- and sham-iTBS was randomized across subjects.

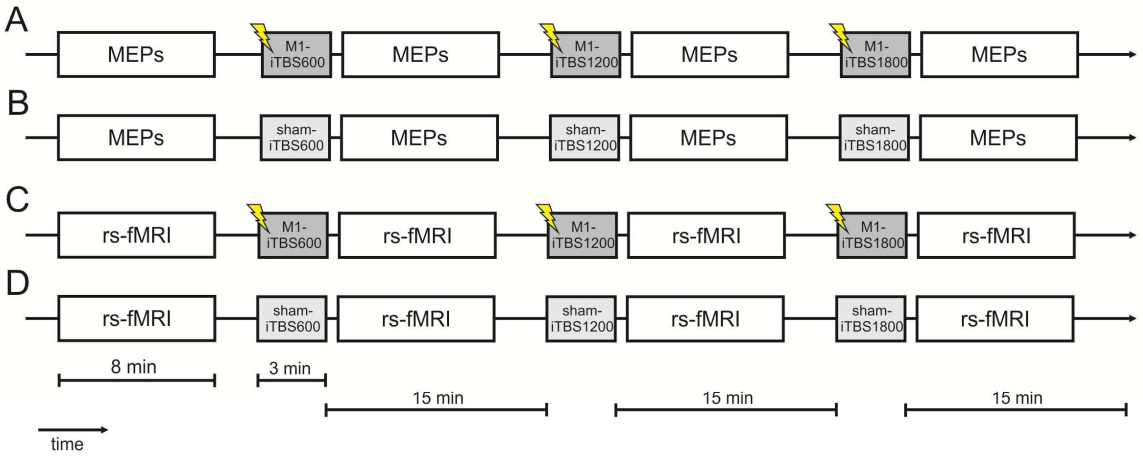

Figure 1
Nettekoven et al.
(2 columns)

Figure 1: Experimental design. Using a within-subjects design each subject took part in four sessions to assess (i) MEPs before and after (A) M1-iTBS and (B) sham-iTBS as well as to assess (ii) rs-fMRI before and after (C) M1-iTBS and (D) sham-iTBS. In each session three iTBS blocks were applied separated by 15 min. Each iTBS block consisted of 600 pulses, leading to a total of 1800 pulses.

2.3 Neuronavigated transcranial magnetic stimulation

The position of the TMS coil was tracked and recorded using a Brain-Sight2 computerized frameless stereotaxic system ensuring a reliable positioning of the stimulation site across all sessions and subjects (Rogue Research Inc., Montreal, Canada). The head of the subject was coregistered with an individual high-resolution anatomical MR image. MEPs were recorded from the abductor pollicis brevis (APB) muscle of the right hand with Ag/AgCl surface electrodes (Tyco Healthcare,

Neustadt, Germany) placed in a belly-tendon montage. The electromyographic (EMG) signal was amplified, filtered (0.5 Hz high pass and 30-300 Hz band pass) and digitized with a Powerlab 26T device and LabChart software package (version 5, ADInstruments, Ltd., Dunedin, New Zealand).

2.4 Theta-burst stimulation

iTBS was delivered over the left M1 using a Magstim SuperRapid 2 with a figure-of-eight coil (70-mm standard coil, Magstim Co., Whitland, Dyfed, UK) according to Huang et al. (2005). As previoulsy described (and evaluated), iTBS was applied during M1- and sham-iTBS at 70% of the resting motor threshold (RMT) instead of 80% of the active motor threshold (AMT) (Cárdenas-Morales et al., 2014; Gentner et al., 2008; Sarfeld et al., 2012) due to the following: We wished to prevent voluntary preactivation of the target muscle, which is necessary for AMT determination but may impact on TBS aftereffects (Gentner et al., 2008; Huang et al., 2008) and may increase inter-subject variability (Goldsworthy et al., 2014).

2.5 MEPs

Neuronavigated single-pulse TMS was applied over the same location as used for iTBS using a Magstim 200^2 stimulator (Magstim Co., Whitland, Dyfed, UK). At baseline and after each iTBS-application (iTBS600, iTBS1200, iTBS1800), stimulus-response curves of MEPs evoked with intensities ranging from 90% to 150% of the RMT were assessed in steps of 10%. Two blocks of five pulses were recorded in a randomized order for each intensity, except for 120%, which was assessed in six blocks at five pulses adding up to a total number of 90 MEPs.

2.6 Data analysis – MEPs

In line with previous experiments, we used “normalized” MEP amplitudes to assess changes in cortical excitability rather than absolute MEP amplitudes to account for variance in RMTs at different stimulation days (i.e., M1- and sham-iTBS) (Cárdenas-Morales et al., 2014; Huang et al., 2005; Nettekoven et al., 2014). Therefore, mean MEP amplitudes acquired after each block of iTBS were normalized to mean baseline values of the respective intensity (i.e., 90-150% of the RMT).

Finally, stimulus-response curves were plotted for each subject using the absolute MEP amplitudes to test for iTBS effects on the slope of the stimulus-response

curves. The steepness of each curve was computed by means of a linear regression analysis and R^2 values were calculated to assess the quality of model-fit using SPSS 21 (Statistical Package for the Social Sciences, IBM, New York/USA).

2.7 Definition of responders

The scope of this paper was to investigate whether inter-individual differences in the electrophysiological response to iTBS (i.e., in MEP amplitudes) are related to the different connectivity profiles of the stimulated region before and after stimulation. Therefore, responders and non-responders were classified according to their increase in MEPs after the first stimulation block (M1-iTBS600): Subjects showing an increase of ≥10% in MEPs compared to baseline were defined as responders (Hinder et al., 2014). This threshold criterion ensured that responders had a clear stimulation aftereffect, possibly accounting for random fluctuations around the baseline-level.

To test for differences between responders and non-responders in the dose-dependent modulation of normalized MEP amplitudes, we set up a four-factorial repeated measures analysis of variance (ANOVA) with the within-subject factors INTERVENTION (2 levels: M1-iTBS, sham-iTBS), DOSE (3 levels: iTBS600, iTBS1200, iTBS1800), INTENSITY (7 levels: 90-150% of the RMT) and the between-subject factor GROUP (2 levels: responders, non-responders) using SPSS 21. The Greenhouse-Geisser alpha-correction was used in case of a violation of the non-sphericity assumption. Post-hoc Student´s t-tests were performed to compare the iTBS response between responders and non-responders and to test for iTBS effects within groups. False discovery rate (FDR)-correction was used to correct for multiple comparisons (Benjamini and Hochberg, 1995). To test whether M1-iTBS differentially modulated the slope of stimulus-response curves in responders and non-responders in a dose-dependent fashion, the curve-steepness was entered into a three-way repeated measures ANOVA with the within-subject factors INTERVENTION (2 levels: M1-iTBS, sham-iTBS), DOSE (3 levels: iTBS600, iTBS1200, iTBS1800) and the between-subject factor GROUP (2 levels: responders, non-responders).

2.8 Magnetic resonance imaging

After assessing the TMS hotspot and the RMT subjects were transported in an MR-compatible wheel chair between the anteroom of the scanner where stimulation was applied and the scanner room. This was to minimize any further movement since pre- or post-interventional neuronal activity can strongly impact on TBS aftereffects (Gentner et al., 2008; Goldsworthy et al., 2014; Huang et al., 2008) and thereby also on the susceptibility to iTBS. Moreover, we aimed to obtain comparable conditions between the resting-state scans. In the scanner, subjects were instructed to lie motionless with open eyes fixating a red cross (resting-state fMRI), which was presented on a TFT screen visible through a mirror attached to the MR head coil. After the baseline fMRI, subjects were transported from the scanner to the anteroom of the MR console. After coregistration with the neuronavigation system, iTBS was applied followed by another 8 min resting-state fMRI. This procedure was repeated three times in total (three blocks of iTBS), always separated by 15 min.

In addition, an active motor task was performed after the baseline resting-state fMRI (and before the first iTBS block) for localization of motor areas. The task consisted of rhythmic thumb ab- and adductions with the right or left hand (please see Nettekoven et al., 2014 for details). Of note, the task activated the same muscle as used for TMS recordings (APB). The motor task was acquired after the first resting-state scan to prevent motor activity to bias rsFC.

2.9 Image acquisition and preprocessing

fMRI images were acquired on a Siemens Trio 3.0 T scanner (Siemens Medical Solutions, Erlangen, Germany) using a gradient echo planar imaging (EPI) sequence with the following parameters: TR = 2070 ms, TE = 30 ms, FOV = 200 mm, 31 slices, voxel size: 3.1 x 3.1 x 3.1 mm^3, 20% distance factor, flip angle = 90°, resting-state: 225 volumes (3 dummy images), localizer task: 202 volumes (3 dummy images). Acquisition planes and slice orientation were identical for the four fMRI assessments (i.e., 1 x baseline, 3 x post iTBS sessions). The slices covered the whole brain extending from the vertex to the lower parts of the cerebellum. fMRI data (resting-state and motor task) were analyzed using Statistical Parametric Mapping (SPM8, http://www.fil.ion.ucl.ac.uk/spm/). The first three volumes (dummy images) of each session were discarded from further analyses to allow for magnetic field saturation. All remaining EPI volumes were realigned to the mean image of each time series and

coregistered with the structural T1-weighted image. In a next step, all images were spatially normalized to the standard template of the Montreal Neurological Institute (MNI, Canada) using the unified segmentation approach (Ashburner and Friston, 2005) and smoothed with an isotropic Gaussian kernel of 8 mm full-width at half-maximum.

To exclude the possibility that head movements during the resting-state scans contributed to group differences in rsFC we tested for differences in head motion parameters acquired from image realignment by comparing the framewise displacement (FD) and the root mean squared error (RMSE) (Power et al., 2012; Satterthwaite et al., 2012). Importantly, there was no difference between groups neither in the FD nor in the RMSE ($p>0.2$ for all comparisons, FDR-corrected). Likewise, FD and RMSE were not significantly different between the multiple stimulation blocks within responders and non-responders. Therefore, neither between nor within group differences in head movements are likely to have biased the rsFC results.

2.10 Statistical analysis – resting-state fMRI

For the statistical analysis of the resting-state data, variance that could be explained by known confounds was removed from the smoothed fMRI time-series. Confound regressors included the tissue-class-specific global signal intensities and their squared values, the six head motion parameters, their squared values and their first-order derivatives (Satterthwaite et al., 2012). A band-pass filter was used to preserve only frequencies between 0.01 and 0.08 Hz in the time-series data.

We computed a seed-based whole-brain analysis. Here, the time-course within a sphere of 10 mm-diameter centered on the seed voxel (left M1, single-subject coordinates derived from localizer task, please cf. Nettekoven et al., 2014) was correlated with the time course of every other voxel in the brain by means of linear Pearson´s correlation (Eickhoff and Grefkes, 2011; zu Eulenburg et al., 2012). Correlation coefficients were converted to Fisher´s Z-scores using the formula $Z = (1/2) \times \ln(1+r)/(1-r) = \operatorname{atanh}(r)$ to yield approximately normally distributed data.

In order to determine changes in functional connectivity following iTBS, individual baseline functional connectivity maps were subtracted from the respective maps post iTBS for each subject (Nettekoven et al., 2014). For group-level analysis, the individual subtraction maps were entered into a “full factorial” general linear model

(GLM) analysis as implemented in SPM8 with the factors GROUP (2 levels: responders, non-responders), INTERVENTION (2 levels: M1-iTBS, sham-iTBS) and DOSE (3 levels: iTBS600, iTBS1200, iTBS1800). Differential contrast were computed (i) between M1- and sham-iTBS for iTBS600, iTBS1200 and iTBS1800 (separately for responders and non-responders), (ii) between the different stimulation blocks (i.e., iTBS1800-iTBS1200, iTBS1800-iTBS600, iTBS1200-iTBS600; separately for responders and non-responders), and (iii) between responders and non-responders for M1- versus sham-iTBS for different stimulation blocks (i.e., iTBS600, iTBS1200, iTBS1800). The resting-state maps were masked by cytoarchitectonic probability maps of frontoparietal sensorimotor areas (Brodmann areas 6, 4 a/b, 3 a/b, 2, 1) as provided by the SPM Anatomy Toolbox (Eickhoff et al., 2005) to focus inference on rsFC within the cortical sensorimotor network. The statistical threshold was set to $p \leq 0.05$, family-wise error (FWE) corrected at the cluster-level.

3. Results

We here exclusively report findings related to iTBS responsiveness at the MEP and the fMRI network level. General effects have been reported elsewhere (Nettekoven et al., 2014). Seven of the subjects were classified as responders (i.e., increase in MEP amplitudes of ≥10% after the first iTBS block; Hinder et al., 2014) and nine as non-responders. This ratio is similar to what has been found in other studies (Hamada et al., 2013).

Table 1. Differences between responders and non-responders in RMTs before iTBS and MEPs at baseline[a]

	Responders	Non-Responders	p
baseline RMTs			
sham-iTBS	36.71 ± 8.79	30.78 ± 4.84	0.286
M1-iTBS	35.14 ± 7.40	30.00 ± 4.44	0.551
baseline MEPs			
sham-iTBS	0.97 ± 0.68	0.87 ± 0.48	0.757
M1-iTBS	0.93 ± 0.72	0.83 ± 0.42	1.000

[a]p-values are FDR-corrected for multiple comparisons.

3.1 Baseline measures

There were no significant differences in RMT at baseline and baseline MEPs when directly comparing M1-iTBS as well as sham-iTBS between responders and non-responders (Table 1). However, non-responders (relative to responders) featured a significantly higher baseline rsFC before M1-iTBS between the stimulated (left) M1 and bilateral dorsal premotor cortex (dPMC) as well as supplementary motor area (SMA) ($p \leq 0.05$, FWE-corrected at the cluster-level; Figure 2). The reverse contrast yielded no significant effects. That is, in responders (compared to non-responders) no area featured significantly stronger rsFC at baseline with left M1.

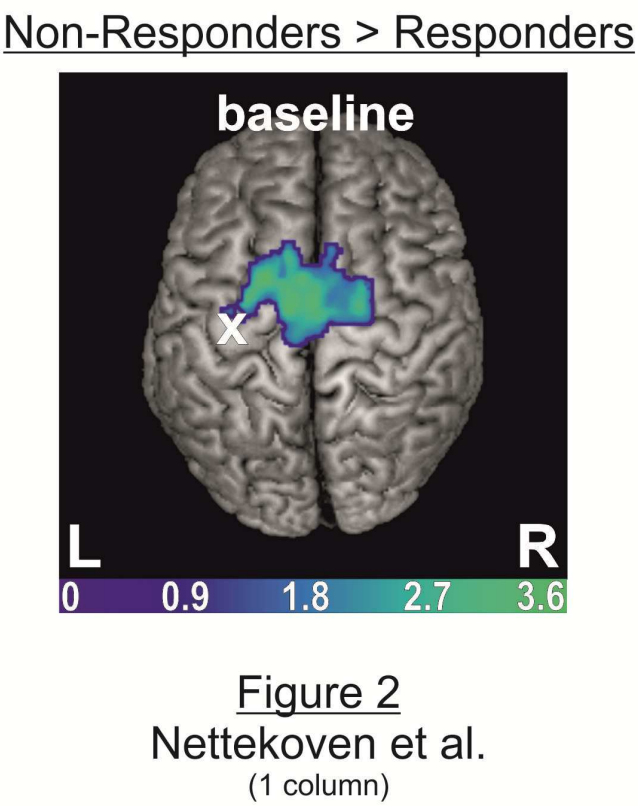

Figure 2
Nettekoven et al.
(1 column)

Figure 2. Baseline rsFC. Non-responders featured a higher baseline rsFC between M1 and a bilateral network including premotor areas (SMA, dPMC) compared to responders. Color bar represents t-values. Only clusters surviving a cluster level FEW-correction ($p \leq 0.05$) are shown. The X indicates the stimulated M1.

Within groups, RMTs at baseline were not significantly different between M1- and sham-iTBS for responders ($p=0.365$, FDR-corrected for multiple comparisons) and non-responders ($p=1.000$, FDR-corrected). Likewise, baseline MEP amplitudes did

not differ between sham- and M1-iTBS neither for responders (p=0.685, FDR-corrected) nor non-responders (p=0.753, FDR-corrected).

3.2 iTBS-induced plasticity: MEP amplitudes

A four-way repeated measures ANOVA assessing MEP differences after iTBS between responders and non-responders revealed a significant main effect of GROUP ($F_{1,14}$=10.362, p=0.006) as well as an interaction effect of the factors INTERVENTION x GROUP ($F_{1,14}$=10.246, p=0.006). However, there was no interaction effect of the factor INTENSTIY so that we averaged MEPs across all intensities for further analysis. Post-hoc Student`s t-tests on averaged MEP amplitudes revealed a significantly higher increase of MEP amplitudes in responders compared to non-responders after all three blocks of M1-iTBS. However, there was no significant difference between responders and non-responders in the steepness of stimulus-response curves. Moreover, post-hoc Student´s t-tests on MEP amplitudes revealed a dose-dependent decrease between sham-iTBS1200 and sham-iTBS1800 in non-responders (p=0.039, FDR-corrected) (Figure 3A). Importantly, no significant differences were found after sham-iTBS between groups. Furthermore, there were no significant increases neither for M1-iTBS compared to baseline nor between M1-iTBS and sham-iTBS for non-responders. By contrast, in responders MEP amplitudes significantly increased after M1- compared to sham-iTBS (iTBS600: p=0.032, iTBS1200: p=0.018, iTBS1800: p=0.030, FDR-corrected) as well as after M1-iTBS compared to baseline (iTBS600: p=0.010, iTBS1200: p=0.015, iTBS1800: p=0.023, FDR-corrected) (Figure 3B). Statistical trends suggesting dose-dependent increases in responders could be found between iTBS600 and iTBS1800 (p=0.076, FDR-corrected) as well as between iTBS1200 and iTBS1800 (p=0.076, FDR-corrected). Moreover, there were no significant effects on the steepness of the stimulus-response curves within the responder and the non-responder group.

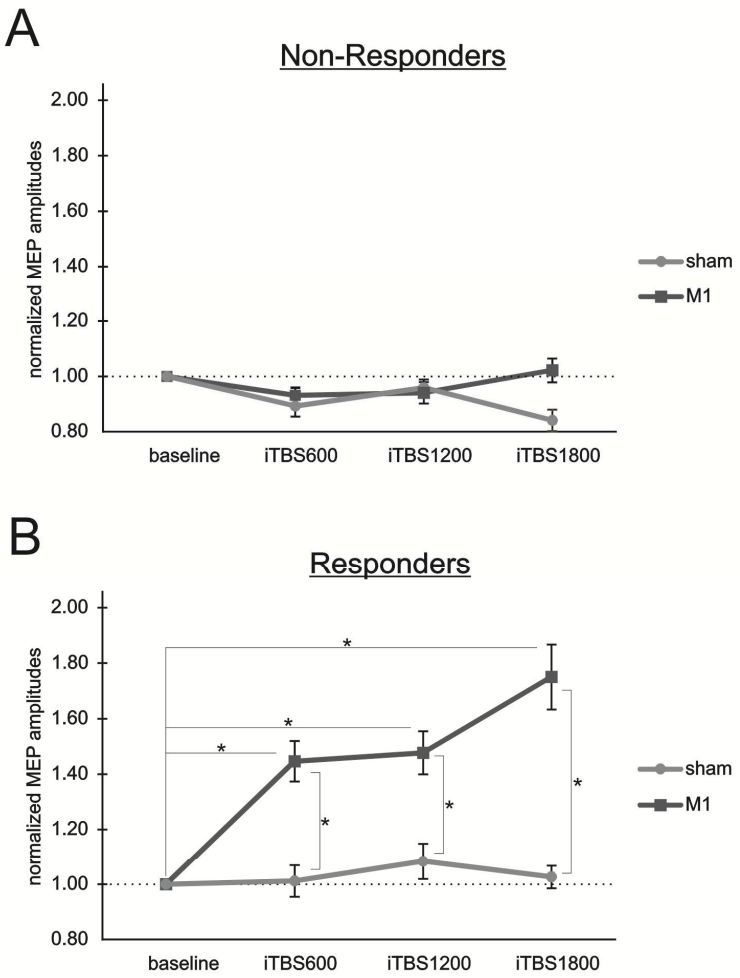

Figure 3
Nettekoven et al.
(1.5 columns)

Figure 3. Changes in normalized MEP amplitudes after iTBS. A. Non-responders. M1-iTBS did not lead to changes in normalized MEPs compared to sham-iTBS or baseline. MEP amplitudes decreased significantly between sham-iTBS1200 and sham-iTBS1800. **B. Responders.** M1-iTBS led to a significant increase in MEPs compared to baseline and sham-iTBS after all three iTBS blocks. Sham-iTBS did not lead to changes in MEPs compared to baseline. For M1-iTBS a statistical trend was evident for the increase between iTBS600 and iTBS1800 as well as between iTBS1200 and iTBS1800. * p≤0.05 (post-hoc Student´s t-test, FDR-corrected).

Taken together, the repeated application of iTBS did not modulate cortical excitability in non-responders but rather enhanced the aftereffects observed after iTBS600 in responders. Moreover, responders showed a significantly higher increase in cortical excitability compared to non-responders.

3.3 iTBS-induced plasticity: resting-state functional connectivity

When comparing rsFC after iTBS between responders and non-responders for different iTBS doses, we found in responders a significantly higher increase in rsFC for M1-iTBS vs. sham-iTBS for iTBS600 ($p=0.006$, FWE-corrected at the cluster-level) as well as iTBS1800 ($p\leq0.001$, FWE-corrected at the cluster-level) and a statistical trend after iTBS1200 ($p=0.071$, FWE-corrected at the cluster-level) (Figure 4A). Here, rsFC was significantly enhanced between M1 and a bilateral network comprising premotor areas (i.e., dPMC and SMA), parts of the somatosensory cortex as well as the contralateral M1.

Within groups we found a significant increase in rsFC after M1-iTBS compared to sham-iTBS after each block only in the responder group ($p\leq0.05$, FWE-corrected at the cluster-level, Figure 4B). Functional connectivity was enhanced between M1 and bilateral SMA and dPMC as well as parts of the somatosensory cortex and contralateral M1. In contrast, non-responders showed no significant increase after M1-iTBS compared sham-iTBS. Between the different stimulation blocks responders showed a significant dose-dependent increase from iTBS1200 to iTBS1800 ($p\leq0.05$, FWE-corrected at the cluster-level, Figure 5), but no significant increases were evident in the non-responder group.

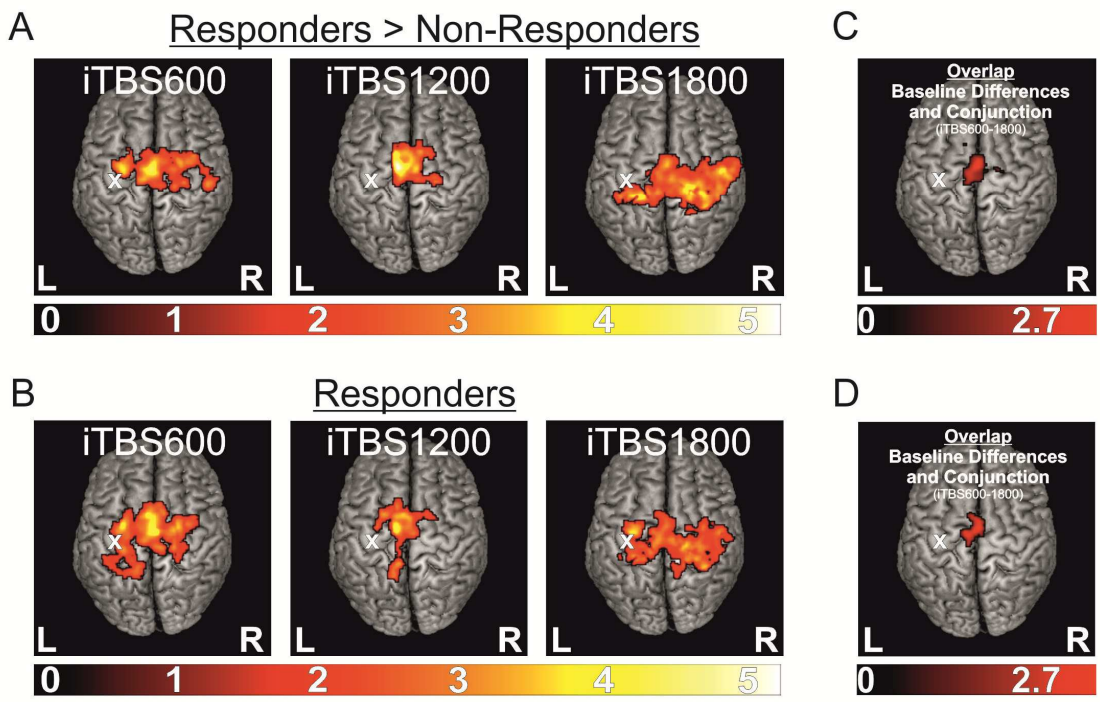

Figure 4
Nettekoven et al.
(2 columns)

Figure 4. Changes in rsFC after iTBS. A. Responders vs. non-responders. Responders (compared to non-responders) featured a significantly higher increase in rsFC for M1-iTBS > sham-iTBS after iTBS600 and iTBS1800. Likewise, a statistical trend was evident for iTBS1200. **B. Responders.** A significant increase in rsFC after M1-iTBS compared to sham-iTBS was found for responders after all three blocks of iTBS. In contrast, non-responders did not show a significant increase in rsFC. Color bar represents t-values. Only clusters surviving a cluster level FWE-correction ($p \leq 0.05$) are shown. The X indicates the stimulated M1. **Overlap with baseline differences. C. Responders vs. non-responders.** The areas showing baseline differences between responders and non-responders (Figure 2) overlapped with areas showing a stronger increase in rsFC after all three blocks of iTBS (conjunction iTBS600-1800) in responders compared to non-responders ($p \leq 0.05$, uncorrected). The overlap is present in the SMA. **D. Responders.** A similar overlap with baseline differences was found for the conjunction of the increase in rsFC after M1-iTBS600-1800 compared to sham-iTBS in the responder group ($p \leq 0.05$, uncorrected).

Interestingly, we found that areas showing different rsFC between responders and non-responders at baseline (non-responders > responders, Figure 2) overlapped with areas showing a higher increase in rsFC after all three iTBS blocks (conjunction iTBS600-1800) for responders compared to non-responders (p≤0.05, uncorrected). As shown in Figure 4C this overlap was present in the SMA. A similar overlap was evident for the increase in rsFC after all three M1-iTBS blocks compared to sham-iTBS (conjunction iTBS600-1800) in the responder group (p≤0.05, uncorrected, Figure 4D).

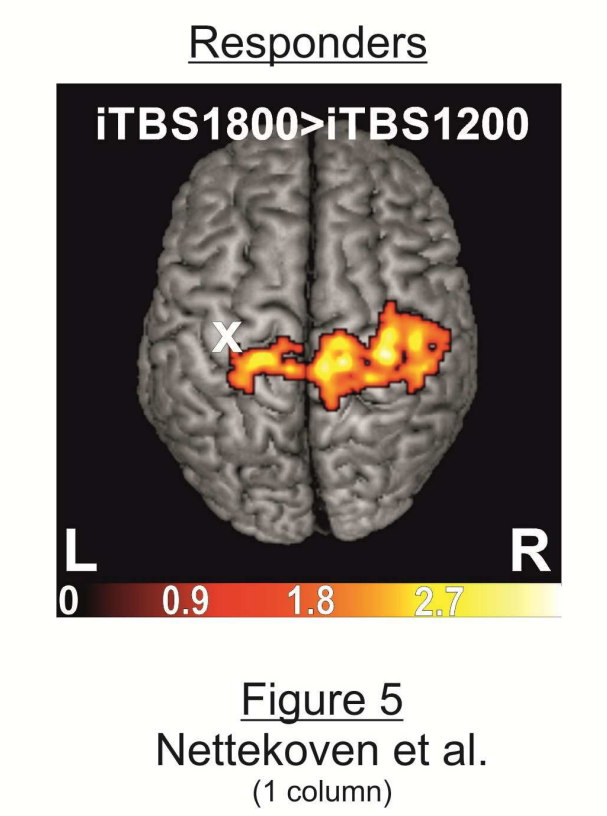

Figure 5. Dose-dependent increase in rsFC for iTBS responders. rsFC significantly increased after iTBS1800 compared to iTBS1200 (M1-iTBS > sham-iTBS) only in the responder group. p≤0.05, FWE-corrected on the cluster. The X indicates the stimulated M1.

In summary, only responders featured a significant increase in rsFC after iTBS as seen for MEP amplitudes. Likewise, rsFC increased dose-dependently between the second and third block only in the responder group. Moreover, rsFC was higher (significantly or statistical trend) in the responder group compared to the non-responder group for all three blocks of iTBS.

4. Discussion

4.1 Summary of findings

iTBS non-responders compared to responders featured higher pre-interventional levels of M1-connectivity with a cortical network comprising bilateral premotor areas. Furthermore, responders and non-responders differed in iTBS-induced aftereffects on MEP amplitudes as well as rsFC: only responders showed an increase in MEP amplitudes and in rsFC in a bilateral motor network comprising premotor areas as well as the contralateral M1 and somatosensory areas. Likewise, dose-dependent increases in MEPs and rsFC were found exclusively in responders. Of note, the network in which connectivity was significantly modulated by iTBS overlapped with areas showing baseline differences in connectivity between responders and non-responders.

4.2. Inter-individual variability in iTBS-responses (MEPs)

Recent studies reported no group-level effect of TBS on cortical excitability (Hamada et al., 2013; López-Alonso et al., 2014; Martin et al., 2006). Although in our cohort of subjects ~56% were classified as non-responders, we still observed a significant increase in MEP amplitudes across the entire sample (please cf. Nettekoven et al., 2014). We here found that this effect was driven by 44% of our subjects that featured strong canonical responses, i.e., increases in cortical excitability already after one block of iTBS. Note that responsiveness to iTBS in our cohort was slightly lower but similar compared to previous studies reporting 50% - 73% of their subjects to respond as expected, i.e., with an increase in MEPs after iTBS (Hamada et al., 2013; Hinder et al., 2014). Importantly, response rates observed between studies are similar, although different cut-offs regarding changes in MEP amplitudes were used to define responders and non-responders: above or below 100%, 110% or 120% (Goldsworthy et al., 2014; Hamada et al., 2013; Hinder et al., 2014; López-Alonso et al., 2014). Therefore, the choice of the distinction-criterion seems less critical. Remaining variance in response rates may result from, e.g., different time points and durations of MEP-assessment after iTBS as well as intensities used to obtain MEPs. We chose our criterion in accordance to Hinder and colleagues (2014) since changes in MEP amplitudes less than 10% might be due to variance of MEP assessment or represent rather negligible effects regarding behavioral or clinical implications.

However, whether or not a MEP increase of 10% actually leads to a relevant improvement in motor function needs to be investigated in future studies.

Our data on dose-dependent effects revealed that non-responders could not be turned into responders. Only responders benefited from a higher number of stimuli in terms of dose-dependent increases in cortical excitability, whereas non-responders remained at baseline level, or even dropped below, i.e., decreased in excitability. Taken together, the further enhancement of cortical excitability after iTBS1800 observed in our previous study (Nettekoven et al., 2014) was driven by an amplification of aftereffects in responders, and not from non-responders turning into responders. This finding is of high relevance not only for rTMS/TBS experiments in healthy subjects but also with respect to therapeutic interventions in patients.

4.3 Relationship between baseline measures and increases in cortical excitability

A number of factors have been discussed to contribute to the high inter-individual variability observed in the response to iTBS (and other rTMS protocols) such as daytime, previous history of activity, or genetic polymorphisms (for a review see Ridding and Ziemann, 2010). In line with other studies, we here did not find a significant effect of RMT or MEP amplitudes on changes in cortical excitability after iTBS (Hamada et al., 2013; López-Alonso et al., 2014).

We recently showed that fMRI connectivity between the premotor cortex and the stimulated M1 (in the activated motor system, i.e., when subjects performed an unimanual task) correlated with iTBS-induced increases in cortical excitability after 10 min (Cárdenas-Morales et al., 2014). However, in that study, rsFC did not correlate with MEP changes, a finding which was reproduced in the current study with an independent sample of subjects. This finding implies that MEPs and rsFC are not linearly related. Rather they seem to constitute two independent markers of iTBS aftereffects (Cárdenas-Morales et al., 2014; Nettekoven et al., 2014). However, when dividing subjects into responders and non-responders according to their increase in MEPs after the first stimulation we found a significantly higher baseline rsFC between M1 and premotor areas in non-responder compared to responders (Figure 2). One interpretation is that high baseline levels of rsFC (as found in the non-responder group) could preclude a further increase in rsFC and MEPs, hence constituting a ceiling effect. Indeed, other groups have suggested that ceiling effects with respect to the ability of modulating neural connectivity might underlie absent intervention effects

(Huang et al., 2010; Koch et al., 2008; Quartarone et al., 2003; Salomons et al., 2014). For example, Salomons and colleagues (2014) showed that a high baseline resting-state cortico-thalamic, cortico-striatal and cortico-limbic connectivity was associated with poorer rTMS treatment outcome in patients with major depressive disorder. Of note, a successful intervention effect was also associated with an increase in rsFC as seen for our group of responders.

Taken together, our data suggest that the responsiveness to iTBS (in terms of changes in MEP amplitudes) depends – at least in part - on the baseline level of rsFC between premotor areas and M1, possibly representing a biomarker for the individual responsiveness to iTBS.

4.4. Mechanisms underlying responsiveness to iTBS

Recent evidence from human and animal studies suggests that the individual response to TBS might derive from the stimulation of distinct subpopulations of interneurons (Benali et al., 2011; Funke and Benali, 2011; Hamada et al., 2013). High intensity (suprathreshold) single-pulse TMS with a latero-medial oriented current (LM-TMS) directly activates the axons of the corticospinal neurons resulting in direct waves (D-waves) as shown by epidural recordings (Di Lazzaro et al., 2012). In contrast, anterior-posterior (AP) TMS tends to evoke indirect waves (I-waves) with longer latencies resulting from the transsynaptic (hence indirect) activation of corticospinal neurons. Hamada and colleagues (2013) found that the response to AP-TMS (recruitment of I-waves) varies between subjects, accounting for a part of the inter-individual differences in stimulation aftereffects: Subjects showing the “expected” response to TBS tended to recruit late I-waves (high MEP-latency after AP-TMS relative to LM-TMS), whereas non-responders tended to recruit earlier I-waves (low MEP-latency after AP-TMS relative to LM-TMS). There is evidence that I-wave recruitment (i.e., responsiveness to iTBS) is related to premotor-M1 connectivity (Volz et al., 2014): Functional connectivity between premotor areas and M1 (highly similar to the network obtained here, Figure 2) is lower in subjects preferentially recruiting late I-waves following AP-TMS, resembling responders as described by Hamada and colleagues (2013). These findings fit our present data revealing that subjects, who featured a lower connectivity between M1 and premotor cortex, show a significant response to iTBS (increase in MEPs and rsFC). In contrast, cortical excitability and rsFC did not increase after iTBS in subjects with higher M1-

premotor connectivity at baseline. Premotor input to M1, which has been found to be related to iTBS responsiveness, excites some of the same circuitry that participate in I-wave generation (Di Lazzaro and Ziemann, 2013; Lemon, 2008; Shimazu et al., 2004), providing further evidence for the relationship between responsiveness to iTBS/I-wave recruitment and premotor-M1 connectivity.

Therefore, our data suggest that responsiveness to iTBS not only underlies local M1 excitability, but also the connectivity strength between M1 and premotor areas (which is associated with the recruitment of I-waves). This interpretation is further supported by our post iTBS data as well as other studies reporting that rTMS/TBS does not only lead to changes in cortical excitability of the stimulated region but also in connectivity of the stimulated and remote areas (Grefkes et al., 2010; Nettekoven et al., 2014; Suppa et al., 2008; van der Werf et al., 2011; Vercammen et al., 2010). Although not linearly correlated, increases in MEP amplitudes are paralleled by changes in rsFC (Nettekoven et al., 2014). Moreover, a study in stroke patients could show that patients with lesions affecting the premotor cortex but not M1 were less responsive to rTMS over M1 in terms of behavioural changes (Ameli et al., 2009). In the light of the present data, one explanation could be that the missing propagation of facilitation due to the disrupted connectivity between M1 and the premotor cortex negatively affected the induction of cortical plasticity by rTMS. Hence, the excitability state of premotor-M1 connections and the increase in rsFC between these areas could represent one mechanism underlying responsiveness to iTBS also at the behavioural level.

5. Conclusion

Responsiveness to iTBS seems to be strongly linked to motor network connectivity. Responders revealed increased MEP amplitudes as well as increased connectivity following a higher number of stimuli. The finding that non-responders could not be turned into responders by increasing the number of pulses strongly suggests that motor network connectivity limits the capacity of changes induced by non-invasive brain stimulation. Our findings might also hold implications for the clinical use of non-invasive brain stimulation, i.e., highlighting the necessity to identify patients that might benefit from TMS interventions (and thereby from multiple applications). Finding reliable biomarkers for responsiveness also in patient populations represents an important aim for future research.

6. Acknowledgments

CG was supported by grants from the Deutsche Forschungsgemeinschaft (DFG, GR 3285/2-1; GR3285/5-1 KFO219-TP8). The study additionally supported by the University of Cologne Emerging Groups Initiative (CONNECT group, CG, GRF) implemented into the Institutional Strategy of the University of Cologne and the German Excellence Initiative. SBE was supported by the Deutsche Forschungsgemeinschaft (DFG, EI 816/4-1; EI 816/6-1 and LA 3071/3-1), the National Institute of Mental Health (R01-MH074457), and the European EFT program (Human Brain Project). GRF gratefully acknowledges additional support from the Marga and Walter Boll Stiftung.

7. Literature

Ameli, M., Grefkes, C., Kemper, F., Riegg, F.P., Rehme, A.K., Karbe, H., Fink, G.R., Nowak, D.A., 2009. Differential effects of high-frequency repetitive transcranial magnetic stimulation over ipsilesional primary motor cortex in cortical and subcortical middle cerebral artery stroke. Ann Neurol 66, 298-309.

Andoh, J., Zatorre, R.J., 2011. Interhemispheric Connectivity Influences the Degree of Modulation of TMS-Induced Effects during Auditory Processing. Front Psychol 2, 161.

Andoh, J., Zatorre, R.J., 2013. Mapping interhemispheric connectivity using functional MRI after transcranial magnetic stimulation on the human auditory cortex. Neuroimage 79, 162-171.

Ashburner, J., Friston, K.J., 2005. Unified segmentation. Neuroimage 26, 839-851.

Benali, A., Trippe, J., Weiler, E., Mix, A., Petrasch-Parwez, E., Girzalsky, W., Eysel, U.T., Erdmann, R., Funke, K., 2011. Theta-burst transcranial magnetic stimulation alters cortical inhibition. J Neurosci 31, 1193-1203.

Benjamini, Y., Hochberg, Y., 1995. Controlling the False Discovery Rate: A Practical and Powerful Approach to Multiple Testing. J R Stat Soc Ser B (Methodological) 57, 289-300.

Cárdenas-Morales, L., Volz, L.J., Michely, J., Rehme, A.K., Pool, E.M., Nettekoven, C., Eickhoff, S.B., Fink, G.R., Grefkes, C., 2014. Network Connectivity and Individual Responses to Brain Stimulation in the Human Motor System. Cereb Cortex.

Di Lazzaro, V., Profice, P., Ranieri, F., Capone, F., Dileone, M., Oliviero, A., Pilato, F., 2012. I-wave origin and modulation. Brain Stimulation 5, 512-525.

Di Lazzaro, V., Ziemann, U., 2013. The contribution of transcranial magnetic stimulation in the functional evaluation of microcircuits in human motor cortex. Front Neural Circuits 7, 18.

Downar, J., Geraci, J., Salomons, T.V., Dunlop, K., Wheeler, S., McAndrews, M.P., Bakker, N., Blumberger, D.M., Daskalakis, Z.J., Kennedy, S.H., Flint, A.J., Giacobbe, P., 2014. Anhedonia and reward-circuit connectivity distinguish nonresponders from responders to dorsomedial prefrontal repetitive transcranial magnetic stimulation in major depression. Biol Psychiatry 76, 176-185.

Eickhoff, S.B., Grefkes, C., 2011. Approaches for the integrated analysis of structure, function and connectivity of the human brain. Clin EEG Neurosci 42, 107-121.

Eickhoff, S.B., Stephan, K.E., Mohlberg, H., Grefkes, C., Fink, G.R., Amunts, K., Zilles, K., 2005. A new SPM toolbox for combining probabilistic cytoarchitectonic maps and functional imaging data. Neuroimage 25, 1325-1335.

Funke, K., Benali, A., 2011. Modulation of cortical inhibition by rTMS - findings obtained from animal models. J Physiol 589, 4423-4435.

Gentner, R., Wankerl, K., Reinsberger, C., Zeller, D., Classen, J., 2008. Depression of human corticospinal excitability induced by magnetic theta-burst stimulation: evidence of rapid polarity-reversing metaplasticity. Cereb Cortex 18, 2046-2053.

Goldsworthy, M.R., Muller-Dahlhaus, F., Ridding, M.C., Ziemann, U., 2014. Inter-subject Variability of LTD-like Plasticity in Human Motor Cortex: A Matter of Preceding Motor Activation. Brain Stimul.

Grefkes, C., Nowak, D.A., Wang, L.E., Dafotakis, M., Eickhoff, S.B., Fink, G.R., 2010. Modulating cortical connectivity in stroke patients by rTMS assessed with fMRI and dynamic causal modeling. Neuroimage 50, 233-242.

Hamada, M., Murase, N., Hasan, A., Balaratnam, M., Rothwell, J.C., 2013. The role of interneuron networks in driving human motor cortical plasticity. Cereb Cortex 23, 1593-1605.

Herwig, U., Cardenas-Morales, L., Connemann, B.J., Kammer, T., Schönfeldt-Lecuona, C., 2010. Sham or real - Post hoc estimation of stimulation condition in a randomized transcranial magnetic stimulation trial. Neuroscience Letters 471, 30-33.

Herwig, U., Fallgatter, A.J., Hoppner, J., Eschweiler, G.W., Kron, M., Hajak, G., Padberg, F., Naderi-Heiden, A., Abler, B., Eichhammer, P., Grossheinrich, N., Hay, B., Kammer, T., Langguth, B., Laske, C., Plewnia, C., Richter, M.M., Schulz, M., Unterecker, S., Zinke, A., Spitzer, M., Schonfeldt-Lecuona, C., 2007. Antidepressant effects of augmentative transcranial magnetic stimulation: randomised multicentre trial. Br J Psychiatry 191, 441-448.

Hinder, M.R., Goss, E.L., Fujiyama, H., Canty, A.J., Garry, M.I., Rodger, J., Summers, J.J., 2014. Inter- and Intra-individual variability following intermittent theta burst stimulation: implications for rehabilitation and recovery. Brain Stimul 7, 365-371.

Huang, Y.Z., Edwards, M.J., Rounis, E., Bhatia, K.P., Rothwell, J.C., 2005. Theta burst stimulation of the human motor cortex. Neuron 45, 201-206.

Huang, Y.Z., Rothwell, J.C., Edwards, M.J., Chen, R.S., 2008. Effect of physiological activity on an NMDA-dependent form of cortical plasticity in human. Cereb Cortex 18, 563-570.

Huang, Y.Z., Rothwell, J.C., Lu, C.S., Wang, J., Chen, R.S., 2010. Restoration of motor inhibition through an abnormal premotor-motor connection in dystonia. Mov Disord 25, 696-703.

Koch, G., Schneider, S., Baumer, T., Franca, M., Munchau, A., Cheeran, B., Fernandez del Olmo, M., Cordivari, C., Rounis, E., Caltagirone, C., Bhatia, K., Rothwell, J.C., 2008. Altered dorsal premotor-motor interhemispheric pathway activity in focal arm dystonia. Mov Disord 23, 660-668.

Lemon, R.N., 2008. Descending pathways in motor control. Annu Rev Neurosci 31, 195-218.

López-Alonso, V., Cheeran, B., Rio-Rodriguez, D., Fernandez-Del-Olmo, M., 2014. Inter-individual variability in response to non-invasive brain stimulation paradigms. Brain Stimul 7, 372-380.

Martin, P.G., Gandevia, S.C., Taylor, J.L., 2006. Theta burst stimulation does not reliably depress all regions of the human motor cortex. Clin Neurophysiol 117, 2684-2690.

Nettekoven, C., Volz, L.J., Kutscha, M., Pool, E.M., Rehme, A.K., Eickhoff, S.B., Fink, G.R., Grefkes, C., 2014. Dose-dependent effects of theta burst rTMS on cortical excitability and resting-state connectivity of the human motor system. J Neurosci 34, 6849-6859.

Oldfield, R.C., 1971. The assessment and analysis of handedness: the Edinburgh inventory. Neuropsychologia 9, 97-113.

Power, J.D., Barnes, K.A., Snyder, A.Z., Schlaggar, B.L., Petersen, S.E., 2012. Spurious but systematic correlations in functional connectivity MRI networks arise from subject motion. Neuroimage 59, 2142-2154.

Quartarone, A., Bagnato, S., Rizzo, V., Siebner, H.R., Dattola, V., Scalfari, A., Morgante, F., Battaglia, F., Romano, M., Girlanda, P., 2003. Abnormal associative plasticity of the human motor cortex in writer's cramp. Brain 126, 2586-2596.

Salomons, T.V., Dunlop, K., Kennedy, S.H., Flint, A., Geraci, J., Giacobbe, P., Downar, J., 2014. Resting-state cortico-thalamic-striatal connectivity predicts response to dorsomedial prefrontal rTMS in major depressive disorder. Neuropsychopharmacology 39, 488-498.

Sarfeld, A.S., Diekhoff, S., Wang, L.E., Liuzzi, G., Uludag, K., Eickhoff, S.B., Fink, G.R., Grefkes, C., 2012. Convergence of human brain mapping tools: neuronavigated TMS parameters and fMRI activity in the hand motor area. Hum Brain Mapp 33, 1107-1123.

Satterthwaite, T.D., Elliott, M.A., Gerraty, R.T., Ruparel, K., Loughead, J., Calkins, M.E., Eickhoff, S.B., Hakonarson, H., Gur, R.C., Gur, R.E., Wolf, D.H., 2012. An improved framework for confound regression and filtering for control of motion artifact in the preprocessing of resting-state functional connectivity data. Neuroimage 64, 240-256.

Shimazu, H., Maier, M.A., Cerri, G., Kirkwood, P.A., Lemon, R.N., 2004. Macaque ventral premotor cortex exerts powerful facilitation of motor cortex outputs to upper limb motoneurons. J Neurosci 24, 1200-1211.

Suppa, A., Ortu, E., Zafar, N., Deriu, F., Paulus, W., Berardelli, A., Rothwell, J.C., 2008. Theta burst stimulation induces after-effects on contralateral primary motor cortex excitability in humans. J Physiol 586, 4489-4500.

van der Werf, Y.D., Sanz-Arigita, E.J., Menning, S., van den Heuvel, O.A., 2011. Modulating spontaneous brain activity using repetitive transcranial magnetic stimulation. BMC Neurosci 11, 145.

Vercammen, A., Knegtering, H., Liemburg, E.J., den Boer, J.A., Aleman, A., 2010. Functional connectivity of the temporo-parietal region in schizophrenia: effects of rTMS treatment of auditory hallucinations. J Psychiatr Res 44, 725-731.

Volz, L.J., Benali, A., Mix, A., Neubacher, U., Funke, K., 2013. Dose-dependence of changes in cortical protein expression induced with repeated transcranial magnetic theta-burst stimulation in the rat. Brain Stimul 6, 598-606.

Volz, L.J., Hamada, M., Rothwell, J.C., Grefkes, C., 2014. What Makes the Muscle Twitch: Motor System Connectivity and TMS-Induced Activity. Cereb Cortex.

zu Eulenburg, P., Caspers, S., Roski, C., Eickhoff, S.B., 2012. Meta-analytical definition and functional connectivity of the human vestibular cortex. Neuroimage 60, 162-169.

3. Discussion

The aim of the present thesis was to investigate the mechanisms underlying cortical plasticity in the human motor system induced by iTBS as well as the factors contributing to the high inter-individual variability in the response to iTBS. These issues were here addressed by using functional neuroimaging and connectivity analyses of the human cortical motor system. In the following sections, the main findings of the present thesis will be discussed. First, the focus will be on the correlation between iTBS aftereffects (increase in MEP amplitudes) and the level of BOLD-activity as well as effective connectivity between motor areas. Next, the effect of multiple stimulation blocks on MEP amplitudes and resting-state functional connectivity (rsFC) revealing possible mechanisms underlying iTBS-induced cortical plasticity will be discussed. Finally, the contribution of rsFC to the understanding of inter-individual iTBS aftereffects will be elucidated as well as the influence of multiple stimulation blocks on the individual susceptibility to iTBS.

3.1 Network connectivity and individual responses to brain stimulation in the human motor system

The first study focused on the relationship between iTBS-induced aftereffects on cortical excitability (MEP amplitudes) and neural activity (BOLD activity) as well as connectivity of the stimulated motor system. Therefore, 12 right-handed subjects underwent resting-state fMRI as well as fMRI while performing a simple hand motor task. Sham-controlled aftereffects of iTBS applied over the left M1 were investigated in a separate session for up to 25 min post-stimulation via single-pulse TMS. A whole-brain analysis as well as a seed-to-seed analysis were used to assess rsFC. For the motor task data, task-induced activation (BOLD activity) and effective connectivity (via DCM) were estimated.

Our findings revealed that the magnitude of changes in cortical excitability were strongly related to the level of BOLD activity at the stimulated, left M1 and to effective connectivity between distinct motor areas of the stimulated hemisphere. More precisely, large clusters of movement-related M1 activity were negatively correlated with changes in MEP amplitudes at 10 min post stimulation (strongest iTBS group effect). This finding indicates that subjects with a more focused BOLD activity at the

stimulated M1 show a stronger response to iTBS. Further support for this hypothesis stems from a study showing that iTBS led to a decrease in BOLD activity during a hand choice reaction task compared to sham stimulation, i.e., increased efficacy of neural signal transmission induced by iTBS (Cárdenas-Morales et al., 2011). Likewise, motor recovery in patients is going along with a focusing of motor system activity after an initial extension (Chollet et al., 1991; Ward et al., 2003; Eickhoff et al., 2008; Grefkes et al., 2008). Hence, more focal BOLD activity patterns induced by a simple motor task seem to reflect a more efficient cortical motor network, i.e., that less neural resources are needed for task performance. Subjects featuring an efficient cortical motor network might also feature a greater capacity to respond with increased cortical excitability after plasticity enhancing iTBS.

A correlation between changes in cortical excitability and rsFC could not be found in this study. This null result might derive from a high inter-individual variability in rsFC and MEP amplitudes or the assessment of rsFC and MEP amplitudes on separate days. However, this seems unlikely given the high retest-reliability of both parameters (Shehzad et al., 2009; Cacchio et al., 2011) and the fact that a high correlation could be found for DCM and BOLD activity, which were assessed in the same session as rsFC. The analyses of effective connectivity revealed that high coupling estimates between vPMC and SMA as well as between vPMC and M1 of the left hemisphere were correlated with a high increase in MEP amplitudes post iTBS. Therefore, not only the stimulated M1, but also the whole motor network including vPMC and SMA might contribute to iTBS aftereffects. Similar results have been reported for the auditory system, where a better response to rTMS could be predicted by DCM connectivity of the primary auditory cortex (Andoh and Zatorre, 2011). Interestingly, although no correlation with rsFC could be found, the endogenous coupling among motor areas (as reflected by DCM A) also correlated with iTBS aftereffects. In contrast to rsFC, which is defined as the temporal dependence of neuronal activity patterns of anatomically separated brain regions at (Friston et al., 1993), the endogenous connectivity in DCM represents the constant part of connectivity in the activated motor system which is specific to the particular fMRI experiment (Friston et al., 2003). Therefore, the coupling of motor areas in the activated motor system prior to stimulation might also enable a high susceptibility to iTBS and might have a predictive value for iTBS interventions.

In conclusion, strong aftereffects of iTBS could be predicted by a low level of BOLD activity at M1 and a strong effective connectivity between left vPMC and SMA as well as between left vPMC and M1. No correlation could be found for functional connectivity measured at rest. Therefore, changes in cortical excitability seem to be related to the task dependent interplay of M1, vPMC and SMA. Moreover, cortical excitability changes after the induction of cortical plasticity via iTBS seem to depend not only on local properties, but also on the interaction between distinct motor areas.

3.2 Dose-dependent effects of theta burst rTMS on cortical excitability and resting-state connectivity of the human motor system

In study II, dose-dependent effects of iTBS on cortical excitability and rsFC were tested to investigate whether aftereffects can be amplified by multiple stimulation blocks and to find out about possible mechanisms underlying iTBS aftereffects. Accordingly, 16 healthy, right-handed subjects received stimulation over M1 and the parieto-occipital vertex (sham) on different days. In each session, three blocks of iTBS (i.e., iTBS600, iTBS1200 and iTBS1800) were applied separated by 15 min. Aftereffects on MEP amplitudes and rsFC were assessed in separate sessions, leading to a total of four sessions (i.e., M1-iTBS_MEPs, sham-iTBS_MEPs, M1-iTBS_rs-fMRI, sham-iTBS_rs-fMRI). A seed-based whole-brain analysis was conducted to estimate rsFC.

For the first time, it could be shown that cortical excitability can be enhanced by increasing the number of iTBS stimuli from 600 up to 1,800 and by using an inter-stimulus interval of 15 min. Previous studies using different inter-stimulus intervals ranging from 0 to 20 min could not observe a further increase in MEP amplitudes after two blocks of iTBS (Gamboa et al., 2010; Gamboa et al., 2011), which is similar to our finding after iTBS1200. The finding after two blocks of iTBS can nicely be explained in the framework of homeostatic metaplasticity (Bienenstock-Cooper-Munro theory, Bienenstock et al., 1982): increasing cortical excitability (induction of LTP) might increase the threshold for inducing further synaptic plasticity since the induction of LTD by the next stimulation is favored. However, after 1,800 pulses the threshold for inducing further LTP-like effects must be overcome. Another explanation for dose-dependent effects of iTBS comes from an animal study investigating iTBS aftereffects on the cellular level in rats using the same stimulation protocol and inter-session

interval as used for this study (Volz et al., 2013). Volz and colleagues reported that iTBS dose-dependently modified the inhibitory cortical system, i.e., the expression-patterns of subgroups of GABAergic inhibitory interneurons. For example, the protein expression of parvalbumin-positive cells, which constitute the largest group of interneurons, was significantly decreased after three blocks of iTBS (iTBS1800). Therefore, the dose-dependent increase in MEP amplitudes observed in our study might - at least partly - be explained by the dose-dependent decrease of inhibitory interneuron activity. Furthermore, we found that dose-dependent iTBS aftereffects seem to be more pronounced when MEPs are evoked with intensities near threshold (i.e., 90%-110% of the resting motor threshold) compared to higher intensities (i.e., 120%-150% of the resting motor threshold). TMS at high intensities directly activates the axons of corticospinal neurons and most likely evokes D-waves, which are not modified by changes in cortical excitability (Di Lazzaro et al., 2012). Contrariwise, near-threshold intensities activate corticospinal neurons transsynaptically via axonal projections of interneurons thereby recruiting I-waves, which are modified by changes in cortical excitability (Di Lazzaro et al., 2008; Di Lazzaro et al., 2012). Therefore, our observation nicely fits the hypothesis on the involvement of interneurons in the dose-dependent modulation following iTBS.

Moreover, iTBS did not only lead to changes in cortical excitability, but also in motor network connectivity. After iTBS, rsFC was enhanced between the stimulated M1 and bilateral premotor areas like SMA and dPMC as well as areas of the somatosensory and superior parietal cortex. Changes in rsFC after iTBS might derive from activity conduction via corticocortical fibers since these regions are densely connected with each other (Stepniewska et al., 1993; Geyer et al., 2000). Concurrent activation of two regions might increase their synchronicity of neural activity, thereby increasing the functional connectivity between them (Fries, 2005; Veniero et al., 2013). Therefore, iTBS effects on the systems level might derive from an increase in coherence of brain activity after the timely dependent activation of interconnected brain areas. Moreover, dose-dependent increases in cortical excitability were found to be paralleled by dose-dependent changes in rsFC between M1 and premotor areas (i.e., dPMC). Increases in rsFC might therefore promote the beneficial effect of iTBS on the behavioral level together with changes in cortical excitability. However, increases in cortical excitability

were not linearly correlated to increases in rsFC. Therefore, MEP amplitudes and rsFC seem to be two independent markers of iTBS aftereffects.

Taken together, a possible benefit from multiple stimulation block using an inter-stimulus interval of 15 min could be found for the first time, thereby highlighting the importance of choosing the right inter-stimulus interval for optimizing stimulation protocols. Moreover, our findings on dose-dependent increases in cortical excitability after iTBS gave evidence that the distinct activation of interneurons might be one possible mechanism underlying iTBS aftereffects. Another important finding was that iTBS also had an effect on the functional connectivity of the cortical motor system. Increases in cortical excitability were paralleled by increases in rsFC. However, they seem to be two independent markers of iTBS response.

3.3 Inter-individual variability in cortical excitability and motor network connectivity following multiple blocks of rTMS

The aim of study III was to investigate whether responsiveness to iTBS can be altered by applying multiple stimulation blocks. Furthermore, the question was whether responders and non-responders to iTBS differ regarding their pre-interventional rsFC as well as their changes in rsFC induced by iTBS. Therefore, the data of study II were re-analyzed with respect to the inter-individual variability in the response to iTBS.

Responders and non-responders were classified according to their increase in MEP amplitudes after one block of iTBS (responders: ≥10%, Hinder et al., 2014). This criterion resulted in seven responders (44%) and nine non-responders (56%). This is slightly lower but similar to previous studies, which reported that 50%-73% of their subjects did not respond to TBS in the “canonical” manner (Hamada et al., 2013; Hinder et al., 2014). Although a number of studies recently reported no effect of TBS on cortical excitability on the group level (Martin et al., 2006; Hamada et al., 2013; López-Alonso et al., 2014), a significant increase in cortical excitability across all subjects could be found here (study II). Interestingly, our data on dose-dependent effects showed that only responders showed a further increase in MEP amplitudes after multiple stimulation blocks. In contrast, non-responder after one block (increase in MEP amplitudes <10%) remained around baseline level or showed a decrease in MEP amplitudes even after two or three iTBS blocks. Hence, the increase seen in

study II over the whole group of subjects seems to be driven by an amplification of aftereffects in responders, and not from non-responders turning into responders. Therefore, our data suggest that responsiveness cannot be altered by increasing the number of pulses, but rather represents an intrinsic property.

Further support for this hypothesis stems from our finding that responders and non-responders differed in their rsFC between M1 and premotor areas before stimulation, i.e., non-responders featured a stronger rsFC of M1 with premotor areas (dPMC) and SMA compared to responders. Moreover, increases in rsFC after iTBS could only be observed in the responder group, giving evidence that responsiveness to iTBS in terms of MEP increases is paralleled by increases in rsFC. Thus, the individual susceptibility to iTBS manifests not only on the local level (M1 excitability) but also on the network level (rsFC between distinct motor areas). One interpretation would be that high baseline levels of rsFC preclude a further increase, both in rsFC and cortical excitability, constituting a ceiling effect. This hypothesis is in line with other studies, also reporting a ceiling effect in the ability to modulate neural connectivity to underlie missing intervention effects (Quartarone et al., 2003; Koch et al., 2008; Huang et al., 2010; Salomons et al., 2014). A recent study of our group suggested that functional connectivity between premotor areas, SMA and M1 (similar areas as found here) is lower in subjects preferentially recruiting late I-waves after stimulation with AP-TMS relative to LM-TMS (Volz et al., 2014). According to Hamada and colleagues (2013) subjects preferentially recruiting late I-waves show the “expected” response to iTBS, i.e., are responders. Together, these findings suggest that responsiveness to iTBS is related to functional connectivity within the motor system. Again, this hypothesis could be confirmed by the present study (III). Furthermore, a study in stroke patients could show that patients with lesions affecting premotor regions are less responsive to rTMS over M1 on the behavioral level (Ameli et al., 2009). Non-responsiveness, therefore, seems to result from a missing propagation of facilitation caused by the missing connection between M1 and premotor regions or a high baseline rsFC between M1 and premotor regions (limited capacity for modifications) as found here.

Taken together, the excitability state of premotor-M1 connections and SMA-M1 connections as well as the increase in rsFC between these areas could represent one mechanism underlying responsiveness to iTBS. Importantly, non-responders could not be turned into responders by increasing the stimulation dose. Only responders after

the first block of iTBS showed a further increase in MEP amplitudes as well as rsFC after three iTBS blocks. This finding is of high relevance not only for rTMS/TBS experiments in healthy subjects but also with respect to therapeutic interventions in patients.

3.4 Methodological limitations

3.4.1 Transcranial magnetic stimulation

One general limitation when using TMS in humans is that findings can only be interpreted indirectly. For instance, the extent or spread of the induced current in the underlying tissue varies between subjects. As one cannot study TMS effects on the cellular/molecular level in humans, it is hard to say which cortical neurons and how much cortical area is affected (Bolognini and Ro, 2010). Moreover, the effect on these neurons could be excitatory, inhibitory, or state-dependent (Ziemann, 2010). Therefore, the explanation on mechanisms underlying dose-dependent effects in humans based on animal studies remains at the very end speculative. A further limitation of TMS is that only cortical areas, but no subcortical areas (e.g., basal ganglia) can be stimulated. Although it might be possible to stimulate some subcortical regions depending on the stimulation intensity and coil (Zangen et al., 2005), stimulation is less focal and cortical regions would always be co-affected. Moreover, a number of factors like contraction of the head and neck muscles and the loud click of the coil (at high intensities) should always be considered when carrying out TMS experiments (Bolognini and Ro, 2010). This problem can be overcome by e.g. wearing earplugs. In addition, the spatial resolution of TMS is relatively low compared to e.g. fMRI. However, depending on the stimulation coil areas within the order of a few millimeters can be stimulated (Ro et al., 1999). In contrast, the temporal resolution of TMS is higher compared to fMRI (due to the hemodynamic response latency).

As outlined in this thesis one factor limiting the use and comparability of non-invasive brain stimulation paradigms such as iTBS is the high inter-individual variability. Intrinsic factors such as genetics (Cheeran et al., 2008), differential recruitment of interneurons (Hamada et al., 2013) or motor network connectivity, as shown here, might influence the response to stimulation protocols. However, these factors rather contribute to between-subject variability than to within-subject variability (Vallence and Ridding,

2014). In contrast, there are many factors contributing to within- and between subject variability that need to be controlled for. For example, time of the day, prior voluntary motor activity or pharmacology might strongly impact on stimulation aftereffects (Ridding and Ziemann, 2010). Therefore, the confounding of these factors should also be taken into account when planning TMS experiments. Besides the high inter-individual variability, the duration of changes induced by stimulation is limited, thereby limiting the usefulness of the stimulation paradigms (Vallence and Ridding, 2014). Changes have been observed for up to 60 min following stimulation (Huang et al., 2005) and are assumed to underlie LTP- and LTD-like mechanisms similar to changes in cortical excitability observed after electrical stimulation in hippocampal rat tissue (Malenka and Bear, 2004). However, they seem to reflect only the very earliest phase of activity-dependent plasticity, which might explain the high variability as well as the modest effects on behavior (Vallence and Ridding, 2014). Animal studies could show that more persistent and later-phase activity dependent plasticity can be induced when stimulation is repeated within short time intervals of 10-15 min compared to a single application (Bliss and Gardner-Medwin, 1973; Barnes, 1979; Abraham, 2003). Recently, a human study could show that two blocks of cTBS applied with an inter-session interval of 10 min led to less variable and longer-lasting results (Goldsworthy et al., 2012). We, here, found similar results regarding the strength of aftereffects. However, time-effects have not been investigated here, but similar results would be expected. Moreover, it needs to be clarified whether aftereffects observed in humans after repeated application within short time intervals also represent later-phase activity dependent plasticity.

3.4.2 Resting-state fMRI

One important pitfall of resting-state fMRI is that subjects might fall to sleep inside the scanner and it is difficult to control for this. Long scanning times promote fatigue. Therefore, a good tradeoff between robustness of the data (signal-to-noise ratio) and fatigue of the subjects is necessary. Van Dijk and colleagues (2010) suggested a scanning-time of ~7 min to be sufficient. Scanning subjects with open eyes, e.g., ask them to fixate a red cross like in our studies, might also prevent fatigue. Other confounding factors are physiological artifacts like heart rate or respiration (Birn et al., 2008) and head movements (Power et al., 2012; Van Dijk et al., 2012). In the studies

of the present thesis, BOLD fMRI data were adjusted for possible confounds by removing variance that could be explained by these known confounds. Confound regressors included the tissue-class-specific global signal intensities, the six head motion parameters, their squared volumes, and their first order derivatives thereby substantially reducing their impact on the resting-state data (Satterthwaite et al., 2012). This is especially critical when studying group differences. Notably, no significant difference in head motion parameters between our groups of responders and non-responders could be found.

When investigating intervention effects of rTMS/TBS on rsFC one should keep in mind, that BOLD fMRI only indirectly measures neuronal activity. Therefore, it may well be that changes in neuronal activity as induced by rTMS/TBS are not detected using fMRI. Here, another approach to investigate aftereffects of rTMS/TBS in humans more precisely on the involvement of neurotransmitters would be magnetic resonance spectroscopy (MRS), which has already been used for studying cTBS intervention effects (Stagg et al., 2009). However, MRS is unfortunately not capable of, e.g., addressing differential effects of iTBS on the activity of distinct subpopulations of GABAergic inhibitory interneuron. Moreover, MRS cannot distinguish between extra- and intracellular origins of the GABA-signal (Stagg et al., 2010). Therefore, further research on TBS aftereffects in animal studies is necessary.

3.4.3 Dynamic causal modeling

In general, the use of DCM is limited by the number of areas that can be included in a model due to the stability of model estimations (Penny et al., 2004; Stephan et al., 2010). Usually, eight to ten regions can be included into the model as implemented in SPM8. In study I, the primary visual cortex was chosen as an input region and bilateral M1, SMA and vPMC. The vPMC was included in our model instead of the dPMC, because monkey studies revealed that neurons in vPMC (areas F4/F5) are engaged in movements of the hands and fingers, which were primarily addressed by our fMRI task. In contrast, the dPMC codes movements of the arm based on visual and somatosensory information (Dum and Strick, 1992; Rizzolatti and Fadiga, 1998). However, in study II and III the dPMC was found to be involved in the dose-dependent modulation of rsFC after iTBS via a seed-based whole-brain analysis. Therefore, our

data suggest that the dPMC should also be considered in DCM models in future studies when testing for the relationship between effective connectivity and iTBS aftereffects.

Another limitation is that DCM is strongly hypothesis-driven since one has to choose a number of limited regions in advance. In contrast, a seed-based whole brain analysis (for resting-state functional connectivity) is less based on a-priori assumptions, because you only have to choose one seed region, whose time-course is correlated with the time-course of every other voxel in the brain. However, functional connectivity only reveals information about a temporal co-activation, but does not provide insights into how correlations are mediated. In contrast, an advantage of DCM is that you can identify positive as well as negative influences that one area exerts over another, i.e., causal influences. Therefore, it is useful to answer your research question by using both, effective and functional connectivity estimates, as it was done in the present thesis.

3.5 Summary & Conclusion

The present studies contributed to the understanding of the mechanisms underlying cortical plasticity induced by non-invasive brain stimulation, i.e., iTBS. It could be shown that the application of 1,800 pulses of iTBS led to a dose-dependent increase in cortical excitability, which were most pronounced when MEPs were evoked with low stimulation intensities. These findings further contribute to the hypothesis that interneuron networks underlie iTBS aftereffects. Moreover, our data gave evidence that responsiveness to iTBS cannot be altered by increasing the number of pulses. Only responders after one stimulation block showed a dose-dependent increase in MEP amplitudes as well as rsFC.

Using connectivity analyses it could be shown that iTBS aftereffects depend not only on local properties of the stimulated region (here: M1), but also on the interaction between distinct brain regions as shown for functional and effective connectivity. Increases in MEP amplitudes correlated significantly with effective connectivity between M1 and distinct premotor areas, suggesting a tight relationship between these two parameters. Investigating the relationship between responsiveness to iTBS and rsFC revealed that non-responder feature a higher rsFC between M1 and premotor areas at baseline compared to responders. Therefore, motor network connectivity

seems to limit the capacity of changes induced by non-invasive brain stimulation (ceiling effect). Furthermore, increases in MEP amplitudes were paralleled by increases in rsFC. However, no correlation was evident. Therefore, rsFC and MEP amplitudes seem to represent to independent markers of iTBS response. Taken together, our findings might contribute to the understanding of the mechanisms underlying TBS-induced cortical plasticity as well as to optimize the use of non-invasive brain stimulation protocols both in basic scientific research as well as for therapeutic use.

3.6 Future prospects

In the light of the present data, it would be reasonable to further investigate whether increasing the dose of iTBS might also improve aftereffects at the behavioral level. Some studies gave evidence that the application of more than a single stimulation block has a positive influence on behavior, resembling the possibility of reaching more consistent effects when applying multiple stimulation blocks (Nyffeler et al., 2009; Cazzoli et al., 2012). Hence, whether or not the application of 1,800 iTBS-pulses applied within a short time-interval (e.g., 15 min) also induces more consistent changes on behavior needs to be investigated in future studies. Likewise, it would be interesting to examine whether the serial application of three iTBS blocks also leads to longer-lasting effects than described after one iTBS block. This would increase the usefulness of neuromodulation as a therapeutic tool.

Moreover, the question arises whether one can expect similar effects on dose-dependent increases in cortical excitability and rsFC after three blocks of iTBS in patients, e.g., suffering from stroke. Previous studies could already show that rTMS is capable of modulating pathological interactions, i.e., effective connectivity between cortical motor areas leading to improvements in motor performance of the paretic hand in stroke patients (Grefkes et al., 2010). Therefore, more pronounced changes in connectivity induced by 1,800 pulses of iTBS might also improve motor function compared to a single application in patients. Most importantly, the data show that it would be necessary to determine responders and non-responders in a group of patients to optimize therapeutic interventions, because non-responders cannot be turned into responders. Here, different therapeutic strategies should be taken into

account. In contrast, responders might benefit from a higher iTBS dose during rehabilitation processes when stimulation is for instance combined with physiotherapy.

4. Literature

Abraham WC (2003) How long will long-term potentiation last? Philosophical transactions of the Royal Society of London Series B, Biological sciences 358:735-744.

Adrian ED, Moruzzi G (1939) Impulses in the pyramidal tract. J Physiol 97:153-199.

Amassian VE, Stewart M, Quirk GJ, Rosenthal JL (1987) Physiological basis of motor effects of a transient stimulus to cerebral cortex. Neurosurgery 20:74-93.

Ameli M, Grefkes C, Kemper F, Riegg FP, Rehme AK, Karbe H, Fink GR, Nowak DA (2009) Differential effects of high-frequency repetitive transcranial magnetic stimulation over ipsilesional primary motor cortex in cortical and subcortical middle cerebral artery stroke. Ann Neurol 66:298-309.

Amunts K, Zilles K (2007) Funktionelle MRT in Psychiatrie und Neurologie. In: Schneider, F., Fink, G.R., editors, . Heidelberg: Springer:pp. 9-59.

Andoh J, Zatorre RJ (2011) Interhemispheric Connectivity Influences the Degree of Modulation of TMS-Induced Effects during Auditory Processing. Frontiers in psychology 2:161.

Aydin-Abidin S, Trippe J, Funke K, Eysel UT, Benali A (2008) High- and low-frequency repetitive transcranial magnetic stimulation differentially activates c-Fos and zif268 protein expression in the rat brain. Exp Brain Res 188:249-261.

Barker AT, Jalinous R, Freeston IL (1985) Non-invasive magnetic stimulation of human motor cortex. Lancet 1:1106-1107.

Barnes CA (1979) Memory deficits associated with senescence: a neurophysiological and behavioral study in the rat. Journal of comparative and physiological psychology 93:74-104.

Beckmann CF, DeLuca M, Devlin JT, Smith SM (2005) Investigations into resting-state connectivity using independent component analysis. Philosophical transactions of the Royal Society of London Series B, Biological sciences 360:1001-1013.

Benali A, Trippe J, Weiler E, Mix A, Petrasch-Parwez E, Girzalsky W, Eysel UT, Erdmann R, Funke K (2011) Theta-burst transcranial magnetic stimulation alters cortical inhibition. J Neurosci 31:1193-1203.

Bestmann S, Baudewig J, Siebner HR, Rothwell JC, Frahm J (2003) Subthreshold high-frequency TMS of human primary motor cortex modulates interconnected frontal motor areas as detected by interleaved fMRI-TMS. Neuroimage 20:1685-1696.

Bestmann S, Baudewig J, Siebner HR, Rothwell JC, Frahm J (2004) Functional MRI of the immediate impact of transcranial magnetic stimulation on cortical and subcortical motor circuits. Eur J Neurosci 19:1950-1962.

Bestmann S, Baudewig J, Siebner HR, Rothwell JC, Frahm J (2005) BOLD MRI responses to repetitive TMS over human dorsal premotor cortex. Neuroimage 28:22-29.

Bienenstock EL, Cooper LN, Munro PW (1982) Theory for the development of neuron selectivity: orientation specificity and binocular interaction in visual cortex. J Neurosci 2:32-48.

Birn RM, Murphy K, Bandettini PA (2008) The effect of respiration variations on independent component analysis results of resting state functional connectivity. Hum Brain Mapp 29:740-750.

Biswal B, Yetkin FZ, Haughton VM, Hyde JS (1995) Functional connectivity in the motor cortex of resting human brain using echo-planar MRI. Magnetic resonance in medicine : official journal of the Society of Magnetic Resonance in Medicine / Society of Magnetic Resonance in Medicine 34:537-541.

Bliss TV, Gardner-Medwin AR (1973) Long-lasting potentiation of synaptic transmission in the dentate area of the unanaestetized rabbit following stimulation of the perforant path. J Physiol 232:357-374.

Bolognini N, Ro T (2010) Transcranial magnetic stimulation: disrupting neural activity to alter and assess brain function. J Neurosci 30:9647-9650.

Brodmann K (1909) Vergleichende Lokalisationslehre der Grosshirnrinde: in ihren Principien dargestellt auf Grund des Zellenbaues. Leipzig: Johann Ambrosius Barth Verlag.

Büchel C, Friston KJ (1997) Modulation of connectivity in visual pathways by attention: cortical interactions evaluated with structural equation modelling and fMRI. Cereb Cortex 7:768-778.

Buxton RB, Wong EC, Frank LR (1998) Dynamics of blood flow and oxygenation changes during brain activation: the balloon model. Magnetic resonance in medicine : official journal of the Society of Magnetic Resonance in Medicine / Society of Magnetic Resonance in Medicine 39:855-864.

Cacchio A, Paoloni M, Cimini N, Mangone M, Liris G, Aloisi P, Santilli V, Marrelli A (2011) Reliability of TMS-related measures of tibialis anterior muscle in patients with chronic stroke and healthy subjects. Journal of the neurological sciences 303:90-94.

Cárdenas-Morales L, Gron G, Kammer T (2011) Exploring the after-effects of theta burst magnetic stimulation on the human motor cortex: a functional imaging study. Hum Brain Mapp 32:1948-1960.

Cárdenas-Morales L, Nowak DA, Kammer T, Wolf RC, Schonfeldt-Lecuona C (2010) Mechanisms and applications of theta-burst rTMS on the human motor cortex. Brain Topogr 22:294-306.

Cárdenas-Morales L, Volz LJ, Michely J, Rehme AK, Pool EM, Nettekoven C, Eickhoff SB, Fink GR, Grefkes C (2014) Network Connectivity and Individual Responses to Brain Stimulation in the Human Motor System. Cereb Cortex.

Cazzoli D, Muri RM, Schumacher R, von Arx S, Chaves S, Gutbrod K, Bohlhalter S, Bauer D, Vanbellingen T, Bertschi M, Kipfer S, Rosenthal CR, Kennard C, Bassetti CL, Nyffeler T (2012) Theta burst stimulation reduces disability during the activities of daily living in spatial neglect. Brain : a journal of neurology 135:3426-3439.

Cheeran B, Talelli P, Mori F, Koch G, Suppa A, Edwards M, Houlden H, Bhatia K, Greenwood R, Rothwell JC (2008) A common polymorphism in the brain-derived neurotrophic factor gene (BDNF) modulates human cortical plasticity and the response to rTMS. J Physiol 586:5717-5725.

Chollet F, DiPiero V, Wise RJ, Brooks DJ, Dolan RJ, Frackowiak RS (1991) The functional anatomy of motor recovery after stroke in humans: a study with positron emission tomography. Ann Neurol 29:63-71.

Chouinard PA, Leonard G, Paus T (2005) Role of the primary motor and dorsal premotor cortices in the anticipation of forces during object lifting. J Neurosci 25:2277-2284.

Conte A, Gilio F, Iezzi E, Frasca V, Inghilleri M, Berardelli A (2007) Attention influences the excitability of cortical motor areas in healthy humans. Exp Brain Res 182:109-117.

Conte A, Belvisi D, Iezzi E, Mari F, Inghilleri M, Berardelli A (2008) Effects of attention on inhibitory and facilitatory phenomena elicited by paired-pulse transcranial magnetic stimulation in healthy subjects. Exp Brain Res 186:393-399.

Damoiseaux JS, Greicius MD (2009) Greater than the sum of its parts: a review of studies combining structural connectivity and resting-state functional connectivity. Brain structure & function 213:525-533.

Damoiseaux JS, Rombouts SA, Barkhof F, Scheltens P, Stam CJ, Smith SM, Beckmann CF (2006) Consistent resting-state networks across healthy subjects. Proc Natl Acad Sci U S A 103:13848-13853.

Day BL, Dressler D, Maertens de Noordhout A, Marsden CD, Nakashima K, Rothwell JC, Thompson PD (1989) Electric and magnetic stimulation of human motor cortex: surface EMG and single motor unit responses. J Physiol 412:449-473.

De Luca M, Beckmann CF, De Stefano N, Matthews PM, Smith SM (2006) fMRI resting state networks define distinct modes of long-distance interactions in the human brain. Neuroimage 29:1359-1367.

Di Lazzaro V, Profice P, Ranieri F, Capone F, Dileone M, Oliviero A, Pilato F (2012) I-wave origin and modulation. Brain Stimulation 5:512-525.

Di Lazzaro V, Restuccia D, Oliviero A, Profice P, Ferrara L, Insola A, Mazzone P, Tonali P, Rothwell JC (1998a) Magnetic transcranial stimulation at intensities below active motor threshold activates intracortical inhibitory circuits. Exp Brain Res 119:265-268.

Di Lazzaro V, Oliviero A, Profice P, Saturno E, Pilato F, Insola A, Mazzone P, Tonali P, Rothwell JC (1998b) Comparison of descending volleys evoked by transcranial magnetic and electric stimulation in conscious humans. Electroencephalography and clinical neurophysiology 109:397-401.

Di Lazzaro V, Pilato F, Saturno E, Oliviero A, Dileone M, Mazzone P, Insola A, Tonali PA, Ranieri F, Huang YZ, Rothwell JC (2005) Theta-burst repetitive transcranial magnetic stimulation suppresses specific excitatory circuits in the human motor cortex. J Physiol 565:945-950.

Di Lazzaro V, Pilato F, Dileone M, Profice P, Oliviero A, Mazzone P, Insola A, Ranieri F, Meglio M, Tonali PA, Rothwell JC (2008) The physiological basis of the effects of intermittent theta burst stimulation of the human motor cortex. J Physiol 586:3871-3879.

Di Lazzaro V, Dileone M, Pilato F, Capone F, Musumeci G, Ranieri F, Ricci V, Bria P, Di Iorio R, de Waure C, Pasqualetti P, Profice P (2011) Modulation of motor cortex neuronal networks by rTMS: comparison of local and remote effects of six different protocols of stimulation. J Neurophysiol 105:2150-2156.

Dum RP, Strick PL (1991) The origin of corticospinal projections from the premotor areas in the frontal lobe. J Neurosci 11:667-689.

Dum RP, Strick PL (1992) Medial wall motor areas and skeletomotor control. Current opinion in neurobiology 2:836-839.

Dum RP, Strick PL (2002) Motor areas in the frontal lobe of the primate. Physiology & behavior 77:677-682.

Dum RP, Strick PL (2005) Frontal lobe inputs to the digit representations of the motor areas on the lateral surface of the hemisphere. J Neurosci 25:1375-1386.

Eickhoff SB, Dafotakis M, Grefkes C, Shah NJ, Zilles K, Piza-Katzer H (2008) Central adaptation following heterotopic hand replantation probed by fMRI and effective connectivity analysis. Experimental neurology 212:132-144.

Eldaief MC, Halko MA, Buckner RL, Pascual-Leone A (2011) Transcranial magnetic stimulation modulates the brain's intrinsic activity in a frequency-dependent manner. Proc Natl Acad Sci U S A 108:21229-21234.

Faraday M (1832) Experimental research in electricity. Phil Trans R Soc Lond 122:125-162.

Fink GR, Frackowiak RS, Pietrzyk U, Passingham RE (1997) Multiple nonprimary motor areas in the human cortex. J Neurophysiol 77:2164-2174.

Freitas C, Perez J, Knobel M, Tormos JM, Oberman LM, Eldaief M, Bashir S, Vernet M, Peña-Gómez C, Pascual-Leone A (2011) Changes in cortical plasticity across the lifespan. Frontiers in Aging Neuroscience 3.

Fries P (2005) A mechanism for cognitive dynamics: neuronal communication through neuronal coherence. Trends Cogn Sci 9:474-480.

Friston KJ (2002) Bayesian estimation of dynamical systems: an application to fMRI. Neuroimage 16:513-530.

Friston KJ, Harrison L, Penny W (2003) Dynamic causal modelling. Neuroimage 19:1273-1302.

Friston KJ, Frith CD, Liddle PF, Frackowiak RS (1993) Functional connectivity: the principal-component analysis of large (PET) data sets. Journal of cerebral blood flow and metabolism : official journal of the International Society of Cerebral Blood Flow and Metabolism 13:5-14.

Friston KJ, Mechelli A, Turner R, Price CJ (2000) Nonlinear responses in fMRI: the Balloon model, Volterra kernels, and other hemodynamics. Neuroimage 12:466-477.

Funke K, Benali A (2010) Cortical cellular actions of transcranial magnetic stimulation. Restorative neurology and neuroscience 28:399-417.

Funke K, Benali A (2011) Modulation of cortical inhibition by rTMS - findings obtained from animal models. J Physiol 589:4423-4435.

Gamboa OL, Antal A, Moliadze V, Paulus W (2010) Simply longer is not better: reversal of theta burst after-effect with prolonged stimulation. Exp Brain Res 204:181-187.

Gamboa OL, Antal A, Laczo B, Moliadze V, Nitsche MA, Paulus W (2011) Impact of repetitive theta burst stimulation on motor cortex excitability. Brain Stimul 4:145-151.

Gentner R, Wankerl K, Reinsberger C, Zeller D, Classen J (2008) Depression of human corticospinal excitability induced by magnetic theta-burst stimulation: evidence of rapid polarity-reversing metaplasticity. Cereb Cortex 18:2046-2053.

Gerloff C, Corwell B, Chen R, Hallett M, Cohen LG (1997) Stimulation over the human supplementary motor area interferes with the organization of future elements in complex motor sequences. Brain : a journal of neurology 120 (Pt 9):1587-1602.

Geyer S, Matelli M, Luppino G, Zilles K (2000) Functional neuroanatomy of the primate isocortical motor system. Anat Embryol (Berl) 202:443-474.

Goebel R, Roebroeck A, Kim DS, Formisano E (2003) Investigating directed cortical interactions in time-resolved fMRI data using vector autoregressive modeling and Granger causality mapping. Magn Reson Imaging 21:1251-1261.

Goldsworthy MR, Pitcher JB, Ridding MC (2012) The application of spaced theta burst protocols induces long-lasting neuroplastic changes in the human motor cortex. Eur J Neurosci 35:125-134.

Grefkes C, Geyer S, Schormann T, Roland P, Zilles K (2001) Human somatosensory area 2: observer-independent cytoarchitectonic mapping, interindividual variability, and population map. Neuroimage 14:617-631.

Grefkes C, Nowak DA, Wang LE, Dafotakis M, Eickhoff SB, Fink GR (2010) Modulating cortical connectivity in stroke patients by rTMS assessed with fMRI and dynamic causal modeling. Neuroimage 50:233-242.

Grefkes C, Nowak DA, Eickhoff SB, Dafotakis M, Kust J, Karbe H, Fink GR (2008) Cortical connectivity after subcortical stroke assessed with functional magnetic resonance imaging. Ann Neurol 63:236-246.

Grezes J, Armony JL, Rowe J, Passingham RE (2003) Activations related to "mirror" and "canonical" neurones in the human brain: an fMRI study. Neuroimage 18:928-937.

Hamada M, Murase N, Hasan A, Balaratnam M, Rothwell JC (2013) The role of interneuron networks in driving human motor cortical plasticity. Cereb Cortex 23:1593-1605.

Harrison L, Penny WD, Friston K (2003) Multivariate autoregressive modeling of fMRI time series. Neuroimage 19:1477-1491.

He SQ, Dum RP, Strick PL (1993) Topographic organization of corticospinal projections from the frontal lobe: motor areas on the lateral surface of the hemisphere. J Neurosci 13:952-980.

He SQ, Dum RP, Strick PL (1995) Topographic organization of corticospinal projections from the frontal lobe: motor areas on the medial surface of the hemisphere. J Neurosci 15:3284-3306.

Heeger DJ, Ress D (2002) What does fMRI tell us about neuronal activity? Nature reviews Neuroscience 3:142-151.

Hess G, Donoghue JP (1996) Long-term potentiation and long-term depression of horizontal connections in rat motor cortex. Acta neurobiologiae experimentalis 56:397-405.

Hinder MR, Goss EL, Fujiyama H, Canty AJ, Garry MI, Rodger J, Summers JJ (2014) Inter- and Intra-individual variability following intermittent theta burst stimulation: implications for rehabilitation and recovery. Brain Stimul 7:365-371.

Hlustik P, Solodkin A, Noll DC, Small SL (2004) Cortical plasticity during three-week motor skill learning. Journal of clinical neurophysiology : official publication of the American Electroencephalographic Society 21:180-191.

Huang YZ, Chen RS, Rothwell JC, Wen HY (2007) The after-effect of human theta burst stimulation is NMDA receptor dependent. Clin Neurophysiol 118:1028-1032.

Huang YZ, Edwards MJ, Rounis E, Bhatia KP, Rothwell JC (2005) Theta burst stimulation of the human motor cortex. Neuron 45:201-206.

Huang YZ, Rothwell JC, Lu CS, Wang J, Chen RS (2010) Restoration of motor inhibition through an abnormal premotor-motor connection in dystonia. Movement disorders : official journal of the Movement Disorder Society 25:696-703.

Iezzi E, Conte A, Suppa A, Agostino R, Dinapoli L, Scontrini A, Berardelli A (2008) Phasic voluntary movements reverse the aftereffects of subsequent theta-burst stimulation in humans. J Neurophysiol 100:2070-2076.

Ilmoniemi RJ, Ruohonen J, Karhu J (1999) Transcranial magnetic stimulation--a new tool for functional imaging of the brain. Critical reviews in biomedical engineering 27:241-284.

Inghilleri M, Conte A, Curra A, Frasca V, Lorenzano C, Berardelli A (2004) Ovarian hormones and cortical excitability. An rTMS study in humans. Clin Neurophysiol 115:1063-1068.

Kiebel SJ, Holmes AP (2007) The general linear model. In: Friston KJ, Ashburner JT, Kiebel SJ, Nichols TE, Penny WD, editors. Statistical parametric mapping: The analysis of functional brain images. London: Elsevier:101-125.

Kleim JA, Chan S, Pringle E, Schallert K, Procaccio V, Jimenez R, Cramer SC (2006) BDNF val66met polymorphism is associated with modified experience-dependent plasticity in human motor cortex. Nat Neurosci 9:735-737.

Koch G, Schneider S, Baumer T, Franca M, Munchau A, Cheeran B, Fernandez del Olmo M, Cordivari C, Rounis E, Caltagirone C, Bhatia K, Rothwell JC (2008) Altered dorsal premotor-motor interhemispheric pathway activity in focal arm dystonia. Movement disorders : official journal of the Movement Disorder Society 23:660-668.

Koch MA, Norris DG, Hund-Georgiadis M (2002) An investigation of functional and anatomical connectivity using magnetic resonance imaging. Neuroimage 16:241-250.

Kornak J, Hall DA, Haggard MP (2011) Spatially extended FMRI signal response to stimulus in non-functionally relevant regions of the human brain: preliminary results. The open neuroimaging journal 5:24-32.

Kurata K, Wise SP (1988) Premotor cortex of rhesus monkeys: set-related activity during two conditional motor tasks. Exp Brain Res 69:327-343.

Larson J, Lynch G (1986) Induction of synaptic potentiation in hippocampus by patterned stimulation involves two events. Science 232:985-988.

Lauterbur P (1973) Image formation by induced local interactions - Examples employing nuclear magnetic-resonance. Nature 242:190-192.

Logothetis NK (2002) The neural basis of the blood-oxygen-level-dependent functional magnetic resonance imaging signal. Philosophical transactions of the Royal Society of London Series B, Biological sciences 357:1003-1037.

Logothetis NK, Pauls J, Augath M, Trinath T, Oeltermann A (2001) Neurophysiological investigation of the basis of the fMRI signal. Nature 412:150-157.

López-Alonso V, Cheeran B, Rio-Rodriguez D, Fernandez-Del-Olmo M (2014) Inter-individual variability in response to non-invasive brain stimulation paradigms. Brain Stimul 7:372-380.

MacDermott AB, Mayer ML, Westbrook GL, Smith SJ, Barker JL (1986) NMDA-receptor activation increases cytoplasmic calcium concentration in cultured spinal cord neurones. Nature 321:519-522.

Malenka RC, Bear MF (2004) LTP and LTD: an embarrassment of riches. Neuron 44:5-21.

Mansfield P, Grannell PK (1973) NMR diffraction in solids. J Physics C Solid 6:L422-L426.

Martin PG, Gandevia SC, Taylor JL (2006) Theta burst stimulation does not reliably depress all regions of the human motor cortex. Clin Neurophysiol 117:2684-2690.

Matelli M, Luppino G, Rizzolatti G (1985) Patterns of cytochrome oxidase activity in the frontal agranular cortex of the macaque monkey. Behavioural brain research 18:125-136.

Matelli M, Luppino G, Rizzolatti G (1991) Architecture of superior and mesial area 6 and the adjacent cingulate cortex in the macaque monkey. The Journal of comparative neurology 311:445-462.

McIntosh AR, Gonzalez-Lima F (1994) Network interactions among limbic cortices, basal forebrain, and cerebellum differentiate a tone conditioned as a Pavlovian excitor or inhibitor: fluorodeoxyglucose mapping and covariance structural modeling. J Neurophysiol 72:1717-1733.

Murata A, Fadiga L, Fogassi L, Gallese V, Raos V, Rizzolatti G (1997) Object representation in the ventral premotor cortex (area F5) of the monkey. J Neurophysiol 78:2226-2230.

Nettekoven C, Volz LJ, Kutscha M, Pool EM, Rehme AK, Eickhoff SB, Fink GR, Grefkes C (2014) Dose-dependent effects of theta burst rTMS on cortical excitability and resting-state connectivity of the human motor system. J Neurosci 34:6849-6859.

Nyffeler T, Cazzoli D, Hess CW, Muri RM (2009) One session of repeated parietal theta burst stimulation trains induces long-lasting improvement of visual neglect. Stroke; a journal of cerebral circulation 40:2791-2796.

Ogawa S, Lee TM, Kay AR, Tank DW (1990) Brain magnetic resonance imaging with contrast dependent on blood oxygenation. Proc Natl Acad Sci U S A 87:9868-9872.

Pascual-Leone A, Amedi A, Fregni F, Merabet LB (2005) The plastic human brain cortex. Annual review of neuroscience 28:377-401.

Pascual-Leone A, Freitas C, Oberman L, Horvath JC, Halko M, Eldaief M, Bashir S, Vernet M, Shafi M, Westover B, Vahabzadeh-Hagh AM, Rotenberg A (2011) Characterizing brain cortical plasticity and network dynamics across the age-span in health and disease with TMS-EEG and TMS-fMRI. Brain Topogr 24:302-315.

Patton HD, Amassian VE (1954) Single and multiple-unit analysis of cortical stage of pyramidal tract activation. J Neurophysiol 17:345-363.

Peinemann A, Reimer B, Loer C, Quartarone A, Munchau A, Conrad B, Siebner HR (2004) Long-lasting increase in corticospinal excitability after 1800 pulses of subthreshold 5 Hz repetitive TMS to the primary motor cortex. Clin Neurophysiol 115:1519-1526.

Penny WD, Stephan KE, Mechelli A, Friston KJ (2004) Comparing dynamic causal models. Neuroimage 22:1157-1172.

Picard N, Strick PL (1996) Motor areas of the medial wall: a review of their location and functional activation. Cereb Cortex 6:342-353.

Picard N, Strick PL (2001) Imaging the premotor areas. Current opinion in neurobiology 11:663-672.

Power JD, Barnes KA, Snyder AZ, Schlaggar BL, Petersen SE (2012) Spurious but systematic correlations in functional connectivity MRI networks arise from subject motion. Neuroimage 59:2142-2154.

Quartarone A, Bagnato S, Rizzo V, Siebner HR, Dattola V, Scalfari A, Morgante F, Battaglia F, Romano M, Girlanda P (2003) Abnormal associative plasticity of the human motor cortex in writer's cramp. Brain : a journal of neurology 126:2586-2596.

Rademacher J, Burgel U, Geyer S, Schormann T, Schleicher A, Freund HJ, Zilles K (2001) Variability and asymmetry in the human precentral motor system. A cytoarchitectonic and myeloarchitectonic brain mapping study. Brain : a journal of neurology 124:2232-2258.

Rehme AK, Eickhoff SB, Wang LE, Fink GR, Grefkes C (2011) Dynamic causal modeling of cortical activity from the acute to the chronic stage after stroke. Neuroimage 55:1147-1158.

Ridding MC, Rothwell JC (2007) Is there a future for therapeutic use of transcranial magnetic stimulation? Nature reviews Neuroscience 8:559-567.

Ridding MC, Ziemann U (2010) Determinants of the induction of cortical plasticity by non-invasive brain stimulation in healthy subjects. J Physiol 588:2291-2304.

Rizzolatti G, Fadiga L (1998) Grasping objects and grasping action meanings: the dual role of monkey rostroventral premotor cortex (area F5). Novartis Foundation symposium 218:81-95; discussion 95-103.

Ro T, Cheifet S, Ingle H, Shoup R, Rafal R (1999) Localization of the human frontal eye fields and motor hand area with transcranial magnetic stimulation and magnetic resonance imaging. Neuropsychologia 37:225-231.

Roland PE, Larsen B, Lassen NA, Skinhoj E (1980) Supplementary motor area and other cortical areas in organization of voluntary movements in man. J Neurophysiol 43:118-136.

Salomons TV, Dunlop K, Kennedy SH, Flint A, Geraci J, Giacobbe P, Downar J (2014) Resting-state cortico-thalamic-striatal connectivity predicts response to dorsomedial prefrontal rTMS in major depressive disorder. Neuropsychopharmacology : official publication of the American College of Neuropsychopharmacology 39:488-498.

Salvador R, Suckling J, Schwarzbauer C, Bullmore E (2005) Undirected graphs of frequency-dependent functional connectivity in whole brain networks. Philosophical transactions of the Royal Society of London Series B, Biological sciences 360:937-946.

Satterthwaite TD, Elliott MA, Gerraty RT, Ruparel K, Loughead J, Calkins ME, Eickhoff SB, Hakonarson H, Gur RC, Gur RE, Wolf DH (2012) An improved framework for confound regression and filtering for control of motion artifact in the preprocessing of resting-state functional connectivity data. Neuroimage 64:240-256.

Shehzad Z, Kelly AM, Reiss PT, Gee DG, Gotimer K, Uddin LQ, Lee SH, Margulies DS, Roy AK, Biswal BB, Petkova E, Castellanos FX, Milham MP (2009) The resting brain: unconstrained yet reliable. Cereb Cortex 19:2209-2229.

Smith SB (2001) Preparing fMRI data for statistical analysis. In: Jezzard P, Matthews PM, Smith SB, editors. Functional MRI: an introduction to methods. New York: Oxford University Press; p. 229-41.

Sparing R, Buelte D, Meister IG, Paus T, Fink GR (2008) Transcranial magnetic stimulation and the challenge of coil placement: a comparison of conventional and stereotaxic neuronavigational strategies. Hum Brain Mapp 29:82-96.

Stagg CJ, O'Shea J, Johansen-Berg H (2010) Imaging the effects of rTMS-induced cortical plasticity. Restorative neurology and neuroscience 28:425-436.

Stagg CJ, Wylezinska M, Matthews PM, Johansen-Berg H, Jezzard P, Rothwell JC, Bestmann S (2009) Neurochemical effects of theta burst stimulation as assessed by magnetic resonance spectroscopy. J Neurophysiol 101:2872-2877.

Stephan KE, Harrison LM, Kiebel SJ, David O, Penny WD, Friston KJ (2007) Dynamic causal models of neural system dynamics:current state and future extensions. Journal of biosciences 32:129-144.

Stephan KE, Penny WD, Moran RJ, den Ouden HE, Daunizeau J, Friston KJ (2010) Ten simple rules for dynamic causal modeling. Neuroimage 49:3099-3109.

Stepniewska I, Preuss TM, Kaas JH (1993) Architectonics, somatotopic organization, and ipsilateral cortical connections of the primary motor area (M1) of owl monkeys. The Journal of comparative neurology 330:238-271.

Stöcker T, Shah NJ (2006) Grundlagen der MR-Bildgebung. In: Schneider F, Fink GR, editors. Funktionelle MRT in Psychiatrie und Neurologie. Heidelberg: Springer; p. 62-78.

Talelli P, Cheeran BJ, Teo JT, Rothwell JC (2007) Pattern-specific role of the current orientation used to deliver Theta Burst Stimulation. Clin Neurophysiol 118:1815-1823.

Touge T, Gerschlager W, Brown P, Rothwell JC (2001) Are the after-effects of low-frequency rTMS on motor cortex excitability due to changes in the efficacy of cortical synapses? Clin Neurophysiol 112:2138-2145.

Trippe J, Mix A, Aydin-Abidin S, Funke K, Benali A (2009) theta burst and conventional low-frequency rTMS differentially affect GABAergic neurotransmission in the rat cortex. Exp Brain Res 199:411-421.

Vallence AM, Ridding MC (2014) Non-invasive induction of plasticity in the human cortex: uses and limitations. Cortex; a journal devoted to the study of the nervous system and behavior 58:261-271.

Vallence AM, Kurylowicz L, Ridding MC (2013) A comparison of neuroplastic responses to non-invasive brain stimulation protocols and motor learning in healthy adults. Neurosci Lett 549:151-156.

van den Heuvel MP, Hulshoff Pol HE (2010) Exploring the brain network: a review on resting-state fMRI functional connectivity. European neuropsychopharmacology : the journal of the European College of Neuropsychopharmacology 20:519-534.

van der Werf YD, Sanz-Arigita EJ, Menning S, van den Heuvel OA (2011) Modulating spontaneous brain activity using repetitive transcranial magnetic stimulation. BMC Neurosci 11:145.

Van Dijk KR, Sabuncu MR, Buckner RL (2012) The influence of head motion on intrinsic functional connectivity MRI. Neuroimage 59:431-438.

Van Dijk KR, Hedden T, Venkataraman A, Evans KC, Lazar SW, Buckner RL (2010) Intrinsic functional connectivity as a tool for human connectomics: theory, properties, and optimization. J Neurophysiol 103:297-321.

Veniero D, Ponzo V, Koch G (2013) Paired associative stimulation enforces the communication between interconnected areas. J Neurosci 33:13773-13783.

Vercammen A, Knegtering H, Liemburg EJ, den Boer JA, Aleman A (2010) Functional connectivity of the temporo-parietal region in schizophrenia: effects of rTMS treatment of auditory hallucinations. J Psychiatr Res 44:725-731.

Volz LJ, Hamada M, Rothwell JC, Grefkes C (2014) What Makes the Muscle Twitch: Motor System Connectivity and TMS-Induced Activity. Cereb Cortex.

Volz LJ, Benali A, Mix A, Neubacher U, Funke K (2013) Dose-dependence of changes in cortical protein expression induced with repeated transcranial magnetic theta-burst stimulation in the rat. Brain Stimul 6:598-606.

Ward NS, Brown MM, Thompson AJ, Frackowiak RS (2003) Neural correlates of motor recovery after stroke: a longitudinal fMRI study. Brain : a journal of neurology 126:2476-2496.

Watanabe T, Hanajima R, Shirota Y, Ohminami S, Tsutsumi R, Terao Y, Ugawa Y, Hirose S, Miyashita Y, Konishi S, Kunimatsu A, Ohtomo K (2013) Bidirectional effects on interhemispheric resting-state functional connectivity induced by excitatory and inhibitory repetitive transcranial magnetic stimulation. Hum Brain Mapp.

Wu T, Chan P, Hallett M (2008) Modifications of the interactions in the motor networks when a movement becomes automatic. J Physiol 586:4295-4304.

Xiong J, Ma L, Wang B, Narayana S, Duff EP, Egan GF, Fox PT (2009) Long-term motor training induced changes in regional cerebral blood flow in both task and resting states. Neuroimage 45:75-82.

Yousry TA, Schmid UD, Alkadhi H, Schmidt D, Peraud A, Buettner A, Winkler P (1997) Localization of the motor hand area to a knob on the precentral gyrus. A new landmark. Brain : a journal of neurology 120 (Pt 1):141-157.

Zangen A, Roth Y, Voller B, Hallett M (2005) Transcranial magnetic stimulation of deep brain regions: evidence for efficacy of the H-coil. Clin Neurophysiol 116:775-779.

Ziemann U (2010) TMS in cognitive neuroscience: virtual lesion and beyond. Cortex; a journal devoted to the study of the nervous system and behavior 46:124-127.

5. Eigene Beteiligung an den Veröffentlichungen

Studie I (Network connectivity and individual responses to brain stimulation in the human motor system; Cárdenas-Morales L, Volz LJ, Michely J, Rehme AK, Pool EM, Nettekoven C, Eickhoff SB, Fink GR, Grefkes C.; Cereb Cortex. 2014 Jul;24(7):1697-707):

- Planung und Design der Studie (anteilig)
- Durchführung der Experimente
- Analyse der Daten (anteilig)
- Editierung der Veröffentlichung

Studie II (Dose-dependent effects of theta burst rTMS on cortical excitability and resting-state connectivity of the human motor system; Nettekoven C, Volz LJ, Kutscha M, Pool EM, Rehme AK, Eickhoff SB, Fink GR, Grefkes C.; J Neurosci. 2014 May 14;34(20):6849-59):

- Planung und Design der Studie
- Durchführung der Experimente
- Analyse der Daten
- Verfassung der Veröffentlichung
- Beantworten der Gutachterkommentare (peer-review)

Studie III (Inter-individual variability in cortical excitability and motor network connectivity following multiple blocks of rTMS; Nettekoven C, Volz LJ, Kutscha M, Pool EM, Rehme AK, Eickhoff SB, Fink GR, Grefkes C.; under review):

- Planung und Design der Studie
- Durchführung der Experimente
- Analyse der Daten
- Verfassung der Veröffentlichung
- Beantworten der Gutachterkommentare (peer-review)

6. Danksagung

An erster Stelle möchte ich Prof. Dr. Christian Grefkes für seine Betreuung und Förderung in den letzten Jahren danken. Vielen Dank für deine Zeit, deine Korrekturen und Anmerkungen und die vielen Möglichkeiten, die du mir während der Promotionszeit geboten hast.

Ein großer Dank gilt auch allen Mitgliedern meiner Arbeitsgruppe Neuromodulation & Neurorehabilitation. Vielen Dank für die gute Zusammenarbeit und das nette Miteinander auch außerhalb der Arbeit. Besonders danken möchte ich hier vor allem Dr. Lukas Volz, der mir immer hilfsbereit zur Seite stand und viele Stunden investiert hat, um mich zu betreuen.

Weiterhin möchte ich Prof. Dr. Gereon R. Fink für seine Supervision und wertvollen Kommentare danken, sowie Prof. Dr. Simon Eickhoff für seine Hilfe bei jeglichen Fragestellungen.

Vielen Dank auch an Prof. Dr. Ansgar Büschges, dass er meine Betreuung von Seiten der Universität übernommen hat und sich um alle organisatorischen Dinge gekümmert hat. Vielen Dank für Ihr Interesse an meinen Forschungsarbeiten und die nette Betreuung.

Ein ganz besonders großer Dank gilt meiner Familie und meinen Freunden, die mir vom Beginn meiner Schulzeit bis hin zur Promotion den Rücken gestärkt haben und mich bekräftigt haben in dem was ich tue. Ohne eure Unterstützung, euer offenes Ohr und die vielen schönen Ablenkungen hätte ich diese Zeit nicht so gut hinter mich gebracht. Ich freue mich diesen Abschnitt meines Lebens mit euch zu feiern.

7. Erklärung

Ich versichere, dass ich die von mir vorgelegte Dissertation selbstständig angefertigt, die benutzten Quellen und Hilfsmittel vollständig angegeben und die Stellen der Arbeit – einschließlich Tabellen, Karten und Abbildungen -, die anderen Werken im Wortlaut oder dem Sinn nach entnommen sind, in jedem Einzelfall als Entlehnung kenntlich gemacht habe; dass diese Dissertation noch keiner anderen Fakultät oder Universität zur Prüfung vorgelegen hat; dass sie – abgesehen von unten angegebenen Teilpublikationen – noch nicht veröffentlicht worden ist, sowie, dass ich eine solche Veröffentlichung vor Abschluss des Promotionsverfahrens nicht vornehmen werde.

Die Bestimmungen der Promotionsordnung sind mir bekannt. Die von mir vorgelegte Dissertation ist von Prof. Dr. Ansgar Büschges und Prof. Dr. Christian Grefkes betreut worden.

(Charlotte Maria Nettekoven)